SPRINGER BRIEFS IN MOLECULAR SCIENCE

José Antonio Fornés

Electrical Fluctuations in Polyelectrolytes

Springer

SpringerBriefs in Molecular Science

More information about this series at http://www.springer.com/series/8898

José Antonio Fornés

Electrical Fluctuations in Polyelectrolytes

Springer

José Antonio Fornés
Federal University of Goiás
Goiânia, Goiás, Brazil

ISSN 2191-5407 ISSN 2191-5415 (electronic)
SpringerBriefs in Molecular Science
ISBN 978-3-319-33839-2 ISBN 978-3-319-33840-8 (eBook)
DOI 10.1007/978-3-319-33840-8

Library of Congress Control Number: 2016940063

Printed on acid-free paper

This Springer imprint is published by Springer Nature
The registered company is Springer International Publishing AG Switzerland

Preface

To my wife, Nélida, who was always a source of love and inspiration. In memory

"*Science is an evolution of ideas and approximations,*" *José A. Fornés, 1998.*

The importance of estimating fluctuations in physics is because they contain a lot of information: Electromagnetic fluctuations are the origin of London (van der Waals) forces (1937) between molecules and Lifchitz forces (1956) between macro-objects. Protonic fluctuations are the origin of Kirkwood and Schumaker forces (1952) between molecules and pH fluctuations (Fornés et al. 1999). Also protonic fluctuations could be the cause of the dielectric increment of proteins in solution. Local electrical fluctuations can influence chemical reactions. Polyelectrolytes are present in almost all the biological systems. In order to understand how these systems work, it is important to know the size of their electrical fluctuations. The present book represents the work the author has performed on this subject while he was professor at the Institute of Physics of Goiás University. I am grateful to my many friends and colleagues. I would like especially to acknowledge the help I received from Amando S. Ito, Joaquim Procopio, and José Nicodemos T. Rabelo, who influenced very much my scientific career, and also the help I received from Salviano de Araújo Leão, who was always ready to help me with computational softwares. Also I want to acknowledge the help I received from Daniel Leite in the design of the figures. Also, I would like to thank to Luis Furtado, Springer's editor in Brazil, whose perfect orientation and cordial treatment made this book reality. It has been a considerable pleasure to work with him. Finally, I want to express my gratitude to Susan Westendorf, my book project coordinator, Springer Nature, in New York, who always was ready to give a hearty assistance, related to the book production. *March 2016, José Antonio Fornés Instituto de Física UFG, Brazil*. I want to express my recognition to Sarumathi Hemachandirane, Project Manager Publishing SPi Global in India and her Team, for such a careful and perfect job in the production of the book.

Goiânia, Goiás, Brazil — José Antonio Fornés

Contents

Chapter 1
The Electrical Capacitance, the Link to the Electrical Fluctuations

Abstract In this chapter, we develop a method in order to estimate the electrical fluctuations in small systems. The method consists in knowing the electrical capacitance that emerges as a consequence of the processes or the system's interfaces. We use results given by the fluctuation-dissipation theorem in the classical limit. Estimating the electrical capacitance is important because it is the link to the knowledge of the fluctuation of several physical quantities, voltage and field fluctuations, dipole moment, pH, and charge, and also to knowledge of the polarizability and the dielectric dispersion of colloidal and polyelectrolytes systems.

Keywords Charge fluctuation capacitance • Small systems • Electrical fluctuations

1.1 Electrical Fluctuations

The importance of local field fluctuations in biological systems was raised by several authors: Weaver and Astumian [21] have presented a calculation of the effects of weak fields upon cells. Procopio and Fornés [16], using the fluctuation-dissipation theorem (FDT), have presented a calculation of the voltage fluctuations across cell membranes. Protonic fluctuations could be the cause of the dielectric increment of proteins in solution [11, 20]. For fluctuations of ion distribution in colloid and polyelectrolyte solutions, see, for instance, [4, 13, 14], see also the next chapters. Also local fluctuations can influence chemical reactions, see [1]. Oosawa [15] has also calculated the magnitude of fluctuating voltage and field across different points of an electrolyte solution constituted of point ions using the method of the mode expansion [1, 3–6, 13–15, 18, 19]. Also Brownian motors are small physical micro- or even nano-machines that operate far from thermal equilibrium by extracting the energy from both thermal and non-equilibrium fluctuations in order to generate work

Part reprinted from [José A. Fornés, *J. Colloid Interface Sci.* **226**, 172, (2000)] Copyright (2000), with permission from Elsevier.

J.A. Fornés, *Electrical Fluctuations in Polyelectrolytes*, SpringerBriefs in Molecular Science, DOI 10.1007/978-3-319-33840-8_1

against external loads. They present the physical analogue of bio-molecular motors that also work out of equilibrium to direct intracellular transport and to control motion in cells, Fornés [9].

In this chapter, we develop a method in order to estimate the electrical fluctuations in small systems. The method consists in knowing the electrical capacitance that emerges as a consequence of the processes or by the proper interfaces in the systems [7], e.g.: Protonation–deprotonation equilibrium at interfaces and in the bulk, the fluctuation of the ionic atmosphere surrounding a charged surface or macroion in an electrolyte solution, also the cell and the inner mitochondrial membranes and the ionic channels, can be well represented by combinations of resistances and capacitances, etc. The electrical capacitance is the link to the knowledge of the fluctuation of several physical quantities: voltage and field fluctuations [4–6, 16, 17, 21], dipole moment [5, 6, 8], pH and charge [10]. Also to the knowledge of the polarizability and the dielectric dispersion of molecular systems [5, 8].

1.2 The Fluctuation-Dissipation Theorem

One way of formulating the FDT is by formally regarding the spontaneous fluctuations of a quantity x as due to the action of some random force f, meaning that the environment senses the system through the *generalized susceptibility*, $\alpha(\omega)$, and respond with a fluctuating force. The Fourier components x_ω and f_ω are related by:

$$x_\omega = \alpha(\omega) f_\omega \tag{1.1}$$

The relation between the *generalized impedance* $Z(\omega)$ and $\alpha(\omega)$ is

$$Z(\omega) = -\frac{1}{i\omega\alpha(\omega)} \tag{1.2}$$

with i being the imaginary unit. As $x_\omega = x_{0\omega} e^{-i\omega t}$ we can write

$$f_\omega = Z(\omega)\frac{dx_\omega}{dt} \tag{1.3}$$

The spectral densities of the fluctuation are given by

$$(x^2)_\omega = \mid \alpha(\omega) \mid^2 (f^2)_\omega \tag{1.4}$$

The results of the FDT are

$$(x^2)_\omega = \hbar\alpha''(\omega) coth\frac{\hbar\omega}{2kT} \tag{1.5}$$

Correspondingly:

$$(f^2)_\omega = \frac{\hbar\alpha''(\omega)}{\mid \alpha(\omega) \mid^2} coth\frac{\hbar\omega}{2kT} \tag{1.6}$$

The mean square of the fluctuating quantity is

$$< x^2 >= \frac{1}{\pi}\int_0^\infty (x^2)_\omega d\omega = \frac{\hbar}{\pi}\int_0^\infty \alpha''(\omega) coth\frac{\hbar\omega}{2kT} d\omega \tag{1.7}$$

These formulae constitute the FDT, established by Callen and Welton [2]. They relate the fluctuations of physical quantities to the dissipative properties of the system. At energies $kT \gg \hbar\omega$ (classical limit) we have $coth(\hbar\omega/2kT) \approx 2kT/\hbar\omega$ and $\mid \alpha(\omega) \mid^2 \approx \mid \alpha'(0) \mid^2$. Then Eq. 1.7 becomes

$$< x^2 >= \frac{2kT}{\pi}\int_0^\infty \frac{\alpha''(\omega)}{\omega} d\omega \tag{1.8}$$

Using the Kramers and Kronig's relations this integral can be written as [12]:

$$< x^2 >= kT \mid \alpha'(0) \mid \tag{1.9}$$

Averaging Eq. 1.4 in frequency in the classic region, we have

$$< x^2 >=< (x^2)_\omega >=<\mid \alpha(\omega) \mid^2 (f^2)_\omega > \tag{1.10}$$

and in order for Eqs. 1.9 and 1.10 to be compatible, we obtain

$$< f^2 >= \frac{kT}{\mid \alpha'(0) \mid} \tag{1.11}$$

From Eqs. 1.9 and 1.11 we obtain

$$< x^2 >< f^2 >= (kT)^2 \tag{1.12}$$

This is the classical analogy of the Heisenberg uncertainty principle.

1.2.1 Electrical Circuit

In an electric circuit the relation between the Fourier components of the spontaneous fluctuational current I_ω and voltage, V_ω is given by:

$$V_\omega = Z(\omega) I_\omega, \tag{1.13}$$

Equation 1.13 can be written as

$$q_\omega = \alpha(\omega) V_\omega \tag{1.14}$$

where q_ω is the Fourier component of the fluctuational charge.

In case of an RC circuit in series, we have

$$Z(\omega) = R + \frac{1}{i\omega C} \tag{1.15}$$

Correspondingly from Eq. 1.2, $\alpha(\omega)$ is given by:

$$\alpha(\omega) = \frac{-C}{1 + (\tau\omega)^2} + i\frac{\tau\omega C}{1 + (\tau\omega)^2} \tag{1.16}$$

Then

$$\alpha'(\omega) = \frac{-C}{1 + (\tau\omega)^2}, \quad \alpha''(\omega) = \frac{\tau\omega C}{1 + (\tau\omega)^2} \tag{1.17}$$

From Eqs. 1.5 and 1.17 and considering the classical limit, we obtain[1]

$$(q^2)_\omega = \frac{2kT\tau C}{1 + (\tau\omega)^2} \tag{1.18}$$

and

$$(V^2)_\omega = \frac{2kT\tau}{C(1 + (\tau\omega)^2)} \tag{1.19}$$

Then from Eq. 1.19:

$$< q^2 >= \frac{1}{\pi}\int_0^\infty (q^2)_\omega d\omega = kTC \tag{1.20}$$

Correspondingly the mean quadratic fluctuation of the voltage, $< V^2 >=< q^2 > C^{-2}$, will be

$$< V^2 >= \frac{kT}{C} \tag{1.21}$$

[1]In this limit, whether the circuit is in series or parallel is irrelevant concerning fluctuating magnitudes [16].

1.3 The Electrical Capacitance

The time scale of the mentioned processes is in the μs-ns range, hence we can make use of the FDT in the classical limit ($kT \gg \hbar\omega$ or $\omega \ll kT\hbar^{-1} = 4 \times 10^{13}\,\mathrm{s}^{-1}$) [5],[2] [7], namely

$$\left\langle (\Delta x)^2 \right\rangle^{1/2} \left\langle (\Delta f)^2 \right\rangle^{1/2} = kT \tag{1.22}$$

where $\left\langle (\Delta x)^2 \right\rangle^{1/2}$is the square root of the mean square of the spontaneous fluctuations of a quantity x, as due to the action of some random force f senses by the environment, whose corresponding square root of the mean square of the fluctuations is $\left\langle (\Delta f)^2 \right\rangle^{1/2}$.

In order to simplify the notation we rewrite Eq. 1.22 as

$$\delta x.\delta f = kT \tag{1.23}$$

This equation shows a constant equilibrium between the system and the environment, when δf increases in the ambient, the system reacts in such a way to inhibit the fluctuation of the corresponding physical quantity x and vice versa in order to maintain the product constant equal to kT. We also observe that the product $x \times f$ has dimension of energy.

Examples of Eqs. 1.23 and 1.22 are the following relations:

$$\begin{aligned} \delta q.\delta\psi &= kT \\ \delta p.\delta E &= kT \\ \delta V.\delta P &= kT \\ \delta A.\delta\Pi &= kT \end{aligned} \tag{1.24}$$

In the first relation of the former equations, δq can be the statistical fluctuation of charge produced in a capacitor as due to the action of some random potential ψ sensed by the environment whose statistical fluctuation is $\delta\psi$. In the second relation p is the dipole moment and E is the electric field, in the third one V is the volume and P is the pressure and in the fourth relation A is the area per molecule and Π is the surface pressure ($\mathrm{N.m}^{-1}$) in a Langmuir–Adam surface balance.

[2] In this reference we used the notation x for Δx

1.3.1 Capacitance Definition

As an example of Eq. 1.23 we can consider in a capacitor the relation between the statistical fluctuation of charge, δq, and the corresponding fluctuation of potential, $\delta\psi$, sensed by the environment,

$$\delta q.\delta\psi = kT \tag{1.25}$$

We can define the capacitance as:

$$C = \frac{\delta q}{\delta\psi} \Rightarrow \delta q = C.\delta\psi \tag{1.26}$$

From Eqs. 1.25 and 1.26 we obtain the following relations:

$$C = \frac{(\delta q)^2}{kT}, \qquad \delta\psi = \left(\frac{kT}{C}\right)^{1/2}, \qquad \delta q = (kT.C)^{1/2} \tag{1.27}$$

These relations have already been used by several authors in various situations, see [1, 3–11, 13–21].

The SI system of units is employed throughout the whole book, namely: ε_o is the permittivity of vacuum ($\varepsilon_o = 8.85 \times 10^{-12}\ \mathrm{C^2N^{-1}m^{-2}}$), ε is the dielectric constant of the medium ($\varepsilon = 80$), e_o is the proton charge ($e_o = 1.602 \times 10^{-19}$ C), k is Boltzmann constant ($k = 1.381 \times 10^{-23}$ J/K) and T is the absolute temperature.

In Table 1.1 are shown numerically the relations of Eq. 1.27. From the third and fourth column we can observe the increase of potential and field fluctuations with the decrease of the capacitor value and size. The fifth column shows the diminution of charge fluctuations (number of elementary charges) with the corresponding decrease of the capacitor value and size. The minimum capacitance value at room temperature supporting one elementary charge fluctuation is $\frac{(e_o)^2}{kT} = 6.2$ aF, which corresponds to a cubic capacitor in water of side $d = 87$ Å. Inside vesicular biological systems in water with sizes approximately lower than this, charge fluctuations are fractions of one elementary charge (see discussion on this subject in [10]). Biological polyelectrolyte systems have the property of storing great amount of charge in a small volume (great electrical capacitance), as a consequence the electrical fluctuations are smaller than the example of the cubic capacitor. For example [5], a DNA molecule of 7800 Å (4627 charged groups) has an electrical capacitance of 133 pF ($\delta E = 1687\ \mathrm{V\,m^{-1}}$).

Table 1.1 Potential, electric field and charge fluctuations as related to given values and sizes of the capacitors, from [7]

C	$d = \frac{C}{\varepsilon\varepsilon_o}$	$\delta\psi$	$\delta E = \frac{\delta\psi}{d}$	$\frac{\delta q}{eo}$
1 pF	1.4 mm	64 μV	$46\frac{\text{mV}}{\text{m}}$	402
1 fF	1.4 μm	2 mV	$1.4\frac{\text{kV}}{\text{m}}$	13
100 aF	1400 Å	6 mV	$43\frac{\text{kV}}{\text{m}}$	4
10 aF	140 Å	20 mV	$1.4\frac{\text{MV}}{\text{m}}$	1.3
$\frac{(e_o)^2}{kT} = 6.2$ aF	87 Å	26 mV	$9.6\frac{\text{MV}}{\text{m}}$	1
1 aF	14 Å	64 mV	$46\frac{\text{MV}}{\text{m}}$	0.4

Cubic capacitor: $C = (A/d)\varepsilon\varepsilon_o, A = d^2$,
$\varepsilon = 80$, aF $\equiv$ attoF $= 10^{-18}$ F

References

1. Astumian, R.D., Bier, M.: Fluctuation driven ratchets - Molecular motors. Phys. Rev. Lett. **72**, 1766–1769 (1994)
2. Callen, H.B., Welton, T.A.: Irreversibility and generalized noise. Phys. Rev. **83**, 34 (1951)
3. Chandler, D., Andersen, H.: Mode expansion in equilibrium statistical mechanics. II. A rapidly convergent theory of ionic solutions. J. Chem. Phys. **54**, 26–33 (1971)
4. Fornés, J.A.: Electrical fluctuations in colloid and ionic solutions. J Colloid Interface Sci. **186**, 90–101 (1997)
5. Fornés, J.A.: Fluctuation-dissipation theorem and the polarizability of rodlike polyelectrolytes: an electric circuit view. Phys. Rev. E **57**, 2110–2114 (1998)
6. Fornés, J.A.: Thermal electrical fluctuations around a charged colloidal cylinder in an electrolyte. Phys. Rev. E **57**, 2104–2109 (1998)
7. Fornés, J.A.: The electrical capacitance of small systems. J. Colloid Interface Sci. **226**, 172–179 (2000)
8. Fornés, J.A.: Dielectric relaxation around a charged colloidal cylinder in an electrolyte. J. Colloid Interface Sci. **222**, 97–102 (2000)
9. Fornés, J.A.: Hydrodynamic interactions introduce differences in the behaviour of a ratchet dimer Brownian motor. J. Biomater. Nanobiotechnol. **6**, 81–90 (2015)
10. Fornés, J.A., Ito, A.S., Curi, R., Procopio, J.: pH fluctuations in unilamellar vesicles. Phys. Chem. Chem. Phys. **1**(22), 5133–5138 (1999)
11. Kirkwood, J.G., Shumaker, J.B.: The influence of dipole moment fluctuations on the dielectric increment of proteins in solution. Proc. Natl. Acad. Sci. U.S.A. **38**, 855–862 (1952)
12. Landau, L.D., Lifshitz, E.M.: Statistical Physics, p. 387. Pergamon Press, Oxford (1988)
13. Oosawa, F.: Counterion fluctuation and dielectric dispersion in linear polyelectrolytes. Biopolymers **9**, 677 (1970)
14. Oosawa, F.: Polyelectrolytes, Chap. 5. Marcel Dekker, New York (1971)
15. Oosawa, F.: Field fluctuation in ionic solutions and its biological significance. J. Theor. Biol. **39**, 373–386 (1973)
16. Procopio, J., Fornés, J.A.: Fluctuation-dissipation theorem imposes high-voltage fluctuations in biological ionic channels. Phys. Rev. E **51**, 829–831 (1995)
17. Procopio, J., Fornés, J.A.: Fluctuations of the proton-electromotive force across the inner mitochondrial membrane. Phys. Rev. E **55**, 6285–6288 (1997)
18. Schurr, J.M.: Theory of quasi elastic light scattering from chemically reactive ionic solutions. J. Phys. Chem. **73**, 2820–2828 (1969)

19. Schurr, J.M.: Dielectric dispersion of linear polyelectrolytes. Biopolymers **10**, 1371–1375 (1971)
20. Schwarz, G.: A theory of the low-frequency dielectric dispersion of colloid particles in electrolyte solution. J. Phys. Chem. **66**, 2636–2642 (1962)
21. Weaver, J.C., Astumian, R.D.: The response of living cells to very weak electric-fields - The thermal noise limit. Science **247**, 459–462 (1990)

Chapter 2
Electrical Fluctuations in Colloid and Ionic Solutions

Abstract A method is developed in order to determine the natural electrical thermal fluctuations and its spectral distribution across two points of a solution of ions or spherical charged particles immersed in an ionic solution. The electrical equivalent between two points of a solution is considered as a capacitor and a resistor in parallel. The method is applied within the Debye–Hückel approximation (linearized Poisson–Boltzmann equation), although it is valid in general. Among the results is the diminution of electrical fluctuations as particle sizes increase, as a consequence large particles produce electrical stabilization in their neighbourhood. Also can be observed that fluctuations are not quite sensitive to ionic concentrations for large particles. When the size of the particles becomes negligible we obtain similar results with the already obtained using the method of the mode expansion.

Keywords Electrical fluctuations • Colloid fluctuations • Ionic fluctuations

2.1 Electrical Fluctuations in Solutions

We use the method developed in the former chapter to determine the natural electrical thermal fluctuations and its spectral distribution across two points of a solution of ions or electrical charged particles immersed in an ionic solution. We consider the solution path as a capacitor and a resistor in parallel.

The equations derived in the present work are valid for the following two cases:

a) A solution of spherical charged particles[1] of radii a immersed in a symmetrical electrolyte solution of pointlike ions, Fig. 2.1a.
b) A symmetrical electrolyte solution which ions have a mean radius a, Fig. 2.1b.

Reprinted from [José A. Fornés, *J. Colloid Interface Sci.* **186**, 90, (1997)] Copyright (1997), with permission from Elsevier.

[1] It can also be polyelectrolytes.

J.A. Fornés, *Electrical Fluctuations in Polyelectrolytes*, SpringerBriefs in Molecular Science, DOI 10.1007/978-3-319-33840-8_2

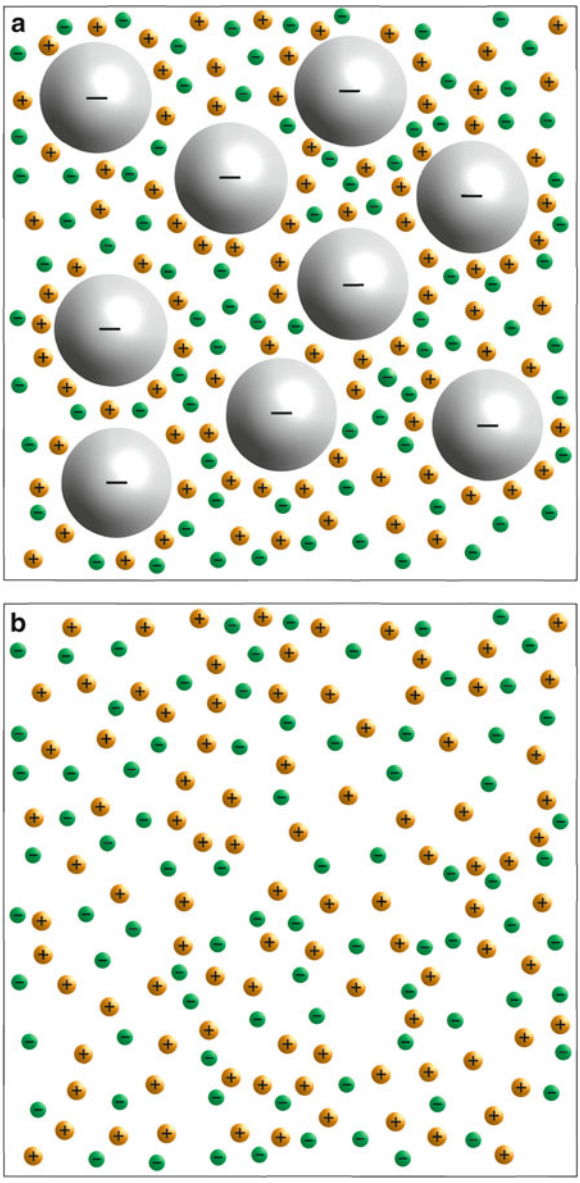

Fig. 2.1 (**a**) Spherical charged particles of radii a immersed in a symmetrical electrolyte solution of pointlike ions. (**b**) Symmetrical electrolyte solution of ions having a mean radius a

In both cases are estimated the electrical fluctuations and their spectral distributions.

The Debye–Hückel theory [2] for a symmetrical electrolyte of valence z with n ions per m^3 gives for the potential, $\psi(r)$ surrounding a spherical ion of charge $Q = ze_0$:

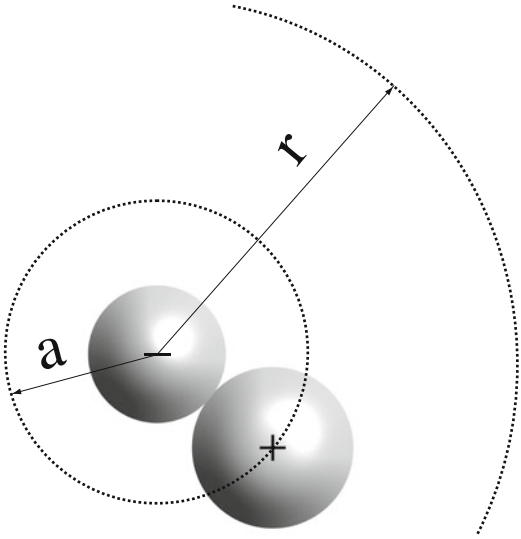

Fig. 2.2 Representation of a, the *distance of closest approach*

$$\psi(r) = \frac{Q}{4\pi\epsilon\epsilon_0}\frac{e^{\kappa a}}{1+\kappa a}\frac{e^{-\kappa r}}{r} \tag{2.1}$$

The SI system of units was employed throughout, in Eq. 2.1 ϵ_0 is the permittivity of vacuum ($\epsilon_0 = 8.85 \times 10^{-12}\ \mathrm{C^2N^{-1}}m^{-2}$), ϵ is the dielectric constant of the medium, e_0 the electron charge ($e_0 = 1.602 \times 10^{-19}\,\mathrm{C}$), a is the *distance of closest approach* equal to the sum of the radii of oppositely charged ions in contact (see Fig. 2.2) and κ, called the

Debye–Hückel reciprocal length parameter, is given by:

$$\kappa^2 = \frac{e_0^2}{\epsilon\epsilon_0 kT}\sum \eta_{i0} z_i^2 = \frac{2000 e_0^2 N_A}{\epsilon\epsilon_0 kT}\left[\frac{1}{2}\sum c_i z_i^2\right] \tag{2.2}$$

The quantity $I = \frac{1}{2}\sum c_i z_i^2$ quantifies the charge in an electrolyte solution and is called the *ionic strength* after Lewis and Randall [8]. In case of a solution of a symmetrical $(z-z)$ electrolyte we have

$$\kappa^2 = \frac{2(e_0 z)^2}{\epsilon_0 \epsilon kT} n = \frac{2(e_0 z)^2}{\epsilon_0 \epsilon kT} N_A c 10^3 \tag{2.3}$$

where k is Boltzmann constant ($k = 1.381 \times 10^{-23}\,\mathrm{J/K}$), T is the absolute temperature, N_A is Avogadro constant and c the solution concentration in *moles*/*liter*.

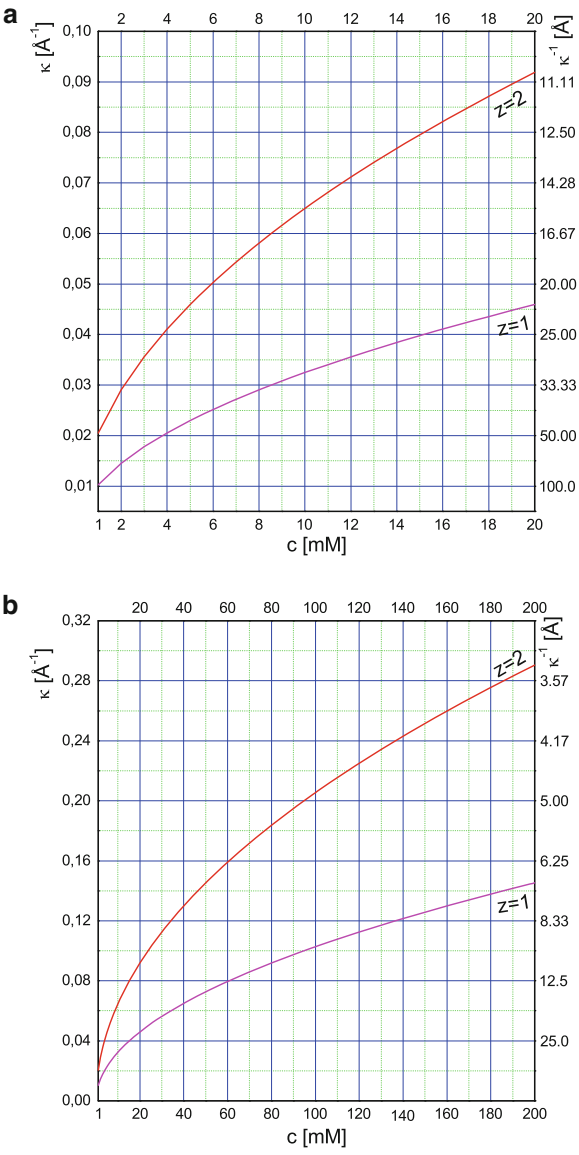

Fig. 2.3 (**a**), (**b**) κ, κ^{-1} for mono and bivalent symmetrical electrolyte solution

In Fig. 2.3a and b are shown κ and κ^{-1} versus c in mM for $z = 1$ and $z = 2$.

In case we have an spherical particle immersed in a solution of pointlike ions Eq. 2.1 remains the same, being Q the charge on the particle and a its radius (see, for instance, [20]).

Equation 2.1 is limited to solutions in which the ratio of the electrical to the thermal energy of the ions is very small, namely[2]:

$$\frac{ze_0\psi(r)}{kT} \ll 1 \tag{2.4}$$

As the potential decreases quite fast from the surface of the particle and in order the former Eq. 2.3 be valid in the neighbourhood of it we can consider the inequality on the particle surface, namely:

$$\frac{ze_0\psi(a)}{kT} = \frac{ze_0 Q}{4\pi\epsilon\epsilon_0 kT(1+\kappa a)a} \ll 1 \tag{2.5}$$

A good approximation is to consider the former equation equal to 10^{-1} and obtain an upper limit to the charge on the particle, Q_{up}, for a given value of a and κ. This value of Q_{up} will satisfy the condition given by Eq. 2.4 in the neighbourhood solution surrounding the particle, namely:

$$Q_{up} = 10^{-1}(ze_0)^{-1}4\pi\epsilon\epsilon_0 kT(1+\kappa a)a \tag{2.6}$$

Of course the actual charge on the particle has to fulfil the condition:

$$ze_0 \leq Q \leq Q_{up} \tag{2.7}$$

In Fig. 2.4 is represented Eq. 2.6 for some particle sizes and electrolyte valence.

In this way the following formulas are only valid preventing the validity of the inequality Eq. 2.5 or Eqs. 2.6 and 2.7.

At the distance of closest approach, $r = a$, then

$$\psi(a) = \frac{Q}{4\pi\epsilon\epsilon_0 a}\frac{1}{1+\kappa a} = \frac{Q}{4\pi\epsilon\epsilon_0 a} - \frac{Q}{4\pi\epsilon\epsilon_0}\frac{\kappa}{1+\kappa a} \tag{2.8}$$

The first term on the right-hand side of Eq. 2.8 is the potential ψ_i at the surface of the ion due solely to the charge on the ion itself. The second term is the portion ψ_a of the total potential that is due to the arrangement of the surrounding ions in the neighbourhood of the central ion and is called *potential of the ionic atmosphere*. The contribution of the cloud to the potential at the site of the central ion or particle can be written as

$$\psi_a(r) = \frac{Q}{4\pi\epsilon\epsilon_0 r}\left[\frac{e^{\kappa(a-r)}}{1+\kappa a} - 1\right] = \frac{-Q}{4\pi\epsilon\epsilon_0 \mathbf{x}} \tag{2.9}$$

[2]This condition comes to approximate $\sinh(ze_0\psi(r)/kT) \approx ze_0\psi(r)/kT$ in the Poisson–Boltzmann equation.

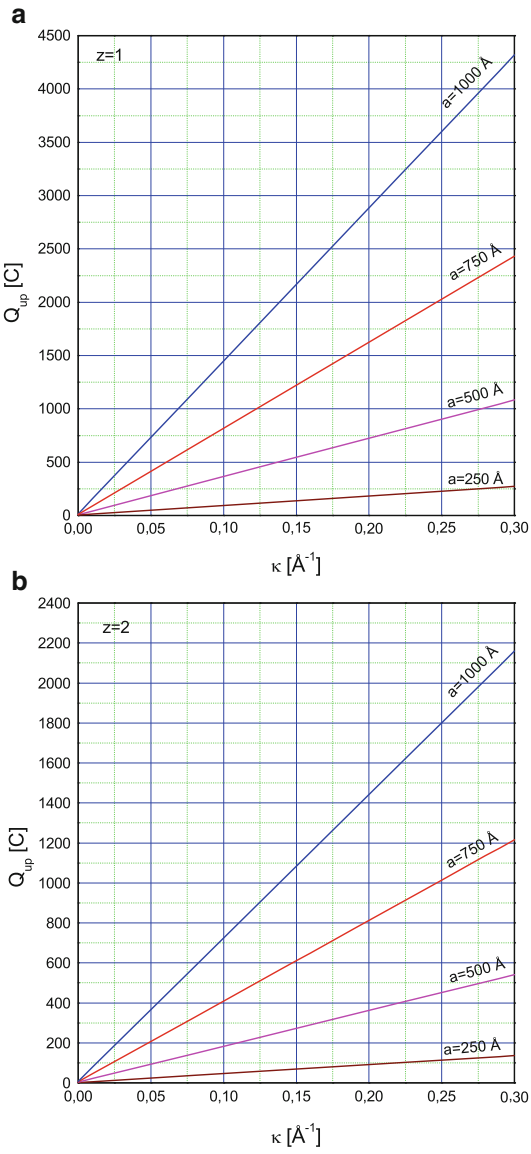

Fig. 2.4 Representation of Eq. 2.6: (**a**), (**b**) for mono and bivalent symmetrical electrolyte solution

with **x** given by:

$$\mathbf{x} = \frac{r(1+\kappa a)}{1+\kappa a - e^{\kappa(a-r)}} \tag{2.10}$$

Because of the spherical symmetry we have transformed the ionic atmosphere into a thin spherical shell with a charge $-Q$ placed at a distance **x** from the site of the

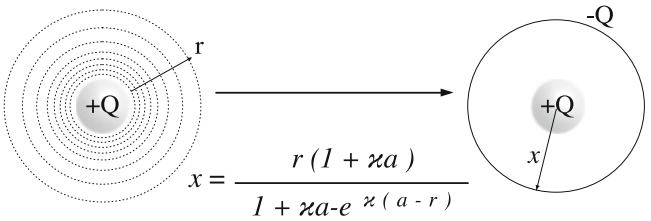

Fig. 2.5 Transformation of the central ion together with its ionic atmosphere into a capacitor

central ion, in this way the central particle or ion and the shell constitute a capacitor, see Fig. 2.5.

For calculating the capacitance we need to compute the difference of potential of the ionic atmosphere between the surface of the particle or ion, $\mathbf{x}(a)$ and $\mathbf{x}(r)$, namely:

$$\psi_a(a) - \psi_a(r) = \frac{-Q}{4\pi\epsilon\epsilon_0 r}\left[\frac{-1 + \kappa(r-a) + e^{\kappa(a-r)}}{1 + \kappa a}\right] \tag{2.11}$$

The corresponding capacitance will be

$$C(r) = \frac{-Q}{\psi_a(a) - \psi_a(r)} = \frac{4\pi\epsilon\epsilon_0 r(1 + \kappa a)}{-1 + \kappa(r-a) + e^{\kappa(a-r)}} \tag{2.12}$$

2.2 Calculation of the Electrical Mean Squares Fluctuations

In order to calculate the voltage thermal fluctuations, $< (\psi_a(r) - \psi_a(a))^2 >$, and its spectral distribution across two points of the solution, $[(\psi_a(r) - \psi_a(a))^2]_\omega$, we resemble the solution path between the two points as an $R(r)C(r)$ circuit in parallel ($R(r)$ is the solution electrical resistance at the distance r from the site of the central ion and $C(r)$ is the corresponding capacitance). The spectral density of the mean square of the fluctuational potential is: (see [16])

$$[(\psi_a(r) - \psi_a(a))^2]_\omega = \frac{2R(r)kT}{1 + [\omega R(r)C(r)]^2} \tag{2.13}$$

and the corresponding mean square of the fluctuating potential will be

$$< (\psi_a(r) - \psi_a(a))^2 >= \frac{1}{\pi}\int_0^\infty [(\psi_a(r) - \psi_a(a))^2]_\omega d\omega = \frac{kT}{C(r)} \tag{2.14}$$

For $\omega \ll \frac{2\pi}{\tau}$, with $\tau = RC$, the spectral density is practically independent of ω; thus, for relatively low frequencies, we have a 'white' spectrum and Eq. 2.13 transforms:

$$[(\psi_a(r) - \psi_a(a))^2]_\omega = 2R(r)kT \tag{2.15}$$

Consequently:

$$< (\psi_a(r) - \psi_a(a))^2 >= \frac{1}{\pi}\int_w^{w+\Delta\omega} 2R(r)kTd\omega = \frac{2}{\pi}R(r)kT\Delta\omega = 4R(r)kT\Delta f \tag{2.16}$$

Where $\omega = 2\pi f$, with f the frequency and the region corresponds to the 'white' noise. Equation 2.16 constitutes the so-called *Nyquist theorem*, [15].

Applying Eqs. 2.12 and 2.14 we get for the mean square of the fluctuating potential difference:

$$< (\psi_a(r) - \psi_a(a))^2 >= \frac{kT[-1 + \kappa(r-a) + e^{\kappa(a-r)}]}{4\pi\epsilon\epsilon_0 r(1+\kappa a)} \tag{2.17}$$

The mean square of the field averaged over the distance r, $< (E_r(r))^2 >=< (\psi_a(r) - \psi_a(a))^2 > r^{-2}$, (see [20] Eqs. (22) and (23)), namely:

$$< (E_r(r))^2 >=< (\vec{\nabla}_r\psi(r))^2 >= \frac{kT[-1 + \kappa(r-a) + e^{\kappa(a-r)}]}{4\pi\epsilon\epsilon_0 r^3(1+\kappa a)} \tag{2.18}$$

For long distances Eqs. 2.17 and 2.18 transform:

$$< (\psi_a(r) - \psi_a(a))^2 > = \frac{kT\kappa}{4\pi\epsilon\epsilon_0(1+\kappa a)} \tag{2.19}$$

$$< (E_r(r))^2 >=< (\vec{\nabla}_r\psi(r))^2 > = \frac{kT\kappa}{4\pi\epsilon\epsilon_0 r^2(1+\kappa a)} \tag{2.20}$$

For a solution of negligible ions size, we can consider $a = 0$ in the former Eqs. 2.17 and 2.18 giving:

$$< (\psi_a(r) - \psi_a(0))^2 >= \frac{kT(-1 + \kappa r + e^{-\kappa r})}{4\pi\epsilon\epsilon_0 r} \tag{2.21}$$

$$< (E_r(r))^2 >=< (\vec{\nabla}_r\psi(r))^2 >= \frac{kT(-1 + \kappa r + e^{-\kappa r})}{4\pi\epsilon\epsilon_0 r^3} \tag{2.22}$$

Equations 2.21 and 2.22 differ by a factor of 2 from those already given by Oosawa [11].

In case we have small potentials and a flat double layer Eq. 2.1 transforms into, see [20]:

$$\psi(r) = \psi_0 e^{-\kappa x} \tag{2.23}$$

It is well known from electrostatics:

$$\sigma = -\epsilon\epsilon_0 \frac{\partial \psi(r)}{\partial x} \mid_{x=0} \tag{2.24}$$

From Eqs. 2.23 and 2.24 we get

$$\psi(x) = \frac{Q}{\epsilon\epsilon_0 \kappa S} e^{-\kappa x} \tag{2.25}$$

The potential profile due solely to the charge on the surface is

$$\psi_s(x) = -\frac{Q}{\epsilon\epsilon_0 S} x \tag{2.26}$$

Then the potential of the ionic atmosphere will be

$$\psi_a(x) = \psi(x) - \psi_s(x) = \frac{Q}{\epsilon\epsilon_0 S}\left[\frac{e^{-\kappa x}}{\kappa} + x\right] \tag{2.27}$$

Correspondingly the capacitance formed by the surface and ionic atmosphere will be

$$C(x) = \frac{-Q}{\psi_a(0) - \psi_a(x)} = \frac{\epsilon\epsilon_0 S}{x\left[1 - \frac{1}{\kappa x}(1 - e^{-\kappa x})\right]} \tag{2.28}$$

Then from Eq. 2.14 we get for the mean square of the fluctuating potential:

$$< (\psi_a(x) - \psi_0(a))^2 >= \frac{kT}{\epsilon\epsilon_0 S} x\left[1 - \frac{1}{\kappa x}(1 - e^{-\kappa x})\right] \tag{2.29}$$

And for the mean square of the field averaged over the distance x, we have

$$< (E_x(x))^2 >=< (\vec{\nabla}_x \psi(x))^2 >= \frac{kT}{\epsilon\epsilon_0 S} \frac{1}{x}\left[1 - \frac{1}{\kappa x}(1 - e^{-\kappa x})\right] \tag{2.30}$$

Equations 2.29 and 2.30 coincide with those given by Oosawa [11].

For long distances we can consider the value of the bracket in Eqs. 2.29 and 2.30 equal to the unit.

2.3 Calculation of the Spectral Density Fluctuations

In order to calculate the spectral density of the mean square of the fluctuational potential difference using Eq. 2.13 we need to know the electrical resistance, $R(r)$, between the surface of the particle or ion and a point r inside the solution. Its relation with the capacitance of the equivalent electrostatic problem is (see, for instance, Reitz and Milford [17]):

$$R(r) = \frac{\epsilon\epsilon_0\rho}{C(r)} \tag{2.31}$$

with ρ being the solution electrical resistivity.

In Fig. 2.6 is represented $C(d)$ and $R(d)$, $(d = r - a)$, from Eqs. 2.12 and 2.31 for a 100 mM KCl solution.

Correspondingly the relaxation time, τ, of the electrical fluctuations will be given by:

$$\tau = \epsilon\epsilon_0\rho \tag{2.32}$$

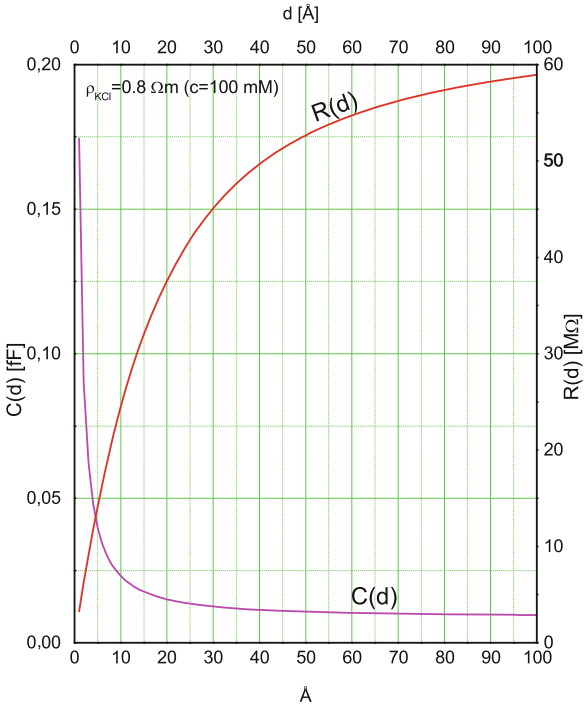

Fig. 2.6 Representation of Eqs. 2.12 and 2.33 for the resistance and capacitance of the solution as a function of the distance from the particle surface. $\rho_{KCl} = 0.8\,\Omega$m was calculated from Eq. A2.7 (see parameters on the figure)

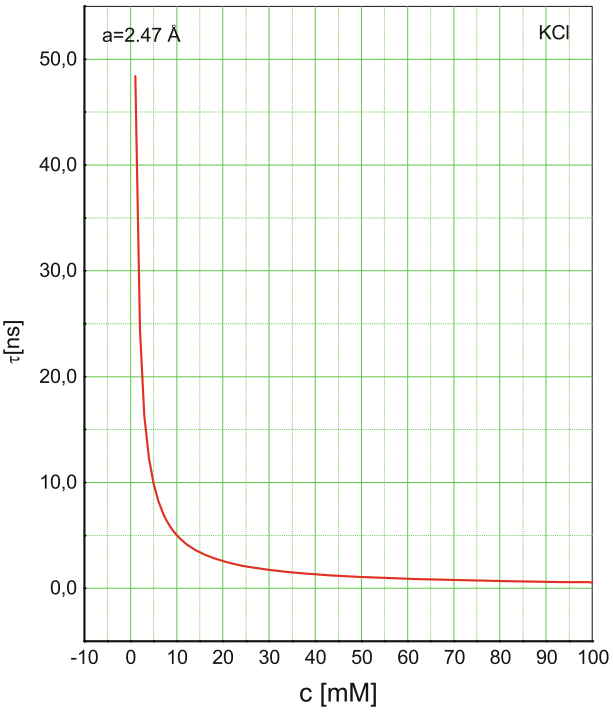

Fig. 2.7 Relaxation time of the fluctuations, τ, as a function of the concentration for a KCl solution, it was calculated using Eqs. 2.32 and A2.7

In Fig. 2.7 is represented τ as a function of concentration for a KCl solution, using Eq. A2.7 for ρ. We can observe a diminution of the relaxation time with concentration because to the corresponding diminution of the electrical resistivity.

From Eqs. 2.12 and 2.31 we get

$$R(r) = \rho \frac{-1 + \kappa(r-a) + e^{\kappa(a-r)}}{4\pi r(1+\kappa a)} \tag{2.33}$$

In case we have a flat double layer from (2.28) and (2.31) we have

$$R(x) = \frac{\rho}{S} x \left[1 - \frac{1}{\kappa x}(1 - e^{-\kappa x}) \right] \tag{2.34}$$

In case of lack of experimental data on ρ we can calculate it from Eq. A2.1 together with Eqs. A2.7 and A2.8, see Appendix.

From Eqs. 2.13, 2.31 and 2.33; we get for the spectral density of the mean square of the fluctuational potential:

$$[(\psi_a(r) - \psi_a(a))^2]_\omega = \frac{2kT\rho}{1 + (4\pi\epsilon\epsilon_0\omega\rho)^2} \frac{-1 + \kappa(r-a) + e^{\kappa(a-r)}}{r(1+\kappa a)} \tag{2.35}$$

Correspondingly the spectral density of the mean square of the fluctuational electric field will be given by:

$$[(E_r(r))^2]_\omega = \frac{2kT\rho}{1 + (4\pi\epsilon\epsilon_0\omega\rho)^2} \frac{-1 + \kappa(r-a) + e^{\kappa(a-r)}}{r^3(1+\kappa a)} \tag{2.36}$$

In Fig. 2.8a is shown the spectral density of the mean square of the fluctuational potential versus the radial frequency of the fluctuations for a KCl solution for given values of concentrations. We can observe a substantial diminution and broaden of the spectrum with increasing concentration with the corresponding diminution of the relaxation time of the fluctuations.

In Fig. 2.8b is shown the spectral density of the mean square of the fluctuational potential as a function of the particle size, we can observe an effect of electrical stabilization, diminution of the amplitude of the fluctuations, with increasing particle size.

2.4 Calculation of the Mean Squares Temporal Averages

We can characterize the time correlation of a physical quantity, $x(t)$, by the mean value of the product $< x(0)x(t) >$ which is related to the spectral resolution, $(x^2)_\omega$, by:

$$< x(0)x(t) >= \frac{1}{2\pi} \int_{-\infty}^{\infty} (x^2)_\omega e^{-i\omega t} d\omega \tag{2.37}$$

In particular, $< x(0)^2 >$ is the mean square of the fluctuating quantity:

$$< x(0)^2 >= \frac{1}{2\pi} \int_{-\infty}^{\infty} (x^2)_\omega d\omega \tag{2.38}$$

In order to compare the fluctuating quantity with the corresponding to a physical event elapsed in a time Δt it is necessary to know the mean square of the fluctuating quantity averaged in this time interval Δt, namely:

$$\overline{< x(0)x(t) >}^{t} = \frac{1}{\Delta t} \int_0^{\Delta t} < x(0)x(t) > dt \tag{2.39}$$

In our case $x \equiv \psi_a(r) - \psi_a(a)$ and from Eq. 2.13 $< x(0)^2 >= \frac{kT}{C(r)}$ and from Eqs. 2.13 and 2.31:

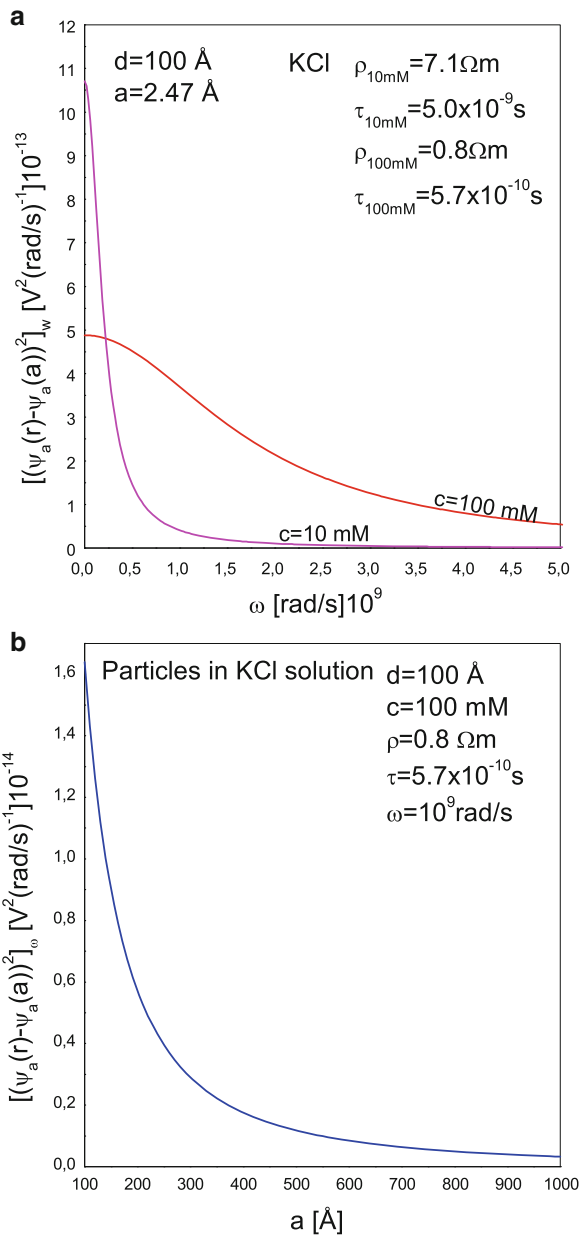

Fig. 2.8 (**a**) Spectral density of the mean square of the fluctuational potential as a function of the fluctuational frequency ω for a pure KCl solution (see parameters on the figure). (**b**) Ditto as a function of particle size

$$[(\psi_a(r) - \psi_a(a))^2]_\omega = \frac{kT}{C(r)} \frac{2}{\tau(\omega - \frac{i}{\tau})(\omega + \frac{i}{\tau})} \tag{2.40}$$

Then from Eqs. 2.35 and 2.38 and adapting the notation to our case, $< x(0)x(t) >=< (\psi_a(r) - \psi_a(a))^2 >$ (to condense notation), we have

$$< (\psi_a(r) - \psi_a(a))^2 >= \frac{kT}{C(r)\pi\tau} \int_{-\infty}^{\infty} \frac{e^{-i\omega t} d\omega}{(\omega - \frac{i}{\tau})(\omega + \frac{i}{\tau})} = \frac{kT}{C(r)} e^{-\frac{t}{\tau}} \tag{2.41}$$

Applying Eq. 2.37 to our case we have

$$\overline{< (\psi_a(r) - \psi_a(a))^2 >}^t = \frac{1}{\Delta t} \int_0^{\Delta t} <(\psi_a(r) - \psi_a(a))^2> dt = \frac{kT}{C(r)} \left[\frac{\tau}{\Delta t}\right] \left[1 - e^{-\frac{\Delta t}{\tau}}\right] \tag{2.42}$$

Analogously for the field fluctuations:

$$\overline{< (E_r(r))^2 >}^t = \frac{kT}{r^2 C(r)} \left[\frac{\tau}{\Delta t}\right] \left[1 - e^{-\frac{\Delta t}{\tau}}\right] \tag{2.43}$$

In Fig. 2.9a–d are shown voltage and field fluctuations as a function of the *Debye–Hückel reciprocal length*, κ^{-1}, for given values of particle sizes at a distance $d = 100\,\text{Å}$ from the particle surface. These figures have to be observed together with Fig. 2.3a and b which give κ^{-1} vs. c for mono and bivalent electrolytes.

Exam of Fig. 2.9 indicates that the fluctuations diminish as particle sizes increase, as a consequence large particles produce electrical stabilization in their neighbourhood.

Also can be observed that fluctuations are not quite sensitive to ionic concentrations for large particles.

Voltage fluctuations, for our range of κ^{-1}, (this range covers most of the current biological and physical chemistry systems) run from tenth of an mV to about 20 mV, with the corresponding field fluctuations spanning a range of $\mu\text{VÅ}^{-1}$–mVÅ^{-1}.

In Fig. 2.9e–h are also shown voltage and field fluctuations as a function of the distance d from the particle surface for different values of κ^{-1} and particle sizes. It can be observed the existence of substantial increase in voltage fluctuations with increasing d, specially for small particles, and up to a limiting value given by Eq. 2.19. Also, for these small particles it can be observed a maximum in the field fluctuations at a distance of the order of κ^{-1}. Also, here, the effect of electrical stabilization with increasing of particle size becomes apparent.

In Fig. 2.10a–d are plotted voltage and field fluctuations for the two extreme cases: (1) an ionic solution of punctual or small ions (Fig. 2.10a, b) and (2) two plates of area $S = 1\,\text{cm}^2$ and separation x immersed in an ionic solution of punctual ions (Fig. 2.10c and d). In case (1) voltage fluctuations remain between 1 and 20 mV converging to the limiting value given by Eq. 2.19 for long distances; the corresponding field fluctuations stay in the range of a few mVÅ^{-1} decreasing with distance.

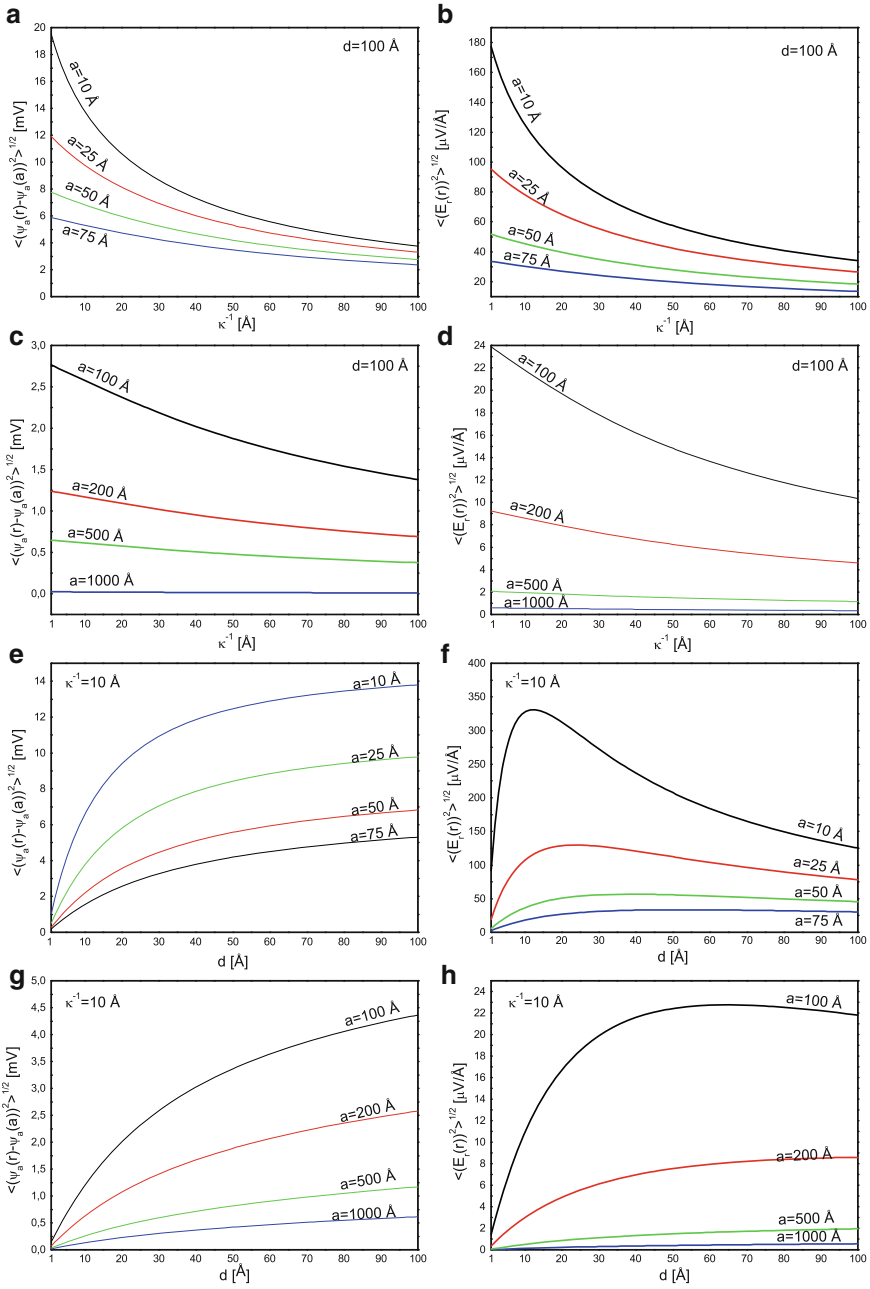

Fig. 2.9 Voltage and field fluctuations as a function of κ^{-1} and the distance d from the particle surface

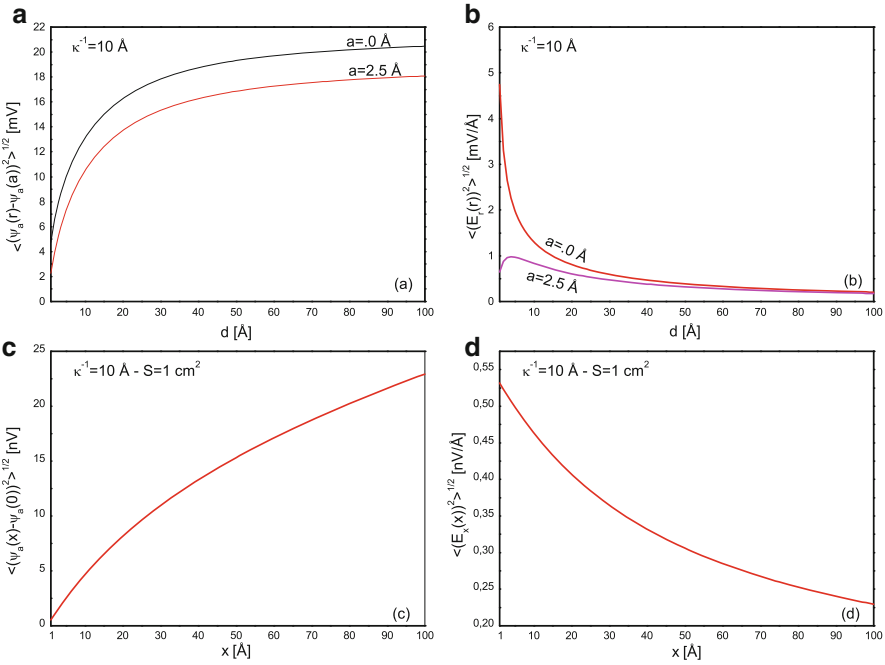

Fig. 2.10 Voltage and field fluctuations: (**a**), (**b**) Ionic solution of pointlike ions. (**c**), (**d**) Two plates of area $S = 1\,\text{cm}^2$ and separation x immersed in an ionic solution of pointlike ions

In case (2) voltage fluctuations increase with distance and are in the two digits nV range. Corresponding electric field fluctuations decrease with distance are in the tenth of $\text{nV}\text{Å}^{-1}$ range.

We have developed a simple method to estimate the electrical fluctuations in colloids and ionic solutions. The steps to perform in order to determine these fluctuations can be summarized as follows:

1. Identification of the molecular–ionic capacitor of the system. The capacitance is given by:

$$C(r) = \left| \frac{Q}{\psi_a(r) - \psi_a(a)} \right|, \tag{i}$$

with Q the charge on the particle or molecule and $\psi_a(r)$ the *potential of the ionic atmosphere*, a the distance from the centre to the surface of the particle or molecule and r the distance from the centre to a point inside the surrounding solution.

2. Estimation of the resistance $R(r)$ or the electrical resistivity ρ of the path associated with the capacitance (electrical path), then the relaxation time, τ, is

$$\tau = R(r)C(r) = \epsilon\epsilon_0\rho, \tag{ii}$$

3. The voltage and field mean square fluctuations are given by:

$$\begin{aligned} &< (\psi_a(r) - \psi_a(a))^2 >= \frac{kT}{C(r)}, \\ &< (E_r(r))^2 >= \frac{< (\psi_a(r) - \psi_a(a))^2 >}{r^2}, \end{aligned} \tag{iii}$$

4. The spectral density of the mean square of the fluctuational potential and field is given by:

$$\begin{aligned} &[(\psi_a(r) - \psi_a(a))^2]_\omega = \frac{2R(r)kT}{1 + [\omega\tau]^2}, \\ &[(E_r(r))^2]_\omega = \frac{[(\psi_a(r) - \psi_a(a))^2]_\omega}{r^2}, \end{aligned} \tag{iv}$$

5. The mean square of the fluctuational potential and field averaged in a time, Δt, is given by:

$$\begin{aligned} &\overline{< (\psi_a(r) - \psi_a(a))^2 >}^t = \frac{kT}{C(r)}\left[\frac{\tau}{\Delta t}\right]\left[1 - e^{-\frac{\Delta t}{\tau}}\right], \\ &\overline{< (E_r(r))^2 >}^t = \frac{\overline{< (\psi_a(r) - \psi_a(a))^2 >}^t}{r^2}, \end{aligned} \tag{v}$$

Voltage fluctuations at a molecular scale cannot be measured due both to unavailability of microscopic probes and to response limitation of measuring electronics. Measurement of these fluctuating voltages is also inherently elusive due to the thermal noise of electronic apparatuses. Molecular systems, on the other hand, are sufficiently small and fast as to both sense and respond to local fluctuating electrical fields (Lauger [7], Hille [6]) or for an efficient processing of information in the form of fast conformational changes [3]. In order to explain any possible mechanism at molecular level, which involves an electric process, this fluctuations have to be considered.

The above described fluctuations are one of the factors that cause the dielectric increment $\Delta\epsilon$ of polyelectrolyte solutions; Oosawa [12] related the field fluctuations to $\Delta\epsilon$ having obtained a good agreement with the experimental data of Takashima [19].

Fluctuations with very long relaxation times appear in or around particles. The lowest relaxation time of fluctuations in counterion density around a long rod-like polyelectrolyte was found to be in the range of 10^{-3}–10^{-4} s (Oosawa [13], Takashima [19], Mandel [9]).

We suggest the application of the present formalism to the determination of the field fluctuations in long rod-like polyelectrolyte solutions in order to estimate the dielectric increment, $\Delta\epsilon$, and compare with the existent experimental data on this kind of systems.

Appendix:Theoretical Calculation of the Electrical Resistivity

When we have highly charged particles or polyelectrolytes immersed in a symmetrical electrolyte solution, another path of electric conduction can be open through this particles or polyelectrolytes and the electrical conductivity $\sigma = \rho^{-1}$ of the solution can be written as:

$$\rho^{-1} = {\rho_i}^{-1} + {\rho_p}^{-1} \tag{A2.1}$$

where ρ_i and ρ_p are the contributions to the total electrical resistivity of the ions and particles, respectively. The relation between the electrical resistivity, ρ_i, and the equivalent conductance Λ is given by:

$$\rho_i = \frac{N_A}{nz\Lambda} \tag{A2.2}$$

According to Debye and Hückel [2] and Onsager [10] interionic attractions and repulsions lead to two *effects* both of which result in the lowering of the equivalent conductance with increasing ion concentrations, correspondingly it can be decomposed into three terms (see [1] for a good treatise on this subject):

$$\Lambda = \Lambda_0 - \Lambda_e - \Lambda_\tau \tag{A2.3}$$

where Λ_0 is the equivalent conductance at infinite dilution, and is given by:

$$\Lambda_0 = \frac{z{e_0}^2 N_A}{kT}({D_0}^+ + {D_0}^-) \tag{A2.4}$$

where ${D_0}^\pm$ are the diffusion constants.

Λ_e is the contribution of the *electrophoretic effect* and tends to diminish Λ_0, is given by:

$$\Lambda_e = \frac{2z{e_0}^2 \kappa N_A}{6\pi\eta(1+\kappa a_i)} \tag{A2.5}$$

where η is the viscosity of the solution and a_i is the mean ions radius.

Λ_τ is called the *time of relaxation effect* and is the other mechanism tending to decrease the equivalent conductance, namely:

$$\Lambda_\tau = \frac{(e_0 z)^2 \kappa}{24\pi\epsilon\epsilon_0 kT} \frac{\sqrt{2}}{1+\sqrt{2}} \Lambda_0 \tag{A2.6}$$

From Eqs. A2.2–A2.6, we get for the ions electrical resistivity:

$$\rho_i = \frac{1}{n(ze_0)^2 \left[\left[1 - \frac{(ze_0)^2 \kappa}{24\pi\epsilon\epsilon_0 kT} \frac{\sqrt{2}}{1+\sqrt{2}} \right] \frac{(D_0{}^+ + D_0{}^-)}{kT} - \frac{\kappa}{3\pi\eta(1+\kappa a_i)} \right]} \tag{A2.7}$$

In Fig. 2.11 is represented Eq. A2.7 for a KCl solution as a function of concentration.

The electrical resistivity corresponding to the particles, ρ_p, is given by:

$$\rho_p = \frac{6\pi\eta a_p (1+\kappa a_p)}{n_p Q^2 (1 + \frac{K_s \rho_i}{a_p}) f(\kappa a_p)} \tag{A2.8}$$

where n_p is the number of particles per m^3, Q is the net charge on the particle, a_p the radius of the particle and $f(\kappa a_p)$ is called Henry's function [4]; it varies between

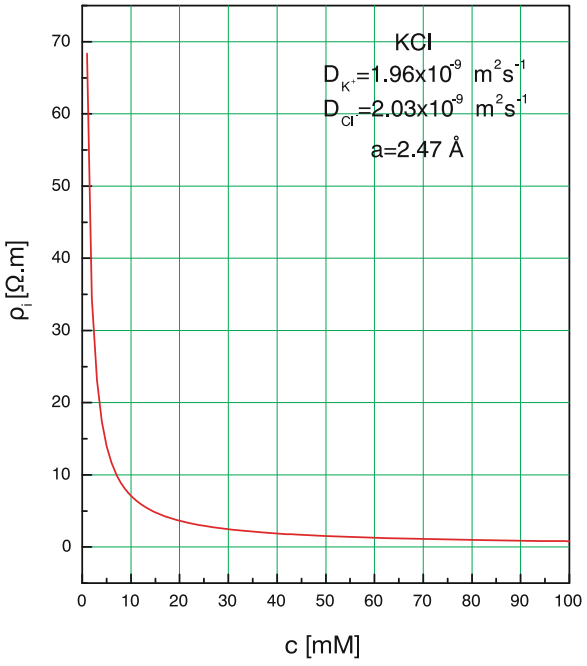

Fig. 2.11 Representation of Eq. A2.7 for ρ_i as a function of concentration for a KCl solution (Eq. 2.3 for κ was also used)

1.0 and 1.5 as κa_p goes from zero to infinity and K_s is the surface conductance of the particle.

In deriving Eq. A2.8 we have used the relation between the current density J (A/m^2) and the external applied field E, namely:

$$J = n_p Q v = \frac{1}{\rho_p} E \tag{A2.9}$$

where v is the velocity of the particles and is given by Henry's equation , Henry [4]:

$$v = \frac{\xi 4\pi\epsilon\epsilon_0}{6\pi\eta} f(\kappa a_p) E \tag{A2.10}$$

where the ξ potential is given by:

$$\xi = \frac{Q}{4\pi\epsilon\epsilon_0 a_p} \frac{1}{1 + \kappa a_p} \tag{A2.11}$$

Henry [5] introduced a correction for the surface conductance, K_s, considering that the mobility of the particle would be reduced on account of the distortion of the spherical symmetry of the electrical double layer, *relaxation effect*. Also, the applied field would be modified in the vicinity of the particle by the electrical conductivity of the double layer.

$$\xi_{\text{corr}} = \xi\left(1 + \frac{K_s \rho_i}{a_p}\right) \tag{A2.12}$$

The surface conductance of the particle can be evaluated using equations due to Street [18]. The relaxation effect may be neglected when (a) the values for ξ potential are far below 25 mV and (b) values for κa_p are small (less than 1) or when $\kappa a_p \gg 1$ (Overbeek [14]).

References

1. Bockris, J.O'M., Reddy, A.K.N.: Modern Electrochemistry, vol. V1, p. 420. Plenum Press, New York (1977)
2. Debye, P., Hückel, E.: On the theory of electrolytes, Z. Phys. **24**, 185, 305 (1923)
3. Fornés, J.A.: Information flow to dissipate an ionic fluctuation through a membrane channel. J. Colloid Interface Sci. **177**, 411 (1996)
4. Henry, D.C.: The cataphoresis of suspended particles. Part I. The equation of cataphoresis. Proc. R. Soc. A. **133**, 106 (1931)
5. Henry, D.C.: The electrophoresis of suspended particles. IV. The surface conductivity effect. Trans. Soc. **44**, 1021 (1948)
6. Hille, B.: Ionic Channels of Excitable Membranes. Sinauer Associates, Inc. Publishers, Sunderland (1992)

7. Lauger, P.: Dynamics of ion transport systems in membranes. Physiol. Rev. **67**, 1296–1331 (1987)
8. Lewis, G.N., Randall, M.: The activity coefficient of strong electrolytes. J. Am. Chem. Soc. **43**, 1112–1154 (1921)
9. Mandel, M.: The electric polarization of rod-like, charged macromolecules. Mol. Phys. **4**, 489 (1961)
10. Onsager, L.: The theory of electrolytes (II). Physik. Z. **28**, 277–298 (1927)
11. Oosawa, F.: Field fluctuation in ionic solutions and its biological significance. J. Theor. Biol. **39**, 373–386 (1973)
12. Oosawa, F.: Counterion fluctuation and dielectric dispersion in linear polyelectrolytes. Biopolymers **9**, 677 (1970)
13. Oosawa, F.: Polyelectrolytes, Chap. 5. Marcel Dekker, New York (1971)
14. Overbeek, J.T.G.: In: Kruyt, H.R. (ed.) Colloid Science, vol. V1, p. 194. Elsevier, Amsterdam (1952)
15. Pathria, R.K.: Statistical Mechanics, p. 474. Pergamon Press, Oxford (1988) [Eq. (31)]
16. Procopio, J., Fornés, J.A.: Fluctuation-dissipation theorem imposes high-voltage fluctuations in biological ionic channels. Phys. Rev. E **51**, 829–831 (1995)
17. Reitz, J.R., Milford, F.J.: Foundations of Electromagnetic Theory, p. 139. Addison-Wesley, Menlo Park (1967) [Eq. (7–34)]
18. Street, N.: Surface conductance of kaolinite. Aust. J. Chem. **9**, 333 (1956)
19. Takashima, S.: Dielectric dispersion of deoxyribonucleic acid. II[1] J. Phys. Chem. Ithaca **70**, 1372 (1966)
20. Verwey, E.J.W., Overbeek, J.Th.G.: "Theory of the Stability of Lyophobic Colloids", p. 38. Elsevier, New York (1948)

Chapter 3
Electrical Fluctuations Around a Charged Colloidal Cylinder in an Electrolyte

Abstract In Chap. 2 we developed a method to determine the natural electrical thermal fluctuations and their spectral distribution across two points in the neighbourhood of a spherical electrically charged particles immersed in an ionic solution. The essence of the method is to consider the charged sphere with its surrounding ionic atmosphere as a capacitor and a resistor in parallel.

In this chapter we apply this method to estimate the electrical fluctuations (field and potential) around rod-like rigid polyelectrolyte bearing a uniform surface charge distribution dispersed in an aqueous salt solution of pointlike ions. We performed computer simulations to solve the Poisson–Boltzmann (P-B) equation and also developed formulas to calculate the fluctuations in the case of a low potential, Debye–Hückel approximation (linearized P-B equation). We apply the formalism to a DNA solution which is a well-known model for a biopolymer. They are shown plots of the potential and electric field fluctuations as a function of the Debye–Hückel length, κ^{-1}, and distance, d, from the polyelectrolyte surface for several molecular sizes.

Keywords Electrical fluctuations • Cylindrical polyelectrolytes

3.1 Electrical Fluctuations Perpendicular to the Polyelectrolyte Axis

We consider a rigid rod-like molecule or particle of radius a, (see Fig. 3.1) (for an excellent bibliography on this subject, see [5]), length $L \gg a$, so that end effects may be neglected, with a charge Q distributed uniformly over the surface with an electrical surface potential ψ_0 immersed in a solution of pointlike ions of a symmetrical electrolyte of valence z with n ions per m^3.

Part of this chapter was reprinted with permission from [José A. Fornés, Phys. Rev. E **57,2**, 2104, (1998)] Copyright (1998) by the American Physical Society.

J.A. Fornés, *Electrical Fluctuations in Polyelectrolytes*, SpringerBriefs in Molecular Science, DOI 10.1007/978-3-319-33840-8_3

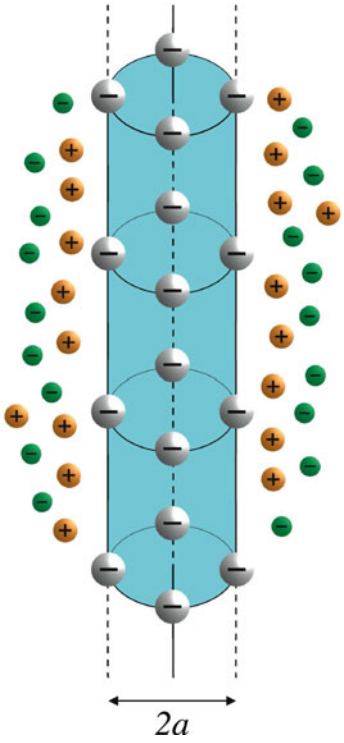

Fig. 3.1 Representation of a rigid rod-like polyelectrolyte

The law governing the potential profile and consequently the ionic distribution ('diffuse' layer) from the surface of the particle is given by the PB equation[1]

$$\triangle \psi = \frac{2ze_0 n}{\epsilon\epsilon_0} \sinh\left(\frac{ze_0\psi}{kT}\right) \tag{3.1}$$

where $\triangle$ is, in our case of cylinder symmetry, the radial part of the Laplace operator. Equation 3.1 can be written, following Stigter [4], as:

$$\frac{1}{x}\frac{d}{dx}\left(x\frac{dy}{dx}\right) = \sinh(y) \tag{3.2}$$

where $y = ze_0\psi/kT$ and $x = \kappa r$ are the dimensionless potential and distance, respectively, r being the distance from the cylinder axis, perpendicular to the surface. At the surface of the cylinder $x = x_0 = \kappa a$ and $y = y_0 = ze_0\psi_0/kT$.

[1]The origin of this equation is the Poisson equation: $\Delta\psi = -\frac{\rho}{\epsilon\epsilon_0}$ with $\rho = ze_0(n_+ - n_-) = nze_0(\exp(-\frac{ze_0\psi}{kT}) - \exp(\frac{ze_0\psi}{kT})) = -2nze_0 \sinh(\frac{ze_0\psi}{kT})$, with n_+ and n_- being the *average* concentration of the ions.

In case the ratio of the electrical to the thermal energy of the ions is very small, namely[2]:

$$\frac{ze_0\psi(r)}{kT} \ll 1, \qquad y \ll 1 \tag{3.3}$$

Equation 3.2 transforms, $\sinh(y) = y$, into the modified Bessel equation of zeroth order, with the boundary conditions $(x, y) = (\infty, 0)$ and

$$\left(\frac{dy}{dx}\right)_{x_0} = -\left(\frac{\sigma}{\epsilon\epsilon_0}\right)\left(\frac{ze_0}{kT\kappa}\right) = -\frac{Qze_0}{2\pi x_0 L\epsilon\epsilon_0 kT} \tag{3.4}$$

This last condition comes from Gauss's electric flux theorem with the surface charge density $\sigma = Q/(2\pi aL)$. The analytic solution (Debye–Hückel approximation) satisfying the former boundary conditions is

$$y = y^{(DH)} = \left(\frac{ze_0}{kT}\right)\frac{Q}{2\pi L\epsilon\epsilon_0 x_0 K_1(x_0)}K_0(x) \tag{3.5}$$

The corresponding derivative function is

$$\frac{dy^{(DH)}}{dx} = -\left(\frac{ze_0}{kT}\right)\frac{Q}{2\pi L\epsilon\epsilon_0 x_0 K_1(x_0)}K_1(x) \tag{3.6}$$

In the former equations $K_0(x)$ and $K_1(x)$ are the modified Bessel functions of zeroth and first order, respectively. For $y \to 0$, Eq. 3.5 is an exact solution of Eq. 3.2.

It is necessary to formulate a few definitions in order to put the equations into the current nomenclature of polyelectrolyte science, namely:

$$\lambda = \frac{Q}{L} = \frac{e_0}{b} = \left(\frac{e_0}{l_B}\right)\xi_0 \tag{3.7}$$

where λ is the linear charge density, $b = L/N$ is the linear charge spacing and N is the number of charged polymer groups. The *Bjerrum length* l_B is the distance at which the coulombic energy is equal to kT ($l_B = 7.13$ Å at 25 °C in water) (for an excellent english reference on this subject, see [1]), namely:

$$l_B = \frac{{e_0}^2}{4\pi\epsilon\epsilon_0 kT} = \xi_0 b \tag{3.8}$$

The dimensionless ratio, ξ_0, which is a reduced linear charge density is particularly useful (a DNA molecule, for instance, has two phosphate charges each at a helical

[2]This condition comes to approximate $\sinh(ze_0\psi(r)/kT) \approx ze_0\psi(r)/kT$ in the Poisson–Boltzmann equation.

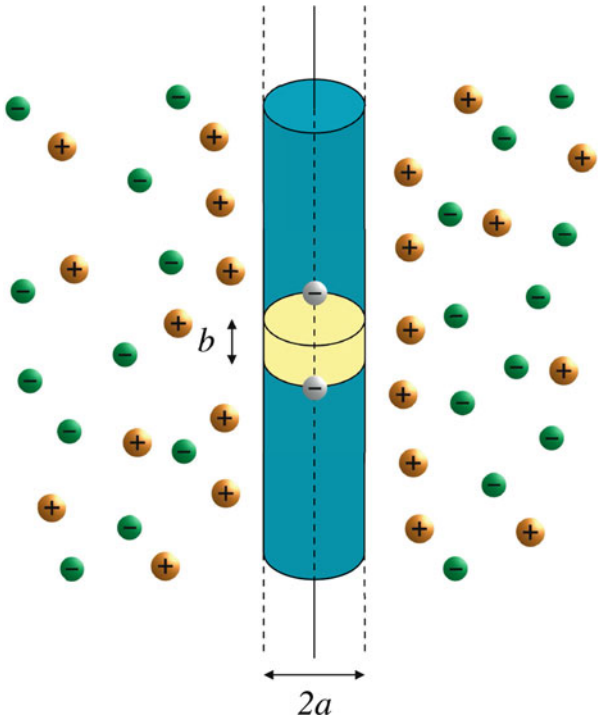

Fig. 3.2 Representation of B-DNA molecule

spacing of 3.37 Å, then $\xi_0 = l_B/b = 7.13 \times (2/3.37) = 4.23$) (see Fig 3.2). As a consequence the surface charge density can be written as:

$$\sigma = \frac{\lambda}{2\pi a} = \left(\frac{e_0}{2\pi a l_B}\right)\xi_0 \tag{3.9}$$

For B-DNA, $a = 12.5$ Å, Eq. 3.11 gives $\sigma = 7.55 \times 10^{17}$ electric charges m^{-2}, which is 28 times less than that for a bidimensional array of Cu atoms. Also the *Debye–Hückel reciprocal length* parameter, κ, (cf, Eq. 2.2, Chap. 2) can be written as:

$$\kappa^2 = 8\pi z^2 l_B n = 8\pi z^2 l_B N_A c 10^3 \tag{3.10}$$

Applying the former definitions Eqs. 3.4–3.6 transform in:

$$\left(\frac{dy}{dx}\right)_{x_0} = -\frac{2z\xi_0}{x_0} \tag{3.11}$$

$$y = y^{(DH)} = \frac{2z\xi_0}{x_0 K_1(x_0)} K_0(x) \tag{3.12}$$

$$\frac{dy^{(DH)}}{dx} = -\frac{2z\xi_0}{x_0 K_1(x_0)} K_1(x) = -y^{(DH)} \frac{K_1(x)}{K_0(x)} \tag{3.13}$$

As the potential decreases quite fast from the surface of the particle and in order for the former Eq. 3.3 be valid in the neighbourhood of it we can consider the inequality on the particle surface, namely:

$$y(x_0) = \frac{2z\xi_0}{x_0 K_1(x_0)} K_0(x_0) \ll 1 \tag{3.14}$$

In general in a polyelectrolyte the real charge is lessened by a factor α because of the presence of counterions within the defining surface of the cylinder, correspondingly in the former equations ξ_0 has to be replaced by $\xi = \alpha \times \xi_0$. Setting the former equation equal to 10^{-1} upper limits for ξ and λ, ξ_{up} and λ_{up}, for given values of a and κ, can be derived. The values ξ_{up} and λ_{up} will satisfy the condition given by Eq. 3.3 in the neighbourhood solution surrounding the particle, namely:

$$\xi_{up} = 10^{-1} \frac{x_0 K_1(x_0)}{2z K_0(x_0)} \tag{3.15}$$

And the condition for the linear charge density, λ, on the particle surface:

$$\lambda_{up} = \left(\frac{e_0}{l_B}\right) \xi_{up} \tag{3.16}$$

Figure 3.3 shows ξ_{up} and λ_{up} as a function of the Debye length for $z = 1$ and $z = 2$ and different particle sizes.

Numerical integration of Eq. 3.2 is obtained by Runge–Kutta method in which Eq. 3.2 is transformed in a system of coupled first order ordinary differential equations, namely:

$$\begin{aligned} \frac{dy_1}{dx} &= y_2, \\ \frac{dy_2}{dx} &= \sinh(y_1) - \frac{y_2}{x} \end{aligned} \tag{3.17}$$

with $y_1 = y$.

Stigter [3, 4] gives the solution of Eq. 3.2 in terms of a correction factor of an analytical expression derived with the help of the Debye–Hückel approximation.

As the set of Eq. 3.17 represents a second order nonlinear differential equation we used an adaptive stepsize control subroutine, odeint, from Numerical Recipes, [2], joining the main program with subroutines: derivs, odeint, rkqs, rkck, bessi0,

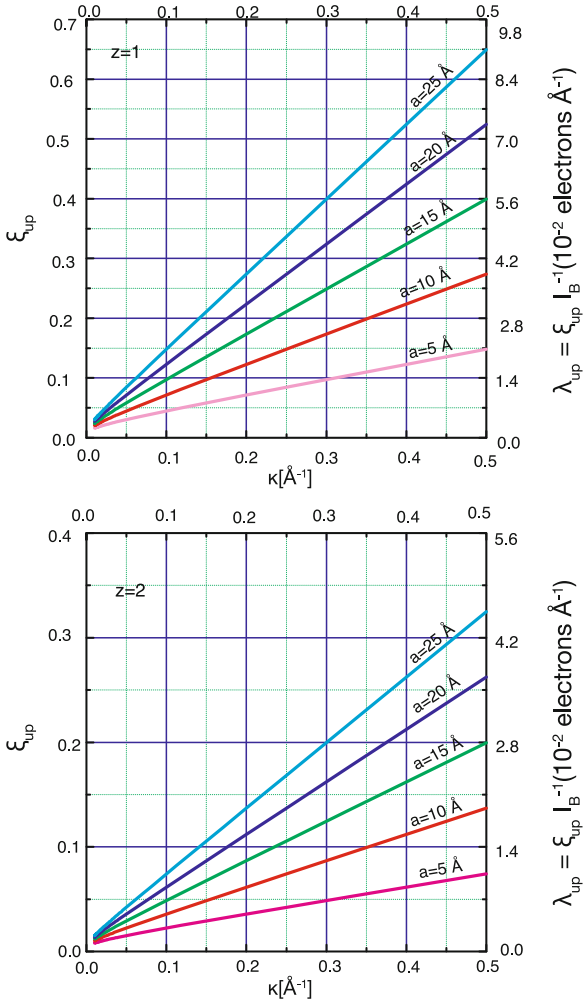

Fig. 3.3 Representation of Eqs. 3.15 and 3.16 for mono and bivalent symmetrical electrolyte solution

bessi1, bessk0, bessk1. We start the integration at low potentials, where Eqs. 3.12 and 3.13 are valid, then the initial conditions for the set of Eqs. 3.17 are

$$(y_1, y_2) = \left(y^{DH}(x_1), -y^{DH}(x_1) \frac{K_1(x_1)}{K_0(x_1)} \right) \tag{3.18}$$

We integrate, as usual, backward, $x_1 \rightarrow x_0$.

In Fig. 3.4 is shown an application of this procedure to obtain the potential profile of DNA immersed in a 100 mM solution of a symmetrical monovalent electrolyte.

The steps of the procedure to calculate the electrical fluctuations in molecular or colloid solutions see (cf. Eqs. To i–v, Chap. 2).

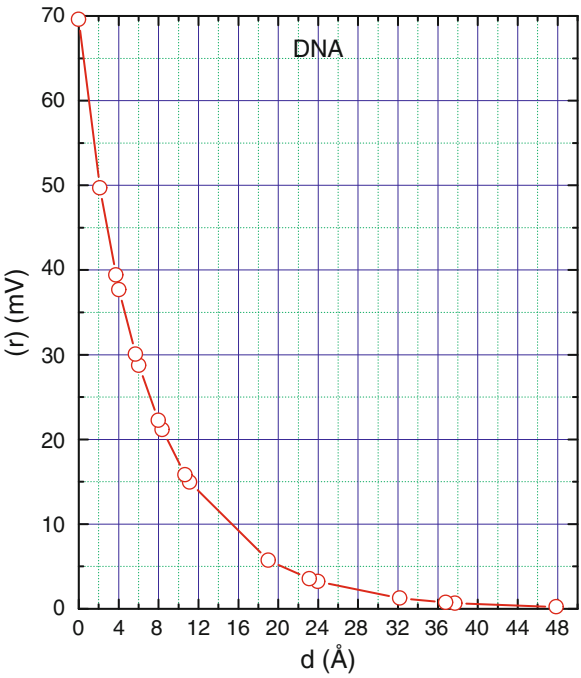

Fig. 3.4 Potential profile (Runge–Kutta solution) for DNA ($\xi_0 = 4.24$, $\alpha = 0.5$, $a = 12.5$ Å, $x_0 = 1.298$, $y_0 = 2.693$) immersed in 100 mM (1-1) electrolyte. d is the distance from the DNA surface

The *potential of the ionic atmosphere*, $\psi_a(r)$, is the contribution of the cloud to the potential at the site of the central ion or particle. It can be written as:

$$\psi_a(r) = \psi(r) - \psi_{\text{bare}}(r) \tag{3.19}$$

where $\psi_{\text{bare}}(r)$ is the potential of the polyion or particle due solely to the charge on the particle itself (without the solution).

Correspondingly for the dimensionless potential, we have

$$y_a(x) = y(x) - y_{\text{bare}}(x) \tag{3.20}$$

In our case of a rod-like polyelectrolyte $\psi_{\text{bare}}(r)$ is given by:

$$\begin{aligned}\psi_{\text{bare}}(r) &= \psi_{\text{bare}}(a) + \frac{1}{2\pi\epsilon\epsilon_0}\frac{Q}{L}\ln\left(\frac{a}{r}\right) \\ &= \psi_{\text{bare}}(a) + \frac{2kT}{e_0}\xi\ln\left(\frac{a}{r}\right)\end{aligned} \tag{3.21}$$

correspondingly

$$y_{\text{bare}}(x) = y_{\text{bare}}(x_0) + 2z\xi\ln\left(\frac{x_0}{x}\right) \tag{3.22}$$

In case of using the Debye–Hückel approximation, from Eqs. 3.12, 3.20 and 3.22 we obtain

$$y_a^{(DH)}(x) = 2z\xi \left[\frac{K_0(x)}{x_0 K_1(x_0)} - y_{\text{bare}}(x_0) - \ln\left(\frac{x_0}{x}\right) \right] \tag{3.23}$$

From Eqs. 4.4 and 3.23, the capacitance of the ionic–molecular capacitor will be given by:

$$C(x) = 2\pi L \epsilon \epsilon_0 \left[\frac{K_0(x) - K_0(x_0)}{x_0 K_1(x_0)} + \ln\left(\frac{x}{x_0}\right) \right]^{-1} \tag{3.24}$$

The corresponding fluctuating magnitudes can be calculated substituting this expression for $C(x)$ in the corresponding Eqs. (cf. Eqs. i–v, Chap. 2)

In case the Debye Hückel approximation is not valid, we can consider the following equation obtained from Eqs. 3.4, 3.11, 4.4, 3.20 and 3.22, ready for computational calculation:

$$C(x) = 2\pi L \epsilon \epsilon_0 \left[\frac{y(x_0) - y(x)}{2z\xi} + \ln\left(\frac{x}{x_0}\right) \right]^{-1} \tag{3.25}$$

In Figs. 3.5 and 3.6 are represented Eqs. iii and iv from Chap. 2, respectively, for DNA immersed in 100 mM NaCl solution.

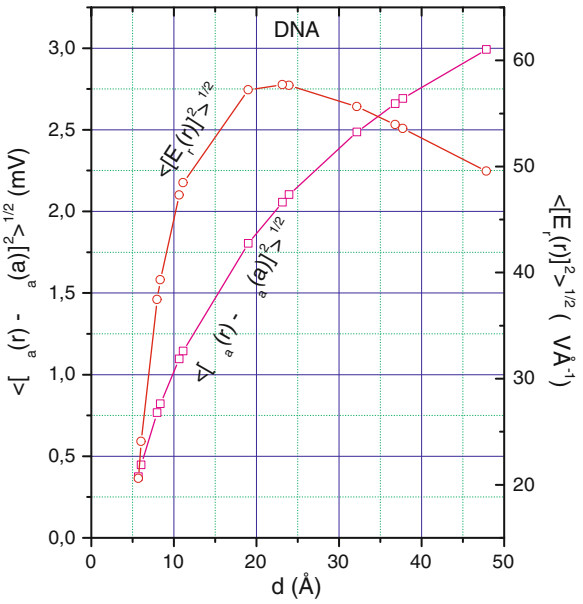

Fig. 3.5 Voltage and field fluctuations (Runge–Kutta solution) for DNA ($\xi_0 = 4.24$, $\alpha = 0.5$, $L = 10^3$ Å, $a = 12.5$ Å) immersed in 100 mM (1-1) electrolyte. d is the distance from the DNA surface

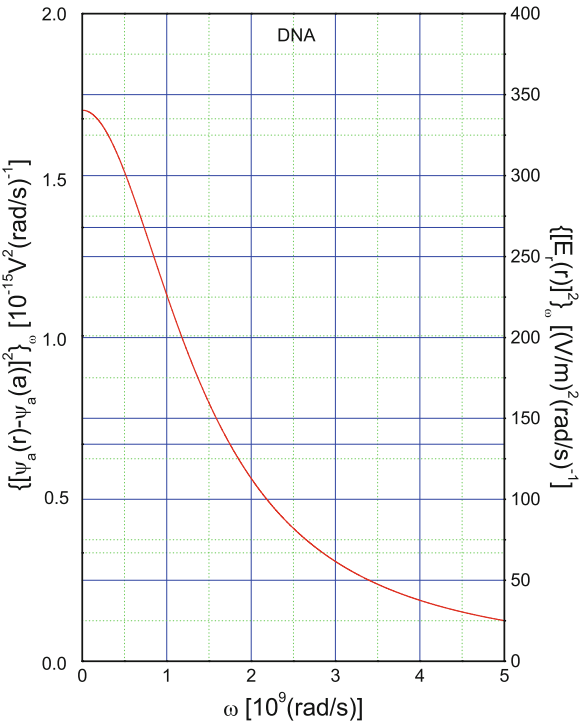

Fig. 3.6 Spectral density (Runge–Kutta solution) of the mean square of the fluctuational potential and field as a function of the fluctuational frequency ω for DNA: $L = 10^3$ Å, $a = 12.5$ Å, $c = 100$ mM NaCl, $\rho_{NaCl} = 1.0\,\Omega$m, $\tau = 7.1 \times 10^{-10}$ s, $r = \kappa^{-1} = 9.73$ Å, $C(\kappa^{-1}) = 3.45 \times 10^{-15}$ F

In Fig. 3.7 is represented the resistance and capacitance (from Eqs. 4.6 and 3.25 in the neighbourhood of a DNA molecule in the same solution.

Figure 3.8a and b shows the voltage and field fluctuations as a function of the *Debye–Hückel length*, κ^{-1}, for given values of particle sizes at a distance $d = 25$ Å from the polyelectrolyte surface. It is interesting to observe these figures together with Fig. 2.3a and b of Chap. 2, which gives κ^{-1} vs. the concentration for mono and bivalent electrolytes.

Examination of Fig. 3.8 indicates that the fluctuations diminish as particle sizes increase, as a consequence large particles produce electrical stabilization in their neighbourhood.

It can also be observed that fluctuations are not quite sensitive to ionic concentrations for large particles. Voltage fluctuations, for our range of κ^{-1}, (this range covers most of the current biological and physical chemistry systems) run from 1 to 12 mV, with the corresponding field fluctuations spanning a range of 10–400 μVÅ^{-1}.

Figure 3.8c–e furthermore shows voltage and field fluctuations as a function of the distance d from the particle surface for a given value of κ^{-1} (10 Å) and particle sizes. It can be observed that voltage fluctuations increase substantially with increasing d, especially for small particles. A maximum of the field fluctuations occurs at a distance of the order of κ^{-1}. The effect of electrical stabilization with increasing of particle size also becomes apparent here. Figure 3.5 also shows a maximum of the field fluctuations.

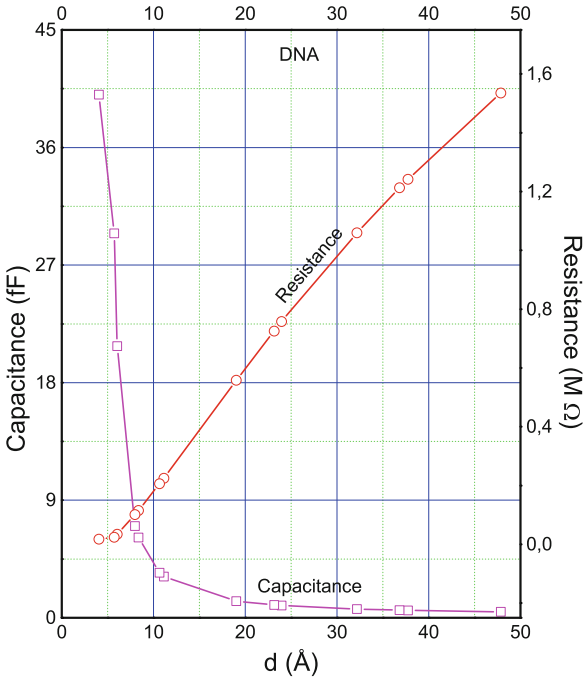

Fig. 3.7 Resistance and capacitance of the solution as a function of the distance d from the DNA surface (Runge–Kutta solution): $L = 10^3$ Å, $a = 12.5$ Å, c = 100mM NaCl, $\rho_{\mathrm{NaCl}} = 1.0\ \Omega$m, $\tau = 7.1 \times 10^{-10}$ s, $r = \kappa^{-1} = 9.73$ Å

References

1. Bockris, J.O'M., Reddy, A.K.N.: Modern Electrochemistry, vol. V1, p. 251. Plenum Press, New York (1977)
2. Press, W.H., Flannery, B.P., Teukolsky, S.A., Vetterling, W.T.: Numerical Recipes: The Art of Scientific Computing. Cambridge University Press, Cambridge (1985)
3. Schellman, J.A., Stigter, D.: Electrical double layer, zeta potential, and electrophoretic charge of double-stranded DNA. Biopolymers **16**, 1415 (1977)
4. Stigter, D.: Electrophoresis of highly charged colloidal cylinders in univalent salt-solutions. J. Colloid Interface Sci. **53**(2), 296 (1975)
5. Stigter, D.: Evaluation of the counterion condensation theory of polyelectrolytes. Biophys. J. **69**, 380 (1995)

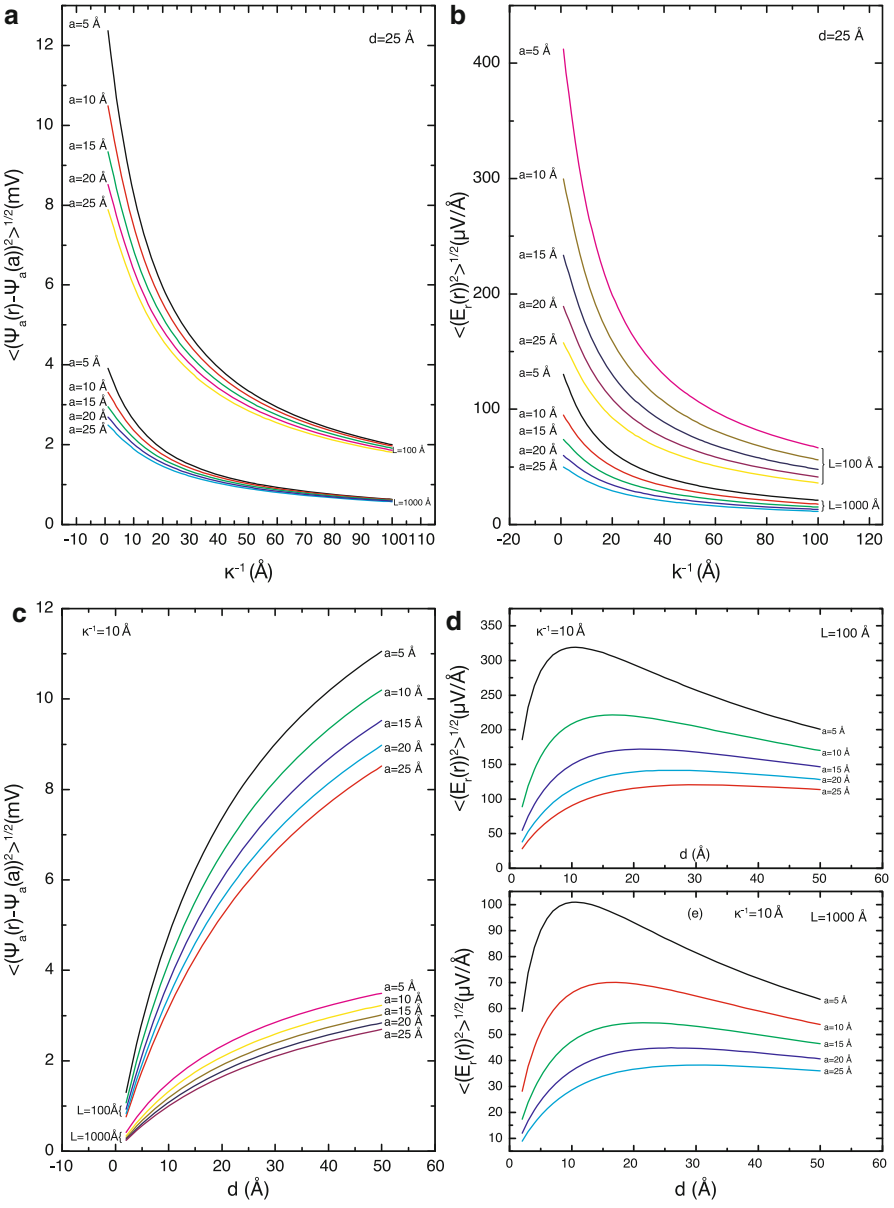

Fig. 3.8 Voltage and field fluctuations as a function of κ^{-1} and the distance d from the polyelectrolyte surface, Debye–Hückel approximation

Chapter 4
Dielectric Relaxation Around a Charged Colloidal Cylinder in an Electrolyte

Abstract The polarizability and the corresponding dielectric relaxation of the Debye–Hückel (DH) atmosphere surrounding a charged rod-like polyelectrolyte immersed in an ionic solution of a symmetrical electrolyte is determined following the method developed in the former chapter.

Several formulas are given to estimate the DH atmosphere parameters, namely: the polarizability at zero frequency, $\alpha(0)$, the relaxation time, τ, the cloud capacitance, $\underline{C}$,the average displacement of the ionic cloud, δ, the square root dipole moment quadratic fluctuation, $< p^2 >^{1/2}$, and the thermal fluctuating field, $< E^2 >^{1/2}$. The Poisson–Boltzmann equation is solved numerically in order to apply the theory to a highly charged polyelectrolyte as DNA in solution, although also are given formulas valid for the DH approximation. It is predicted a dispersion in the polarizability and correspondingly in the dielectric constant of these solutions in the microwave region. For instance, considering the DNA length of 1000 Å, with its reduced linear charge density $\xi_0 = 4.25$, and ionization factor $\gamma = 0.5$, immersed in a NaCl solution (40 mM) we predict a polarizability of the DH atmosphere at zero frequency $\alpha(0) = 1 \times 10^{-33}$ Fm^2 ($\simeq 6.1 \times 10^6$ times greater than the mean value of the polarizability of water) and the corresponding fluctuating dipole moment $p = 2.1 \times 10^{-27}$ cm ($\simeq$ 600 times greater than the permanent dipole moment of water molecule). The relaxation time and the average displacement of the ionic cloud is $\tau = 1.6$ ns and $\delta = 14$ Å, respectively. This displacement is produced by the thermal fluctuating field, which, in this case, at room temperature is $< E^2 >^{1/2} = 2 \times 10^6$ V/m.

Keywords Ionic dielectric relaxation • Ionic polarization • Cylindrical polyelectrolytes

J.A. Fornés, *Electrical Fluctuations in Polyelectrolytes*, SpringerBriefs in Molecular Science, DOI 10.1007/978-3-319-33840-8_4

4.1 Method

We consider a rigid rod-like molecule or particle of radius a , length $L \gg a$, so that end effects may be neglected, with charge Q distributed uniformly over the surface with an electrical surface potential ψ_0 immersed in a solution of punctual ions of a symmetrical electrolyte of valence z with n ions per m^3. The law governing the potential profile and consequently the ionic distribution ("diffuse" layer) from the surface of the particle is given by the Poisson–Boltzmann (PB) equation:

$$\triangle \psi = \frac{2ze_0 n}{\varepsilon\varepsilon_0} \sinh\left(\frac{ze_0\psi}{kT}\right) \tag{4.1}$$

where $\triangle$ is, in our case of cylinder symmetry, the radial part of the Laplace operator. Equation 4.1 can be written as:

$$\frac{1}{x}\frac{d}{dx}\left(x\frac{dy}{dx}\right) = \sinh(y) \tag{4.2}$$

where $y = ze_0\psi/kT$ and $x = \kappa r$ are the dimensionless potential and distance, respectively, r being the distance from the cylinder axis perpendicular to the surface. At the surface of the cylinder $x = x_0 = \kappa a$ and $y = y_0 = ze_0\psi_0/kT$.

The contribution of the ionic cloud to the electrostatic potential at the rod surface will be [1, 4]:

$$y_{\text{cloud}}(x_0) = y(x_0) + 2z\xi \ln(x_0) \tag{4.3}$$

We can then define the ionic cloud capacitance as:

$$\underline{C} = \frac{Q}{\psi_{\text{cloud}}(x_0)} = \frac{4\pi L\varepsilon_0\varepsilon\xi}{y(x_0) + 2z\xi \ln(x_0)} \tag{4.4}$$

where ξ is the reduced linear charge density over the rod surface (see next). In case the ratio of the electrical to the thermal energy of the ions is very small, DH approximation, ($\frac{ze_0\psi(r)}{kT} \ll 1$, or $y \ll 1$), Eq. 4.3 can be written as:

$$\underline{C}_{\text{DH}} = 2\pi L\varepsilon\varepsilon_0 \left[\frac{K_0(x_0)}{x_0 K_1(x_0)} + \ln(x_0)\right]^{-1} \tag{4.5}$$

where $K_0(x_0)$ and $K_1(x_0)$ are the modified Bessel functions of zeroth and first order.

In our range of concentrations we approximate the relaxation time of the DH atmosphere, by that given in [3]:

$$\tau = \underline{R}(r)\underline{C}(r) = \varepsilon\varepsilon_0\rho \tag{4.6}$$

where $\underline{R}(r)$ is the resistance of the electrical path associated with the capacitance and ρ is the electrical resistivity, calculated by (see [3]):

$$\rho = \frac{1}{n(ze_0)^2\left[\left[1 - \frac{(ze_0)^2\kappa}{24\pi\varepsilon\varepsilon_0 kT}\frac{\sqrt{2}}{1+\sqrt{2}}\right]\frac{(D_0{}^{+}+D_0{}^{-})}{kT} - \frac{\kappa}{3\pi\eta(1+\kappa a_i)}\right]} \tag{4.7}$$

where $D_0{}^{\pm}$ are the ionic diffusion constants, η is the viscosity of the solution and a_i is the mean ions radius. Also experimental values for ρ can be used.

In the former chapter we obtained for the longitudinal polarizability $\alpha(0) = \underline{C}\delta^2$, where $\underline{C}$ is the total polyelectrolyte-ionic capacitance and δ the average displacement of the 'bound' ions under the influence of the thermal fluctuating field. Any of the theories which predict $\alpha(0)$, δ, and the relaxation time τ, can be used to estimate $\underline{R}$ and $\underline{C}$, on the other hand, $\underline{R}$, $\underline{C}$ and δ can be obtained independently by modeling the system. Among the results is that the complex polarizability $\alpha(\omega)$:

$$\alpha(\omega) = \frac{\underline{C}\delta^2}{1+(\tau\omega)^2} + i\frac{-\tau\omega\underline{C}\delta^2}{1+(\tau\omega)^2} \tag{4.8}$$

where $\underline{C}$ is the total polyelectrolyte-ionic capacitance and δ the average displacement of the 'bound' ions under the influence of the thermal fluctuating field. τ being the relaxation time of the fluctuation given by Eq. 4.6, and $\alpha(0)$ is given by:

$$\alpha(0) = \underline{C}\delta^2 \tag{4.9}$$

Correspondingly the real and imaginary components of the polarizability are

$$\alpha'(\omega) = \frac{\alpha(0)}{1+(\tau\omega)^2} \qquad ,\alpha''(\omega) = \frac{-\tau\omega\alpha(0)}{1+(\tau\omega)^2} \tag{4.10}$$

Also obtained were the following expressions for the dipole moment quadratic fluctuation, $< p^2 >$, and field, $< E^2 >$:

$$< p^2 >= \alpha(0)kT \tag{4.11}$$

with

$$< E^2 >= \frac{kT}{\alpha(0)} = \frac{kT}{\underline{C}\boldsymbol{\delta^2}} \tag{4.12}$$

Both satisfying the classical analogy of Heisenberg uncertainty principle:

$$< p^2 >< E^2 >= (kT)^2 \tag{4.13}$$

4.2 Polarizability of the Debye–Hückel Atmosphere

We apply these previous results to estimate the DH atmosphere polarizability $\alpha(0) = \text{Ç}\delta^2$. We know that with the application of an electric field the centre of charge of the central polyion is displaced from the centre of charge of its cloud, this is analogous what happen with a spherical ion giving rise to the egg-shaped ionic cloud, see, for instance, [1], the implication is that the ionic cloud is no longer symmetrical around the moving polyion; as a consequence a dipole is formed.

The central polyion practically looses its cloud if it diffuses to a distance δ during the relaxation time τ of the fluctuation. In this way δ is given by:

$$\delta = \tau v_{\text{polyion}} = \tau \mu_{\text{polyion}} < E^2 >^{1/2} \tag{4.14}$$

where v_{polyion} and μ_{polyion} are the velocity and mobility of the polyelectrolyte in the solution. From Eqs. 4.9, 4.12 and 4.14 we get

$$\alpha(0) = \tau \mu_{\text{polyion}} [kT\text{Ç}]^{1/2} \tag{4.15}$$

The mobility of a polyion of charge Q is given by (also can be used formulas given by Ohshima [9–11]):

$$\mu_{\text{polyion}} = \frac{Q}{f} = Q \left[\frac{D_{\text{polyion}}}{kT} \right] \tag{4.16}$$

where f (kg.s^{-1} units) is the frictional coefficient of the polyion and D_{polyion} its diffusion coefficient (m^2 s^{-1}).

For a long rod the frictional coefficient is given by, see [13]:

$$f = \frac{3\pi\eta\text{Ł}}{2ln(L/a) - 0.11} \tag{4.17}$$

Substituting μ_{polyion} given by Eq. 4.18 in Eq. 4.17, we get for $\alpha(0)$:

$$\alpha(0) = \tau Q D_{\text{polyion}} \left[\frac{\text{Ç}}{kT} \right]^{1/2} \tag{4.18}$$

It is necessary to formulate a few definitions in order to put the equations into the current nomenclature of polyelectrolyte science, namely:

$$\lambda = \frac{Q}{L} = \frac{e_0}{b} = \left(\frac{e_0}{l_B} \right) \xi_0 \tag{4.19}$$

where λ is the linear charge density, $b = L/N$ is the linear charge spacing and N is the number of charged polymer groups. The *Bjerrum length* l_B is the distance at

which the coulombic energy is equal to kT, ($l_B = 7.13$ Å at 25 °C in water), for an excellent English reference on this subject, see [1], namely:

$$l_B = \frac{{e_0}^2}{4\pi\varepsilon\varepsilon_0 kT} = \xi_0 b \tag{4.20}$$

The dimensionless ratio, ξ_0, which is a reduced linear charge density is particularly useful (a DNA molecule, for instance, has two phosphate charges each at a helical spacing of 3.37 Å, then $\xi_0 = l_B/b = 7.13 \times (2/3.37) = 4.23$). As a consequence the surface charge density can be written as:

$$\sigma = \frac{\lambda}{2\pi a} = \left(\frac{e_0}{2\pi a l_B}\right)\xi_0 \tag{4.21}$$

For DNA, $a = 12.5$ Å, Eq. 4.21 gives $\sigma = 7.55 \times 10^{17}$ electric charges m^{-2}, which is 28 times less than that for a bidimensional array of Cu atoms.

Then, substituting $Q = L(e_0/l_B)\xi_0$ given by Eq. 4.19 into Eq. 4.18, we get for $\alpha(0)$:

$$\alpha(0) = \tau L\left(\frac{e_0}{l_B}\right)\xi_0 D_{\text{polyion}}\left[\frac{\underline{C}}{kT}\right]^{1/2} \tag{4.22}$$

In general in a polyelectrolyte the real charge is lessened by a factor γ because of the presence of counterions within the defining surface of the cylinder, correspondingly in the former equations ξ_0 has to be replaced by $\xi = \gamma\xi_0$.

In the range of validity of the DH approximation, it can be used Eq. 4.5 to evaluate $\underline{C}_{\text{DH}}$, on the contrary the numerical solution of the Poisson–Boltzmann equation, through Eq. 4.4, has to be used.

To link microscopic parameters such as $\alpha(\omega)$ with macroscopic mensurable ones we make use of the results of the theory of electric polarization (see, for instance, [5]):

$$\varepsilon_0\varepsilon(\omega)E(\omega) = \varepsilon_0\varepsilon_{H_2O}E(\omega) + P(\omega) \tag{4.23}$$

where $E(\omega)$ is the applied macroscopic field, and $P(\omega)$ is the polarization which is given by:

$$P(\omega) = \left(\frac{N_A}{V_M}\right)\alpha(\omega)F(\omega) \tag{4.24}$$

where $F(\omega)$ is the 'inner field' which is the actual field experienced by the molecule and V_M is the molar volume.

From Eqs. 4.23 and 4.24 we obtain the relative increment of the dielectric constant:

$$\frac{\varepsilon(\omega)-\varepsilon_{H_2O}}{\varepsilon_{H_2O}} = B\left(\frac{N_A}{V_M}\right)\frac{1}{\varepsilon_0\varepsilon_{H_2O}}\alpha(\omega) \tag{4.25}$$

With $B(\omega)$ given by:

$$B(\omega) = \frac{F(\omega)}{E(\omega)} \tag{4.26}$$

where $E(\omega)$ is the applied field, B is usually a little larger than unity for a polar solvent [12].

Using the relations

$$\begin{aligned}\varepsilon(\omega) &= \varepsilon'(\omega) - i\varepsilon''(\omega)\\ \alpha(\omega) &= \alpha'(\omega) + i\alpha''(\omega)\end{aligned} \tag{4.27}$$

then for the real and imaginary part of the dielectric constant we have

$$\frac{\varepsilon'(\omega)-\varepsilon_{H_2O}}{\varepsilon_{H_2O}} = B\left(\frac{N_A}{V_M}\right)\frac{1}{\varepsilon_0\varepsilon_{H_2O}}\left[\frac{\alpha(0)}{[1+(\tau\omega)^2]}\right] \tag{4.28}$$

$$\frac{\varepsilon''(\omega)}{\varepsilon_{H_2O}} = -B\left(\frac{N_A}{V_M}\right)\frac{\omega}{\varepsilon_0\varepsilon_{H_2O}}\left[\frac{\tau\alpha(0)}{[1+(\tau\omega)^2]}\right] \tag{4.29}$$

with $\alpha(0)$, and τ given by Eqs. 4.22 and 4.6, respectively. In a more general actual experimental situation of a solution of volume V with N macroions, each one occupying an average volume v, we have to reemplace in Eqs. (4.28 and 4.29) the factor N_A/V_M by $\phi/v = N/V$, with ϕ being the volume fraction.

Figure 4.2 is a representation of Eqs. 4.28 and 4.29 for a DNA solution at room temperature in water.

In Fig. 4.1a–f are plotted the results shown in Table 4.1. Figure 4.1a is a representation of Eq. 4.4. The capacitance formed by the charged polyelectrolyte surface and the ionic atmosphere surrounding it. Figure 4.1b shows the plot of the polarizability $\alpha(0)$ versus concentration (Eq. 4.22), we can observe that the decrease of the relaxation time with concentration domains the polarizability behaviour. This is also manifested on the plot of the fluctuational dipole moment, p/p_{H_2O}, Fig. 4.1e, Eq. 4.11. In Fig. 4.1c is shown the fluctuational displacement, δ, of the cloud with respect to the central polyion, we can also observe a decrease of δ with concentration because the corresponding decrease of the relaxation time with concentration, Eq. 4.14. In Fig. 4.1d is shown the plot of δ versus τ, showing the linear relation. From Fig. 4.1f we can observe the plot p/p_{H_2O} versus the relaxation time τ. The values of the relaxation time are in accordance with those reported by Yoshida and Kikuchi [16], in their Metropolis Monte Carlo Brownian dynamics simulation of the ion atmosphere polarization around a rod-like polyion. Washizu and Kikuchi [14] and Washizu [15] performing computer simulation determined the electric polarizability of DNA, not only in salt-free solution but also in salt

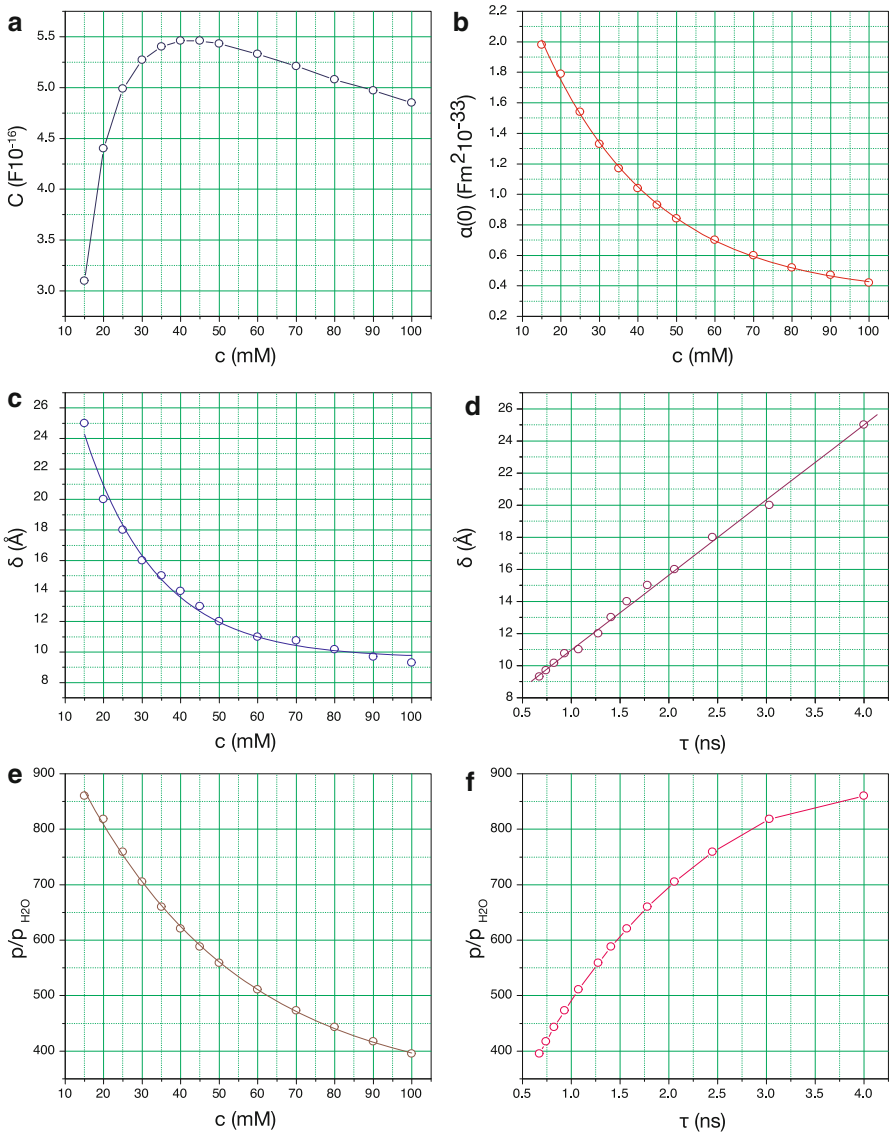

Fig. 4.1 Representation of the Debye–Hückel atmosphere parameters, in accordance with the values of Table 4.1, for DNA immersed in c mM NaCl solution in water

Table 4.1 Debye–Hückel atmosphere parameters by numerical solution of PB equation for DNA immersed in c mM NaCl solution in water[a]

x_o	c (mM)	$y(x_o)$	$\underline{C}$ (10^{-16} F)	$\alpha(0)$ (10^{-33} Fm^2)	δ (Å)	τ (ns)	$(p/p_{H_2O})^b$
0.50	15.0	8.90	3.10	1.98	25	4.0	860
0.58	20.0	6.52	4.40	1.79	20.	3.0	818
0.65	25.0	5.55	4.99	1.54	18.	2.4	759
0.71	30.0	4.96	5.27	1.33	16	2.1	705
0.77	35.0	4.55	5.40	1.17	15	1.8	660
0.82	40.0	4.23	5.46	1.04	14	1.6	621
0.87	45.0	3.98	5.46	0.93	13	1.4	588
0.92	50.0	3.77	5.43	0.84	12	1.3	559
1.00	60.0	3.45	5.33	0.70	11	1.1	511
1.08	70.0	3.20	5.21	0.60	11	0.9	473
1.16	80.0	3.01	5.08	0.52	10.	0.8	443
1.23	90.0	2.84	4.97	0.47	10.	0.7	417
1.30	100.0	2.71	4.85	0.42	9	0.7	395

[a]$L = 1000$ Å, $\xi_0 = 4.25$, $\gamma = 0.5$, $a = 12.5$ Å
[b]Fluctuational dipole moment, p, in units of the dipole moment of water, p_{H_2O}

solution. In both cases they found that the diffuse ion atmospheres play more important role in determining the dependence of the polarizability on salt or polymer concentration than condensed counterions. Contribution from the latter to the radial components of the polarizability tensor is very small, while that from the former is very large. Katsumoto et al. [7] performed dielectric spectroscopy measurements for aqueous solutions of short single-stranded DNA with 30 to 120 bases of thymine over a frequency range of 10^5–10^8 Hz. Dielectric dispersion was found to include two relaxation processes in the ranges from 10^5 to 10^6 and from 10^6 to 10^8 Hz, respectively. Also Fischer and Netz [2] using Brownian dynamics simulations of a salt-free polyelectrolyte solution including hydrodynamic interactions they show that the low-frequency dielectric relaxation process for a single polyelectrolyte chain is due to diffuse (uncondensed) counter ions, while the high- frequency dielectric relaxation mode is due to condensed counter ions. In Fig. 4.2a–c are shown the plots related to the dielectric dispersion due to the relaxation of the DH cloud of a DNA solution. For a DNA electrolyte solution: DNA length 1000 Å, DNA concentration 10^{-2} mol/m^3, electrolyte concentration 15 mM NaCl in water; it is predicted a small increase in the dielectric constant at low frequencies with a relaxation time of 4 ns, this increase can be higher at lower concentrations. We want to emphasize that this relaxation is different of the one caused by the bound ions which is of the order of ms and produces a polarizability parallel to the cylinder axis, $\alpha(0) \simeq 10^{-27}$ Fm^2, described in the former chapter. The DH atmosphere relaxation is in the microwave region of the spectrum and could be measured by the conventional techniques as microwave bridges or microwave resonant cavities,

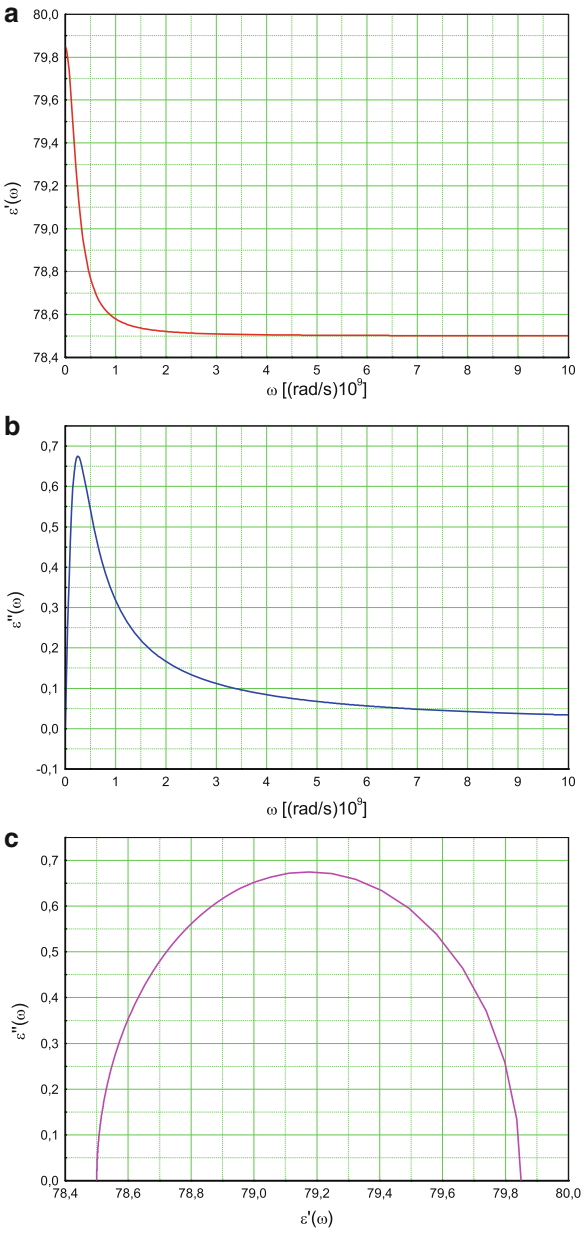

Fig. 4.2 (**a**) Representation of $\varepsilon'(\omega)$ from Eq. 4.23, (**b**) Ditto $\varepsilon''(\omega)$ from Eq. 4.24, (**c**) Cole–Cole plot, for a DNA solution at room temperature in water: $B = 1,\ L = 1000\,\text{Å},\ \xi_0 = 4.25,\ \gamma = 0.5$, molecular weight $M_w = 10^6$, DNA concentration $10^{-2}\,\text{mol/m}^3$ DNA in 15 mM NaCl solution, $\alpha(0) = 1.98 \times 10^{-33}\,\text{Fm}^2,\ \tau = 4.0\,\text{ns}$

[6, 8]. As far our knowledge, the DH atmosphere parameters and their influence on the dielectric relaxation for DNA solutions in this range of concentrations have not been treated by other authors. We hope that these results will stimulate new experiments.

References

1. Bockris, J.O'M., Reddy, A.K.N.: Modern Electrochemistry, vol. 1, p. 200. Plenum Press, New York (1977)
2. Fischer, A., Netz, R.R.: Low-frequency collective exchange mode in the dielectric spectrum of salt-free dilute polyelectrolyte solutions. Eur. Phys. J. E **36**, 117 (2013)
3. Fornés, J.A.: Electrical fluctuations in colloidal and ionic solutions. J. Colloid Interface Sci. **186**, 90 (1997)
4. Fornés, J.A.: Thermal electrical fluctuations around a charged colloidal cylinder in an electrolyte. Phys. Rev. E **57**, 2104 (1998)
5. Hasted, J.B.: Aqueous Dielectrics, p. 11. Chapman and Hall, London (1973)
6. Hill, N.E., Vaughan, W.E., Price, A.H., Davies, M.: "Dielectric Properties and Molecular Behaviour." Van Nostrand Reinhold Company, London (1969)
7. Katsumoto, Y., Omori, S., Yamamoto, D., Yasuda, A.: Dielectric dispersion of short single-stranded DNA in aqueous solutions with and without added salt. Phys. Rev. E **75**, 011911 (2007)
8. Klösgen, B., Reichle, C., Kohlsmann, S., Kramer, K.D.: Dielectric spectroscopy as a sensor of membrane headgroup mobility and hydration. Biophys. J. **71**, 3251 (1996)
9. Ohshima, H.: Henry's function for electrophoresis of a cylindrical colloidal particle. J. Colloid Interface Sci. **180**, 299 (1996)
10. Ohshima, H.: Dynamic electrophoretic mobility of a cylindrical colloidal particle. J. Colloid Interface Sci. **185**, 131 (1997)
11. Ohshima, H.: Electrophoretic mobility of cylindrical soft particles. Colloid Polym. Sci. **275**, 480 (1997)
12. Oosawa, F.: Counterion fluctuation and dielectric dispersion in linear polyelectrolytes. Biopolymers **9**, 677 (1970)
13. Van Holde, K.E.: Physical Biochemistry, p. 81. Prentice-Hall, Englewood Cliffs (1971)
14. Washizu, H., Kikuchi, K.: Simulation of electric polarizability of polyelectrolytes. J. Phys. Chem. B **106**, 11329 (2002)
15. Washizu, H., Kikuchi, K.: Electric polarizability of DNA in aqueous salt solution. J. Phys. Chem. B **110**, 2855 (2006)
16. Yoshida, M., Kikuchi, K.: Metropolis Monte Carlo Brownian dynamics simulation of the ion atmosphere polarization around a rodlike polyion. J. Phys. Chem. **98**, 10303 (1994)

Chapter 5
The Polarizability of Rod-Like Polyelectrolytes: An Electric Circuit View

Abstract In this chapter we use the fluctuation-dissipation theorem (FDT) to estimate the polarizability or dielectric constant as a function of the frequency for low electric field of a polyelectrolyte immersed in an ionic solution; the idea is to consider each charged group within the polyelectrolyte framework and its neighbourhood as a resistor and a capacitor in series. We obtained for the longitudinal polarizability $\alpha_{\parallel}(0) = \mathbf{C}\delta^2$, where $\mathbf{C}$ is the total polyelectrolyte-ionic capacitance and δ the average displacement of the 'bound' ions under the influence of the thermal fluctuating field. Any of the theories which predict $\alpha_{\parallel}(0)$, δ, and the relaxation time τ, can be used to estimate R and C, on the other hand, R, $\mathbf{C}$ and δ can be obtained independently by modeling the system. Using Mandel's results we obtain for the total polyelectrolyte-ionic longitudinal capacitance $\mathbf{C} = n^2 C_0$ where n is the number of condensed but mobile counterions of valence z, and C_0 is the elementary capacitance, $C_0 = (ze_0)^2/kT$. We obtain results that are consistent with the experimental data of Takashima for the dielectric dispersion of DNA solutions.

Keywords Polarizability • Electrical fluctuations • Ionic dielectric relaxation • Cylindrical polyelectrolytes

5.1 Longitudinal Electrical Fluctuations and the Polarizability of Rod-like Polyelectrolytes

Since the pioneer works of Schwarz [15, 16], and Mandel [6] on the polarization of rod-like polyelectrolytes, a lot of work has been performed on this subject, basically because most of the biological macromolecules under physiological conditions are polyelectrolytes in solution and their biological activity depends on their physicochemical properties. Manning [9] used his counterion condensation formalism to generalize the Mandel's model for polarization. Mohanty and Zhao [10] generalized the Mandel–Manning theories even further to include low and high electric field. This paper also contains an excellent biography on this subject.

Part of this chapter was reprinted with permission from [José A. Fornés, Phys. Rev. E **57,2**, 2110, (1998)] Copyright (1998) by the American Physical Society.

J.A. Fornés, *Electrical Fluctuations in Polyelectrolytes*, SpringerBriefs in Molecular Science, DOI 10.1007/978-3-319-33840-8_5

With respect to the dielectric dispersion of polyelectrolyte solutions a lot of work has also been performed since the pioneer works of Oncley and O'Konski on the dielectric behaviour of protein solutions: Oncley [11] has attributed the dielectric properties to orientational relaxation of permanent dipoles, and O'Konski [14] to phenomena due to surface conductivity.

The dielectric dispersion of DNA solutions was first measured by Allgen [1] and Jungner et al. [4] followed by Jerrard and Simmons [3] and Takashima [17, 18] and [19]. Oosawa [12, 13] using the method of the mode expansion explained the experimental results of Takashima. Mandel and Jenard [7, 8] studied the dielectric behaviour of aqueous polyelectrolyte solutions and proposed a model which is based upon the assumption that the polyelectrolyte solution behaves as a suspension of spheroids exhibiting longitudinal polarization which is due to 'bound' ions. This model was improved by Takashima [19] explaining the decrease of the relaxation time with increasing salt concentration.

The main objective of the present work is to show the potential of the FDT in deriving physical properties as well as to give another view of the polarizability of a polyelectrolyte immersed in an ionic solution.

5.2 The Longitudinal Polarizability

The fluctuations we are considering are produced by the ions which according to a Boltzmann distribution are more or less trapped on the surface of the polyelectrolyte and form the fraction of the 'bound' ions. Although they are radially fixed, they still have a certain freedom to move in the longitudinal direction of the molecule. As a consequence of this mobility Schwarz [15, 16], Mandel [6] and Oosawa [12, 13] have predicted a large polarizability $\alpha(\omega)$ for this kind of molecules. In order to determine this polarizability we consider any fixed charge and the 'bound' ions in its neighbourhood as a capacitor and a resistor in series (see Fig. 5.1).

In accordance the total molecular complex generalized impedance $\mathbf{Z}(\omega)$ as a function of the radial frequency ω will be

$$\mathbf{Z}(\omega) = \sum_i n_i Z_i(\omega) \tag{5.1}$$

where Z_i is the impedance associated with each chemical group of class i [1] and n_i is the number of 'bound' ions. In case of only one class of groups Eq. 5.22 transforms in:

$$\mathbf{Z}(\omega) = nZ(\omega) = \mathbf{R} + \frac{1}{i\omega\mathbf{C}} \tag{5.2}$$

[1] A class is defined as a set of chemical groups with the same charge.

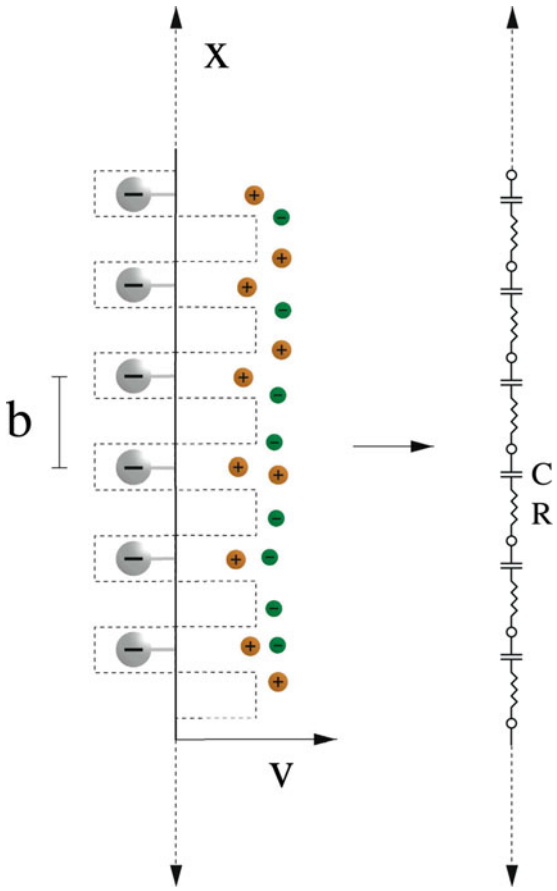

Fig. 5.1 The model: the potential V of the mobile ions is periodic on the x axis, exhibiting a minimum near each charged site, due to the strong , electric attraction of the mobile ion by the fixed charge. We consider any fixed charge and the 'bound' ions in its neighbourhood as a capacitor and a resistor in series

where $\mathbf{R} = nR$ and $\mathbf{C} = C/n$ are the total resistance and capacitance associated with the groups-bound ion system, R and C are the individual resistance and capacitance of each group-bound ions system. The relation between the Fourier components of the spontaneous fluctuational current I_ω and voltage V_ω is given by:

$$V_\omega = \mathbf{Z}(\omega) I_\omega, \tag{5.3}$$

The complex generalized susceptibility is given by:

$$\alpha(\omega) = -\frac{1}{[i\omega \mathbf{Z}(\omega)]} \tag{5.4}$$

Equation 1.14 can also be written as

$$p_\omega = [-\alpha(\omega)\delta^2] E_\omega \tag{5.5}$$

where δ is the average displacement of the 'bound' ions under the influence of the thermal fluctuating field E_ω and p_ω the corresponding Fourier component of the fluctuating dipole moment.

Then the corresponding polarizability parallel to the molecular axis will be

$$\alpha_\parallel(\omega) = -\alpha(\omega)\delta^2 \tag{5.6}$$

From Eqs. 1.16, 3.2 and 3.6 we obtain for the complex polarizability $\alpha_\parallel(\omega)$:

$$\alpha_\parallel(\omega) = \frac{\mathbf{C}\delta^2}{1+(\tau\omega)^2} + i\frac{-\tau\omega\mathbf{C}\delta^2}{1+(\tau\omega)^2} \tag{5.7}$$

τ being the relaxation time of the fluctuation given by:

$$\tau = \mathbf{RC} \tag{5.8}$$

and

$$\alpha_\parallel(0) = \mathbf{C}\delta^2 \tag{5.9}$$

Correspondingly the real and imaginary components of the polarizability are

$$\alpha'_\parallel(\omega) = \frac{\alpha_\parallel(0)}{1+(\tau\omega)^2}, \alpha''_\parallel(\omega) = \frac{-\tau\omega\alpha_\parallel(0)}{1+(\tau\omega)^2} \tag{5.10}$$

Mandel [6], among others, has estimated $\alpha_\parallel(0)$, δ and τ for rod-like, charged macromolecules, we will use his results in order to estimate our electrical molecular parameters. Mandel derived the following three formulae:

$$(i) \qquad \alpha_\parallel(0) = n\frac{(ze_0)^2}{kT}\frac{L^2}{12} = \frac{\gamma z e_0^2 L^3}{12kTb} \tag{5.11}$$

where $\gamma = zn/N$ is the degree of association of the counterions, z the valence of the 'bound' ions, $b = L/N$ is the linear charge spacing, N is the total number of charged polymer sites and L is the length of the rod-like molecule.

$$(ii) \qquad \delta^2 = \frac{(ze_0)^2 L^4}{(12kT)^2}E^2 \tag{5.12}$$

where E is the applied electric field.

$$(iii) \qquad \tau = \frac{ze_0L^2}{12\mu\, kT} \tag{5.13}$$

with μ being the mean mobility of the ions along the polymer framework.

From Eqs. 3.5 and 3.6 we obtain

$$p_\omega = \alpha_\parallel(\omega)E_\omega \tag{5.14}$$

Applying to Eq. 3.14 the results of the fluctuation-dissipation theorem (FDT), Eq. 1.9, in the region of classical fluctuations $kT \gg \hbar\omega$ or $\omega \ll kT\hbar^{-1} = 4 \times 10^{13}\ \mathrm{s}^{-1}$ at room temperature[2]:

$$< p^2 >= \alpha_\parallel(0)kT \tag{5.15}$$

with

$$< E^2 >= \frac{kT}{\alpha_\parallel(0)} = \frac{kT}{\mathbf{C}\delta^2} \tag{5.16}$$

where we have used, in accordance with Eq. 1.12, the relation:

$$< p^2 >< E^2 >= (kT)^2 \tag{5.17}$$

As in our definition δ is produced by the electric thermal fluctuating field, we can consider the applied field in Eq. 3.12 $E^2 =< E^2 >$ Then from Eqs. 3.11, 3.12 and 3.16, we obtain

$$\delta^2 = \frac{L^2}{12n} = \frac{zLb}{12\gamma} \tag{5.18}$$

The corresponding molecular capacitance $\mathbf{C} = \alpha_\parallel(0)/\delta^2$ will be

$$\mathbf{C} = n^2\frac{(ze_0)^2}{kT} = \left(\frac{\gamma L}{b}\right)^2\frac{{e_0}^2}{kT} \tag{5.19}$$

From Eqs. 3.8 and 3.13 we can estimate the resistance $\mathbf{R}$, namely:

$$\mathbf{R} = \frac{b^2z}{12\mu e_0\gamma^2} \tag{5.20}$$

[2]Equation 3.15 was already derived by Oosawa [13] following an averaging procedure.

In order to link microscopic parameters as $\alpha_{\parallel}(\omega)$ with macroscopic measurable ones we make use of the results of the theory of electric polarization, see, for instance, [2, 12]:

$$\epsilon_0 \epsilon(\omega) E(\omega) = \epsilon_0 \epsilon_s + P(\omega) \tag{5.21}$$

where $E(\omega)$ is the applied macroscopic field, and $P(\omega)$ is the polarization which is given by:

$$P(\omega) = \left(\frac{N_A}{V}\right) \alpha_{\parallel}(\omega) F(\omega) \tag{5.22}$$

where $F(\omega)$ is the 'inner field' which is the actual field experienced by the molecule and V is the molar volume.

From Eqs. 3.21 and 3.22 we obtain the relative increment of the dielectric constant:

$$\frac{\epsilon(\omega) - \epsilon_s}{\epsilon_s} = B \left(\frac{N_A}{V}\right) \frac{1}{\epsilon_0 \epsilon_s} \alpha_{\parallel}(\omega) \tag{5.23}$$

With B given by:

$$B(\omega) = \frac{F(\omega)}{E(\omega)} \tag{5.24}$$

B is usually a little larger than unity for a polar solvent [12].

Using the relations:

$$\begin{aligned} \epsilon(\omega) &= \epsilon'(\omega) - i\epsilon''(\omega) \\ \alpha_{\parallel}(\omega) &= \alpha'_{\parallel}(\omega) + i\alpha''_{\parallel}(\omega) \end{aligned} \tag{5.25}$$

Then for the real and imaginary part of the dielectric constant we have

$$\frac{\epsilon'(\omega) - \epsilon_s}{\epsilon_s} = B \left(\frac{N_A}{V}\right) \frac{1}{\epsilon_0 \epsilon_s} \frac{\alpha_{\parallel}(0)}{[1 + (\tau\omega)^2]} \tag{5.26}$$

$$\frac{\epsilon''(\omega)}{\epsilon_s} = B \left(\frac{N_A}{V}\right) \frac{1}{\epsilon_0 \epsilon_s} \frac{\omega\tau\omega\alpha_{\parallel}(0)}{[1 + (\tau\omega)^2]} \tag{5.27}$$

$\alpha_{\parallel}(0)$ and τ are given by Eqs. 3.11 and 3.13, respectively.

Polyelectrolytes such as linear polyacids or DNA show broad dispersion curves of the dielectric constant at low frequencies which cannot be explained by a single relaxation time [12, 13] in order to get a good fit with the experimental curve we have to generalize Eqs. (5.26) and (5.27), namely:

$$\frac{\epsilon'(\omega)-\epsilon_s}{\epsilon_s} = B\left(\frac{N_A}{V}\right)\frac{1}{\epsilon_0\epsilon_s}\sum_k \frac{\alpha_{\|k}(0)}{[1+(\tau_k\omega)^2]} \tag{5.28}$$

$$\frac{\epsilon''(\omega)}{\epsilon_s} = B\left(\frac{N_A}{V}\right)\frac{1}{\epsilon_0\epsilon_s}\sum_k \frac{\omega\tau_k\alpha_{\|k}(0)}{[1+(\tau_k\omega)^2]} \tag{5.29}$$

The objectives raised in the introduction section have been achieved: We derived an expression for the longitudinal polarizability and dielectric constant, $\alpha_\|(\omega)$ and $\epsilon(\omega)$, which as derived from the FDT have the real and imaginary parts satisfying the Kramers and Kronig's dispersion relations.

In this method is defined a local capacitance and resistance surrounding each group in a polyelectrolyte-ionic solution. This can be useful in modeling complex systems for obtaining more realistic approximations, indeed the author envisions science as an evolution of ideas and approximations.

We have used the simple expression for $\alpha_\|(0)$ of Mandel's model [6], which doesn't consider interionic interaction and only one relaxation time. We can see from Fig. 3.1. that the profiles for $\epsilon'(\omega)$ and $\epsilon''(\omega)$ are quite in good agreement with the experimental ones of Takashima [17], in spite of the uncertainty in the factor B [5], in the degree of counterions' association γ and also in the molecular weight of the DNA sample, not reported in the cited paper by Takashima but inferred by us through the reported DNA length of 7800 Å to be approximately 7×10^6. The DNA molecule has two phosphate charges per unit, each with a helical spacing of 3.37 Å, then $b = 3.37\,\text{Å}/2 = 1.68\,\text{Å}$, consequently $N = L/b = 4627$, we considered $\gamma = 1$ (Fig. 5.2).

From Eq. 3.13 and from the experimental value for $\tau = 10^{-3}$ s we estimate the mobility μ of the 'bound' ions as $\mu = 1.96\times10^{-9}\,\text{m}^2\,\text{s}^{-1}\text{V}^{-1}$, which is 26 times smaller than the mobility of Na ions in water, $\mu_{Na^+} = 5.19\times10^{-8}\,\text{m}^2\,\text{s}^{-1}\,\text{V}^{-1}$, showing that these ions are more or less trapped.

From Eq. 3.19 we estimate the total polyelectrolyte-ionic capacitance $\mathbf{C} = 133\,\text{pF}$ and, consequently, the local capacitance will be $C = n\mathbf{C} = 0.61\,\mu\text{F}$. These values are substantially greater than the double layer capacitance surrounding a spherical and rod-like particle in solution which is of the order of fF, see former and next chapters. From the already known values of $\mathbf{C}$ and τ and from Eq. 3.2 we estimate the total 'bound' ions resistance as $\mathbf{R} = 7.5M\Omega$, meaning that the resistance per group is $R = 1621\Omega$. From Eq. 3.18 we obtain the value of the average displacement of the 'bound' ions under the influence of the thermal fluctuating field, giving for our DNA sample $\delta = 33$ Å.

Equation 3.11 gives the value for the static polarizability $\alpha_\|(0) = 1.459\times10^{-27}\,\text{Fm}^2$ which is 9.09×10^{12} greater than the mean polarizability of water molecule $\overline{\alpha}_{H_2O} = 1.6\times10^{-40}\,\text{F m}^2$ [7].

Finally, from the knowledge of $\alpha_\|(0)$ and with the help of Eq. 3.15 we estimate the mean thermal fluctuating dipole moment at room temperature, $\bar{p} =< p^2 >^{1/2} = 2.454\times10^{-24}\,\text{C}\,m = 7.37\times10^5\text{D}$, which is 4×10^5 greater than the permanent dipole moment of a water molecule (1.84D). This dipole moment was produced by the thermal fluctuating field given by Eq. 3.16 which, in this case, is $\bar{E} =< E^2 >^{1/2} = 1687\,\text{V m}^{-1}$.

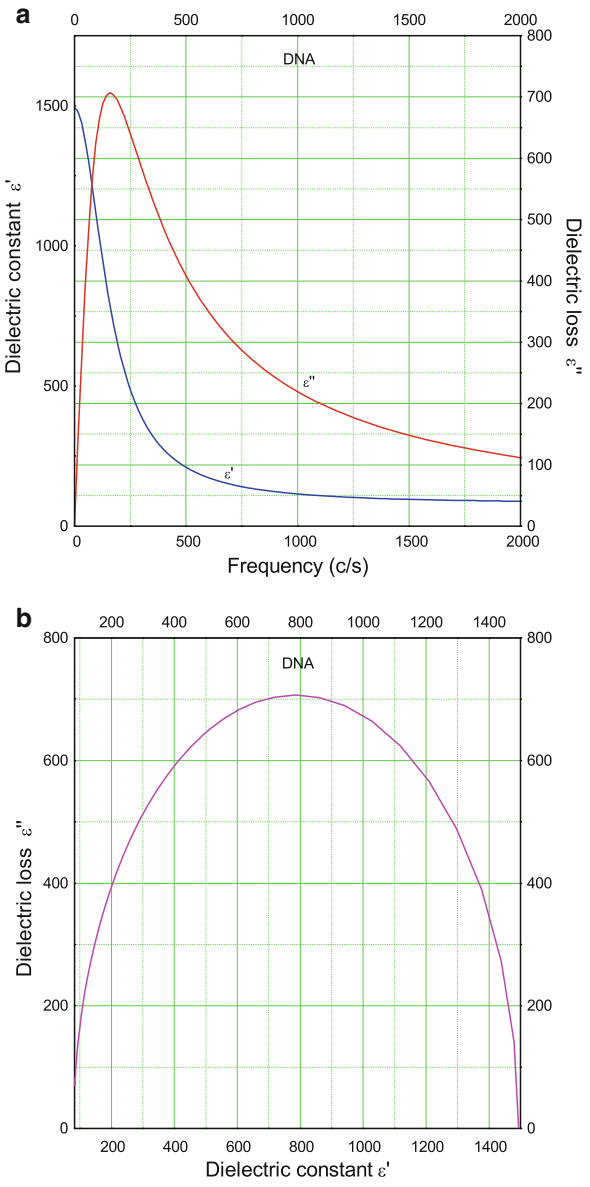

Fig. 5.2 (**a**) Representation of Eqs. 5.26 and 5.27 for a DNA solution at room temperature in water: $L = 7400$ Å, Molecular weight $M_\omega = 7 \times 10^6$, DNA concentration by weight 0.01 %, $\tau = 1$ ms, $\gamma = 1.$, $b = 1.68$ Å, $B = 1.$ (**b**) Ditto, Cole–Cole plot

References

1. Allgen, L.G.: A dielectric study of nucleohistone from calf thymus. Acta Physiol. Scand. Suppl. **22**(Suppl. 76), 1–140 (1950)
2. Hasted, J.B.: Aqueous Dielectrics, p. 11. Chapman and Hall, London (1973)
3. Jerrard, H.G., Simmons, B.A.W.: Dielectric studies on deoxyribonucleic acid. Nature **184**, 1715 (1959)
4. Jungner, G., Jungner, I., Allgen, L.G.: Molecular weight determination on thymonuclelc acid compounds by dielectric measurements. Nature **163**, 849 (1949)
5. Klug, D., Kranbuehl, D., Vanghau, W.: Molecular correlation functions and dielectric relaxation. J. Chem. Phys. **50**, 3904 (1969)
6. Mandel, M.: The electric polarization of rod-like, charged macromolecules. Mol. Phys. **4**, 489 (1961)
7. Mandel, M., Jenard, A.: Dielectric behaviour of aqueous polyelectrolyte solutions. Part 1. Trans. Faraday Soc. **59**, 2158 (1963)
8. Mandel, M., Jenard, A.: Dielectric behaviour of aqueous polyelectrolyte solutions. Part 2. Trans. Faraday Soc. **59**, 2170 (1963)
9. Manning, G.S.: A condensed counterion theory for polarization of polyelectrolyte solutions in high fields. J. Chem. Phys. **99**, 477 (1993)
10. Mohanty, U., Zhao, Y.: Polarization of counterions in polyelectrolytes. Biopolymers **38**, 377 (1996)
11. Oncley, J.L.: The investigation of proteins by dielectric measurements. Chem. Rev. **30**, 433 (1942)
12. Oosawa, F.: Counterion fluctuation and dielectric dispersion in linear polyelectrolytes. Biopolymers **9**, 677 (1970)
13. Oosawa, F.: Polyelectrolytes, Chap. 5. Marcel Dekker, New York (1971)
14. O'Konski, C.T.: Electric properties of macromolecules. V. Theory of ionic polarization in polyelectrolytes. J. Phys. Chem. **64**, 605 (1960)
15. Schwarz, G.: Zur theorie der leitfahigkeitsanisotropie von polyelektrolyten in losung,. Z. Phys. **145**, 563 (1956)
16. Schwarz, G.: Dielectric relaxation of biopolymers in solution. Z. Phys. Chem. **19**, 286 (1959)
17. Takashima, S.: Dielectric dispersion of DNA. J. Mol. Biol. **7**, 455 (1963)
18. Takashima, S.: Dielectric dispersion of deoxyribonucleic acid. J. Phys. Chem. **70**, 1372 (1966)
19. Takashima, S.: Effect of ions on the dielectric relaxation of DNA. Biopolymers **5**, 899 (1967)

Chapter 6
pH Fluctuations in Unilamellar Vesicles

Abstract In this chapter pH fluctuations in small unilamellar vesicles (SUV) are theoretically estimated. We determine that these fluctuations are dependent on macroscopic variables as pH, pK_a, buffer groups concentration and surface electrical potential. Basing on a previously reported definition of buffer electrical capacitance (Procopio & Fornés 1995) it is derived an equation which relates the pH fluctuation, the buffering power and the SUV size.

From our results it is inferred that measurement of pH in small systems has to be performed near the pK of the buffer groups in order that the fluctuational errors be minimized. We show that pH fluctuations diminish with increasing the size of the SUV and the predicted pH fluctuations decrease as the surface potential becomes less negative as a consequence of decreasing density of charged groups in the inner vesicular surface.

It is predicted that measurable effects will appear on the fluorescence detection due to protonic fluctuations close to the pH sensing region of the probes.

Keywords pH fluctuations • Buffer capacity • Shift in the fluorescence spectrum

6.1 Introduction

Artificial unilamellar vesicles (UV) constitute models in which many transport problems have been studied in recent years [7]. The so-called small unilamellar vesicles (SUV) and large unilamellar vesicles (LUV) have been extensively employed to obtain information concerning the passage of different compounds through the cell membrane such as fatty acids (FA) and to serve as vehicles for transport of pharmaceutically relevant substances and, more recently, for genetic materials.

José A. Fornés et al. *Phys. Chem. Chem. Phys.* **1**, 5133, (1999)—Reproduced by permission of the PCCP Owner Societies.

J.A. Fornés, *Electrical Fluctuations in Polyelectrolytes*, SpringerBriefs in Molecular Science, DOI 10.1007/978-3-319-33840-8_6

One of the recent problems studied with the help of vesicular systems is the translocation of fatty acids across the bilayer matrix. Fluorescent probes (FL) have been trapped inside SUV and LUV and served as indicators of pH changes related to FA translocation across the vesicular wall. Half-times of vesicular acidification as low as 25 ms have been measured [11], indicating a fast passage of FA across the bilayer vesicular wall. On the other hand, natural vesicular or vacuolar systems found in the cytoplasm resemble both in size and constitution the artificial vesicles and have important functions in metabolism what permits to extend conclusions obtained in artificial vesicular systems to biology [7]. Many studies using pH sensitive FL have detected intravesicular changes of pH due to FA entry [10].

Vesicles in the range of 25–100 nm, which are produced artificially or found naturally in the cell, are sufficiently small to provide a microscopic enclosure of near molecular dimensions. In such systems the time averaged concentrations of some chemical species and the corresponding intravesicular absolute numbers of ions or molecules may be exceedingly small, in effect often below 1 unit per vesicle. We explore, in this study, the consequences and implications of this for the proton behaviour as well as the meaning of pH in enclosures of near molecular dimensions.

We take, as an example, an SUV of 25 nm diameter and exclude the significant volume contribution of the bilayer (5 nm thickness) proper, what gives a fluid volume of 883 nm^3. Using the classical definition of pH, at pH= 7.4, we obtain an average of about 5×10^{-5} free protons inside the vesicular sac, what means that in a time average a vesicle contains a free proton only 1/20,000 of the time. Equivalently, in an ensemble of 20,000 vesicles only one has a free proton at a given instant. The laws of statistical mechanics establish the equivalence of the two descriptions. In this context the fluctuational means in this work are estimated in the frequency space in accordance to the fluctuation-dissipation theorem. A very schematic rendering of the system being discussed is given in Fig. 6.1, drawn in approximate scale.

In this way it is more appropriate to define the *probability* that a given SUV contains 1 or 2 free protons at a given instant rather than simply defining an intravesicular pH.

Even inside natural vesicles having larger diameters such as 50 or 100 nm we still find that the calculated number of free protons defined by a physiological value of pH is well under unity. Interestingly enough many such natural systems have transporters in their membranes, such as proton pumps, which are necessarily exposed to a coarse grained proton concentration.

A poorly known issue is the typical proton residence time in either free or bound states. This certainly depends on the particular characteristics of the proton donator/acceptor as well as on the buffering properties of the medium. What makes this problem the more interesting is the fact that the interchange between free and bound proton states in a microscopic enclosure can supposedly be identified and measured by molecular machines utilizing or producing proton gradients across the vesicular membrane [5, 7–11]. Such transporters are, in principle, capable of sensing the intense electrical field associated with the proton vicinity and to react appropriately. Also, the transporter itself might change substantially the proton ‘concentration’ in its vicinity. pH sensitive fluorescent probes are also sufficiently fast so as to detect these pH fluctuational changes.

Reasoning from a purely physicochemical standpoint the addition to or removal from one proton in a 25 nm diameter vesicle should, respectively, decrease or increase the pH by 4.3 units with respect to an average 7.4 value. Therefore, in such small system, each protonation/deprotonation event should implicate in a profound change in the physicochemical properties of the vesicular microambient.

6.2 pH Sensitivity of the Fluorescence Response

The proton translocation time across a distance equivalent to a vesicular radius is given by Einstein's well-known diffusion equation:

$$t = \frac{< x^2 >}{2D} \tag{6.1}$$

where x is the travel distance and D the diffusion coefficient. Making $x = 8$ nm and $D = 9.31 \times 10^{-9}\,\mathrm{m^2\,s^{-1}}$ in Eq. 6.1 we obtain that the average proton translocation time is $t = 3.44 \times 10^{-9}$ s. This time is fast relative to the mean free proton dwell time what suggests that the proton can access essentially all the vesicular fluid during its 'free' existence.

According to Gutman and Nachliel [6] the average lifetime of a free proton is given by

$$\tau = \frac{1}{k_a \times [A^-]} \tag{6.2}$$

where $k_a = (1\text{-}3)10^{10}\,\mathrm{M^{-1}\,s^{-1}}$ is the rate of association with the acceptor, A^-. In a solution containing 1 mM buffer we obtain $\tau = 30$ ns, which is comparable with the proton translocation time calculated from Eq. 6.1.

This establishes the radius of action of a pH sensitive probe as the whole vesicular sac and has the meaning that one fluorescent probe can react to the proton activity of the whole content of an SUV, during its response time. It is then apparent that there is a close matching between proton travel time and response time, what allows us to describe the internal vesicular surface and intravesicular fluid as a proton exchange system, governed by its own characteristics and isolated from external medium by the vesicular membrane, during the brief response time of the FL.

In order to sense a fluctuation of pH in a microscopic enclosure, a pH probe must be both small and fast enough.

Biological ion channels, enzymatic molecules, pumps and other molecular machines constitute systems which are, in principle, capable of sensing such fluctuations. pH sensitive FL constitutes, on the other hand, ideal sensors of pH fluctuations, since their response time to pH changes is measured in the nanosecond time frame.

6.3 General Model

The model we consider consists of one pH sensitive FL, fixed at the internal surface of an SUV (Fig. 6.1). Phospholipid (PL) charged headgroups lining the inner bilayer leaflet are considered to be the sole source and sink of protons to the microambient sensed by the fluorophore. The vesicular sap is considered, in a first approach, to have a negligible buffering power, so that only the exchange of protons between the FL molecule and the charged PL groups is considered and the only buffering power is that provided by the PL headgroups. This setting is experimentally achievable, provided the vesicles are formed with no added buffers.

For calculating the buffer concentration [Buffer group], we use data from Kraayenhof et al. [12], Fig. 6.2, where the surface potential, ψ_s, is plotted as a function of the fraction, *f,* of PL headgroups which are dissociable. The corresponding buffer concentration will be

$$[\text{Buffer group}] = \frac{N_{PL}}{N_A V_V} \tag{6.3}$$

where V_V is the vesicular volume, N_A is Avogadro constant and N_{PL} is the total number of PL headgroups in the internal vesicular leaflet given by:

$$N_{PL} = \frac{A}{A_{PL}} f \tag{6.4}$$

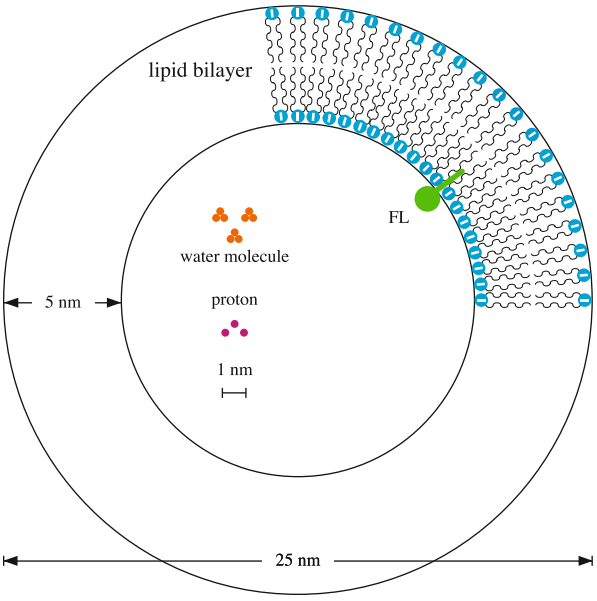

Fig. 6.1 Schematic depiction of the system, consisting of an SUV and one membrane bound probe, drawn in approximate scale

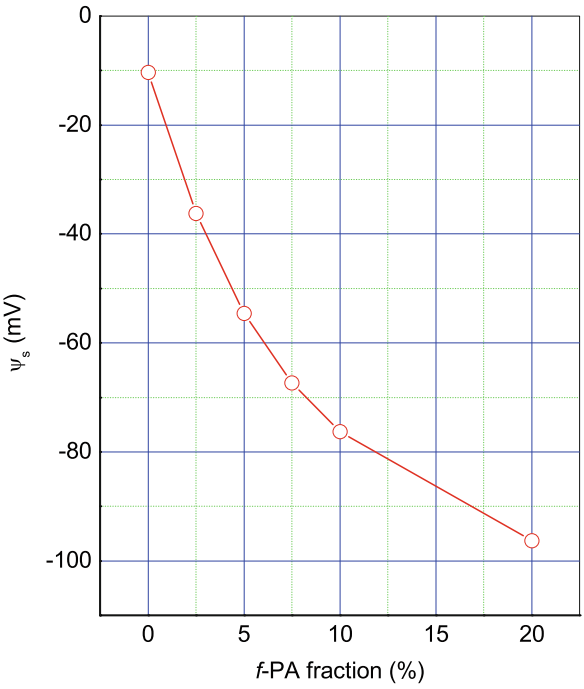

Fig. 6.2 Surface potential, ψ_s, versus the fraction, f,of PL headgroups which are dissociable (data from Kraayenhof et al. [12])

where A is the internal vesicular area and A_{PL} is the phospholipid headgroup area ($\simeq 70\,\text{Å}^2$) [1].

6.4 Electrical Properties of the System

6.4.1 Ionizable Groups

The vesicular surface is assumed to contain acidic ionizable groups at a density $1/S$, where S is the surface area per acidic group. A fraction α (the degree of dissociation) of these groups will be dissociated so that the surface charge density is

$$\sigma = -\frac{e_o \alpha}{S} \tag{6.5}$$

and which will depend on the *dissociation constant, K_a*, for the surface ionizable groups of the lipid corresponding to the reaction:

$$\text{AH} \rightleftarrows \text{A}^- + \text{H}^+ \tag{6.6}$$

whose equilibrium constant is given by:

$$K_a = \frac{[H^+]_s[A^-]}{[AH]} = [H^+]_s \frac{\alpha}{1-\alpha} \tag{6.7}$$

where $[H^+]_s$ is the hydrogen ion concentration at the surface of the lipid. This concentration is related to the one in the bulk solution, $[H^+]$, through the Boltzmann equilibrium condition [1],

$$[H^+]_s = [H^+]e^{-y_s} = 10^{-pH}e^{-y_s} \tag{6.8}$$

or

$$pH_s = pH + 0.434y_s \tag{6.9}$$

where we have used $pH = -\log_{10}[H^+]$ and $y_s = \frac{e_o}{kT}\psi_s$ is the uniform reduced surface potential. The SI system of units was employed throughout, e_o is the electron charge ($e_o = 1.602 \times 10^{-19}$ C), k is the Boltzmann's constant ($k = 1.281 \times 10^{-23}$ J/K) and T is the absolute temperature. Substitution of Eq. 6.8 into Eq. 6.7 yields

$$K_a = 10^{-pH}\, e^{-y_s} \frac{\alpha}{1-\alpha} \tag{6.10}$$

or, in terms of $pK_a = -\log_{10}K_a$

$$pK_a = pH + 0.434y_s - \log_{10}\frac{\alpha}{1-\alpha} \tag{6.11}$$

which is a well-known equation used in protein titration (see, e.g., Tanford [21])

6.4.2 *Electrical and Polarization Shift in the Fluorescence Spectrum*

The electrical potential at the surface of a charged membrane or interface can be measured by a fluorescent probe sufficiently small as to be close to the surface. The interfacial ionization equilibria have been analysed in detail by Fernández and Fromherz [2], followed by Kraayenhof [12], Thelen [23] and Miyazaki [15] and others. The pK_a of any protonable probe group at a membrane interface, pK_a^{int}, will generally differ from the intrinsic value, pK_a^o, in bulk water due to thermodynamic differences in the ionization equilibria at the two locations. In general, the interfacial pK_a^{int} is given by Miyazaki [15] and Kraayenhof [12]:

$$\mathrm{pH} - \mathrm{pH}_s = \mathrm{pK}_a^{\mathrm{int}} - \mathrm{pK}_a^o = \Delta\mathrm{pK}_a^{el} \pm \left|\Delta\mathrm{pK}_a^{\mathrm{pol}}\right| \tag{6.12}$$

where $\Delta\mathrm{pK}_a^{el}$ is the *electrostatic shift* which is a function of the surface potential and is given by:

$$\Delta\mathrm{pK}_a^{el} = -y_s / \ln 10 \tag{6.13}$$

and $\Delta\mathrm{pK}_a^{\mathrm{pol}}$ is the polarity-induced shift which has been attributed to the hydration of the amphiphilic probe at the interface [1], and takes the positive sign for dissociation of a molecular acid ($\mathrm{HA} \rightleftharpoons \mathrm{H}^+ + \mathrm{A}^-$) and the negative sign for the dissociation of a cationic acid ($\mathrm{HB}^+ \rightleftharpoons \mathrm{H}^+ + \mathrm{B}$).

6.4.3 Buffer Capacity

The *buffering power,* β, of a solution is [14, 18]:

$$\beta = \frac{dB}{d\mathrm{pH}} \tag{6.14}$$

where dB is the amount of base added to the solution, and dpH is the change in pH of the solution due to that base addition. The addition of acid to the solution is equivalent to a negative addition of base, -dB. The units of β are mM/pH unit. In a closed system the total buffer concentration remains constant and the buffering power of a weak acid is given by Putnam [18]:

$$\beta = \frac{2.303\,[\mathrm{A}_T]\,\mathrm{K}_a\,a_H}{(\mathrm{K}_a + a_H)^2} \tag{6.15}$$

where $[\mathrm{A}_T]$ is the total concentration of weak acid and a_H is the proton activity.

Substituting in Eq. 6.15, $a_H = [\mathrm{H}^+]_s$, $\alpha = \frac{[\mathrm{A}^-]}{[\mathrm{A}_T]}$, $K_a = [\mathrm{H}^+]_s \frac{\alpha}{1-\alpha}$, we obtain

$$\beta = 2.3\,[\mathrm{A}^-]\,(1-\alpha) = 2.3\,[\mathrm{A}_T]\,\alpha\,(1-\alpha) \tag{6.16}$$

Neglecting, in a first approach, the contribution of free buffers and considering only the PL headgroups buffers, we have that $[\mathrm{A}_T]$ = [buffer group], where [buffer group] stands for the concentration of protonable phospholipid headgroups, namely:

$$\beta = 2.3\,[\text{buffer group}]\,\alpha(1-\alpha) \tag{6.17}$$

From Eq. 6.11 we obtain

$$\alpha = \left[1 + e^{-y_s} 10^{(\mathrm{pK}_a - \mathrm{pH})}\right]^{-1} \tag{6.18}$$

Substituting in Eq. 6.15, we obtain

$$\beta = 2.303 \frac{[\text{buffer group}]}{2 + e^{y_s} 10^{(\text{pH} - \text{pK}_a)} + e^{-y_s} 10^{(\text{pK}_a - \text{pH})}} \tag{6.19}$$

or

$$\beta = 2.3 \frac{[\text{buffer group}]}{2 + e^{y_s} \frac{\text{K}_a}{[\text{H}^+]} + e^{-y_s} \frac{[\text{H}^+]}{\text{K}_a}} \tag{6.20}$$

In general, for a number > 1 of buffer groups, we will have

$$\beta = 2.3 \sum_i \frac{[\text{buffer group}]_i}{2 + e^{y_s} 10^{(\text{pH} - \text{pK}_{ai})} + e^{-y_s} 10^{(\text{pK}_{ai} - \text{pH})}} \tag{6.21}$$

or

$$\beta = 2.3 \sum_i \frac{[\text{buffer group}]_i}{2 + e^{y_s} \frac{\text{K}_{ai}}{[\text{H}^+]} + e^{-y_s} \frac{[\text{H}^+]}{\text{K}_{ai}}} \tag{6.22}$$

The total number of bound protons, $\overline{\nu}$, summed over all types of groups i is

$$\overline{\nu} = \sum_i \nu_i (1 - \alpha_i) \tag{6.23}$$

where ν_i is the number of groups of type i in the lipid.

$$\nu_i = \text{N}_A \, V_V \, [\text{buffer group}]_i \tag{6.24}$$

We can write Eq. 6.23 as:

$$\overline{\nu} = \sum_i \frac{\nu_i}{1 + e^{y_s} \, 10^{(\text{pH} - \text{pK}_{ai})}} \tag{6.25}$$

or

$$\overline{\nu} = \sum_i \frac{\nu_i}{1 + e^{y_s} \frac{\text{K}_{ai}}{[\text{H}^+]}} \tag{6.26}$$

Any one of Eqs. 6.25 and 6.26 describes the titration curve of the phospholipid headgroups with all nonelectrostatic effects on the dissociation described by K_{ai}.

In order to calculate the charge fluctuation associated with the proton we use the electrical equivalent of the buffer capacitance as defined by Procopio and Fornés [17], namely:

$$C_{\text{buffer}} = \frac{\beta V_V}{\ln 10} \frac{F^2}{RT} \tag{6.27}$$

The magnitude of the proton related mean square charge thermal fluctuation is given by Procopio [16] and Fornés [3]:

$$< (\Delta q)^2 > \; = \; kTC_{\text{buffer}} \tag{6.28}$$

After substituting Eq. 6.27 in Eq. 6.28 using Eqs. 6.21 and 6.22, we obtain

$$< (\Delta q)^2 > = e_o^2 \sum_i \frac{\nu_i}{2 + e^{y_s} 10^{(\text{pH} - \text{pK}_{ai})} + e^{-y_s} 10^{(\text{pK}_{ai} - \text{pH})}} \tag{6.29}$$

or

$$< (\Delta q)^2 > = e_o^2 \sum_i \frac{\nu_i}{2 + e^{y_s} \frac{\text{K}_{ai}}{[\text{H}^+]} + e^{-y_s} \frac{[\text{H}^+]}{\text{K}_{ai}}} \tag{6.30}$$

Equation 6.30 with $y_s = 0$ coincides with that given by Kirkwood and Shumaker [13], obtained independently using mechanical statistical methods, when calculating the forces between protein molecules in solution arising from fluctuations in proton charge and configuration.

From Eqs. 6.20, 6.30 and 6.24, we obtain a relation between the mean square of the proton charge fluctuation, $< (\Delta q)^2 >$, and the buffering power β, namely:

$$\beta = \frac{2.3}{e_o^2 \text{N}_A \, V_V} < (\Delta q)^2 > \tag{6.31}$$

Figure 6.3 depicts the average theoretically estimated protonic charge fluctuations, inside a hypothetical 8 nm internal radius SUV bearing phosphatidic acid groups on its internal surface for two surface potentials.

From Eqs. 6.27 and 6.31, we obtain the relation between C_{buffer} and the mean square of the proton charge fluctuation, $< (\Delta q)^2 >$, namely:

$$C_{\text{buffer}} = \frac{< (\Delta q)^2 >}{kT} \tag{6.32}$$

Differentiation of Eq. 6.25 with respect to pH gives

$$\frac{\partial \overline{\nu}}{\partial \text{pH}} = -\frac{2.303}{e_o^2} < (\Delta q)^2 > \tag{6.33}$$

i.e. the slope of the titration curve, Fig. 6.4, at any pH gives the charge fluctuation at that pH. Equation 6.33 was also obtained by Timasheff [22] for the titration of proteins.

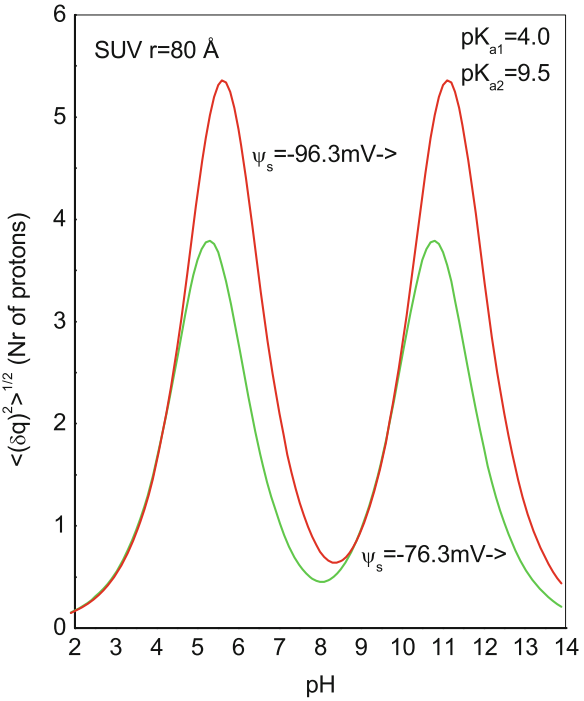

Fig. 6.3 Average theoretically estimated protonic charge fluctuations, inside a hypothetical 8 nm internal radius SUV bearing phosphatidic acid groups on its internal surface for two surface potentials

6.5 pH Fluctuations

The mean square of the fluctuating voltage will be [3, 16]:

$$< (\delta V)^2 >= \frac{kT}{C_{\text{buffer}}} \tag{6.34}$$

Correspondingly, the fluctuation in pH is given by Procopio [17]:

$$< (\delta \text{pH})^2 >^{1/2} = -\frac{e_0}{2.3kT} < (\delta V)^2 >^{1/2} = \frac{e_0}{2.3(kTC_{\text{buffer}})^{1/2}} \tag{6.35}$$

or

$$< (\delta \text{pH})^2 >^{1/2} = \frac{e_0}{2.3 < (\Delta q)^2 >^{1/2}} \tag{6.36}$$

or

$$< (\delta \text{pH})^2 >^{1/2} = \beta^{-1/2}(2.3\text{N}_A V_V)^{-1/2} \tag{6.37}$$

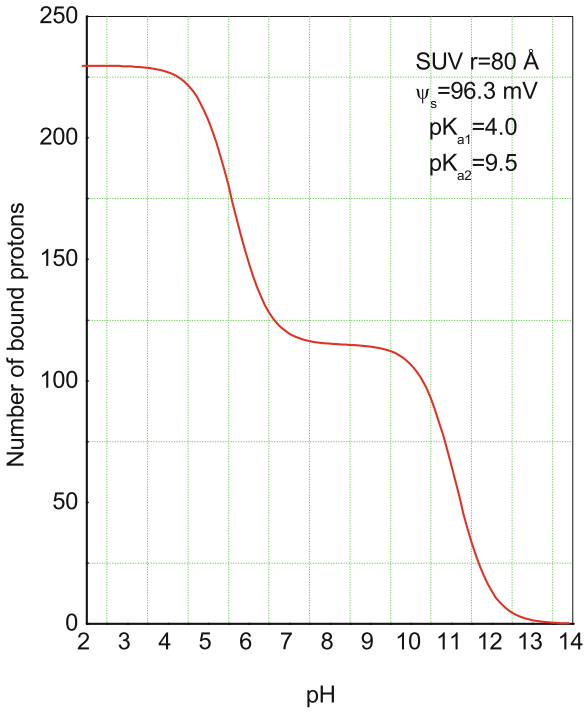

Fig. 6.4 Titration curve, representation of Eq. 6.23

A consequence of Eq. 6.37 is that the relation between the pH fluctuations for two small systems with identical volumes and different buffering powers, β_1 and β_2, is given by:

$$\frac{<(\delta \mathrm{pH}_1)^2>^{1/2}}{<(\delta \mathrm{pH}_2)^2>^{1/2}} = \sqrt{\frac{\beta_2}{\beta_1}} \tag{6.38}$$

In case that the only source of buffer groups is on the surface, as is our case, Eq. 6.36 gives the pH fluctuations on the surface of the buffering system produced by the protonic fluctuations. In order to relate surface pH fluctuations with those in the bulk phase we make use of Eqs. 6.9 and 6.35, namely:

$$\delta \mathrm{pH}_s = \delta \mathrm{pH} + 0.434 \frac{e_o}{kT} \delta \psi_s \tag{6.39}$$

as, in this case, the variation of surface potential is caused by variation in pH, we obtain

$$\delta \psi_s = -2.3 \frac{kT}{e_o} \delta \mathrm{pH}_s \tag{6.40}$$

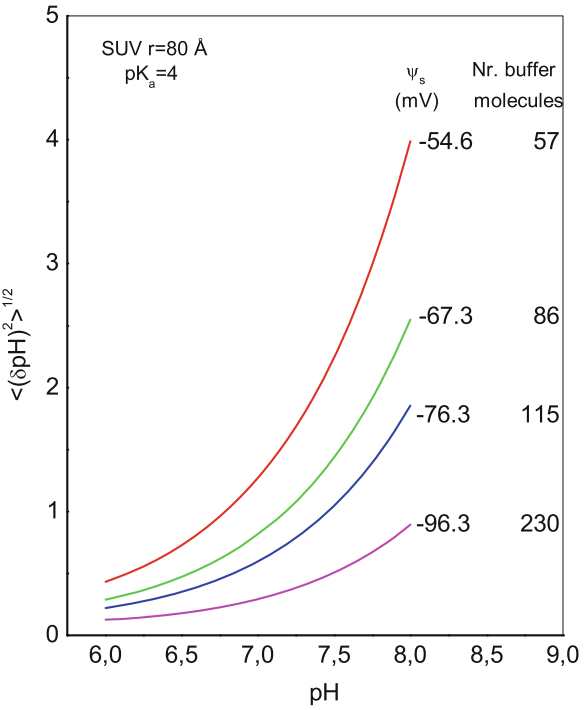

Fig. 6.5 Average pH fluctuations, as a function of the pH, inside a hypothetical 8 nm internal radius SUV with buffer groups having pK$a = 4$

From Eqs. 6.39 and 6.40 and considering the statistical mean of the fluctuations, we obtain

$$< (\delta \mathrm{pH})^2 >^{1/2} = 2 < (\delta \mathrm{pH}_s)^2 >^{1/2} = 2 \frac{e_0}{2.3(kTC_{\mathrm{buffer}})^{1/2}} \tag{6.41}$$

This has the meaning that the mean pH fluctuation in the bulk is twice that on the surface.

Figure 6.5 depicts the average pH fluctuations, as a function of the pH, inside a hypothetical 8 nm internal radius SUV with buffer groups having a single pK$a = 4$ and Fig. 6.6 for an SUV containing groups of phosphatidic acid with pK$_a = 4$ and pK$_a = 9.5$ [1]. Different surface potentials were studied as determined by the fraction of protonable groups to total PL headgroups according to [12] and considering an average area of 70 Å^2 per headgroup [1].

In Fig. 6.7 is shown the variation of pH fluctuations with vesicular size, for a given pK$_a = 4$, it is observed that they are almost negligible for vesicules with 1000 Å radius.

The study of fluctuations in small systems is important not only from an experimental point of view in knowing measurement intervals but also because they provide a deep insight into the occurring mechanisms and processes. Throughout

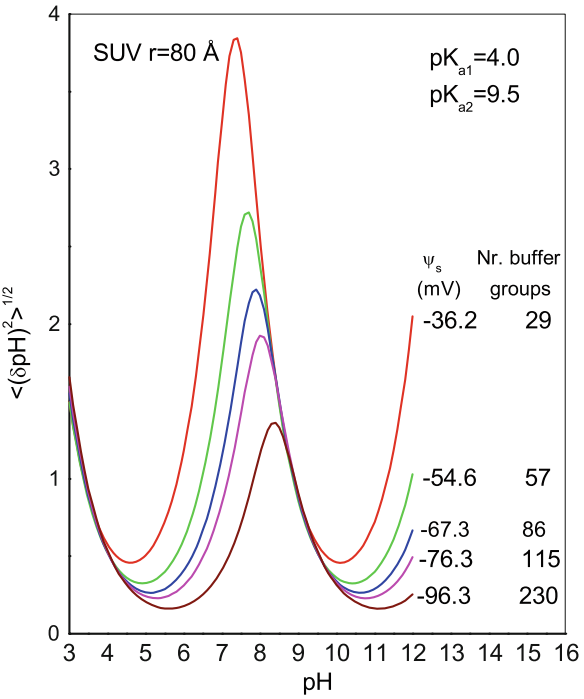

Fig. 6.6 Ditto containing groups of phosphatidic acid $pK_a = 4$ and $pK_a = 9.5$, [1]

this paper we observe that macroscopic defined variables such as buffering power and capacitance and titration curve can be expressed as functions of protonic charge fluctuations.

The validity of our approach through the electrical equivalent of the buffering capacity is reinforced by the coincidence of the results of Eq. 6.30 with the one obtained independently by Kirkwood and Schumaker [13] when calculating the forces between protein molecules, due to proton fluctuations.

From the preceding derivations we infer that these fluctuations are dependent on macroscopic variables such as pH, pK_a and buffer concentration. Equation 6.38 gives the relation between the pH fluctuations for two solutions and the corresponding buffering powers and permits verifying our theoretical predictions of pH noise measurement using a fluorescent probe.

In Fig. 6.3 it is shown the charge fluctuation profile for the same vesicular system. We can observe also here that the maximum in fluctuation is shifted in relation to the corresponding pKs, due to the presence of a surface potential. The number of fluctuating protons increases with the surface potential due to the increase in the number of buffering molecules. The charge fluctuation, as depicted in this figure, is proportional to the derivative of the titration curve Fig. 6.4, see Eq. 6.33.

In Fig. 6.5 is plotted the pH fluctuation, $< (\delta \mathrm{pH})^2 >^{1/2}$, versus pH for given values of the surface potential and number of buffer groups for a lipid with $pK_a = 4$

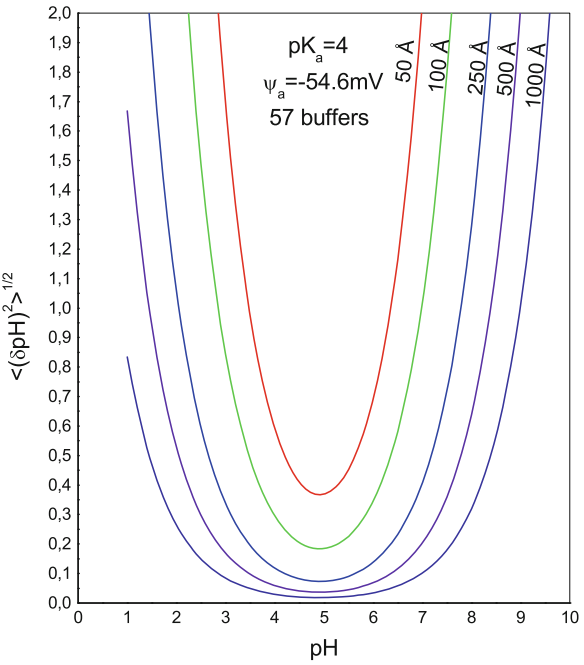

Fig. 6.7 Variation of PH fluctuations with vesicular size

(first pK of PA as reported in [1]) as obtained from Eq. 6.41. We can observe that pH fluctuations for pH values centred about 7.4 (6.4–8.4) are no larger than 1.5 pH units for surface potentials lower than −50 mV.

In Fig. 6.6 we have the same plot of Fig. 6.5 including the second pK$_a$ of PA (also data from [1]) where we have considered the same number of molecules for each pK$_a$. It can be observed that there occurs a maximum in the pH fluctuation between the two pK$_a$. In the interval [pK$_{a1}$,pK$_{a2}$] the pH fluctuation can reach several units of pH except for pH surrounding the corresponding pKs. The shift with respect to the pKs observed in the minima of the curves is due to the surface potential. Also, from Fig. 6.6, we can infer that the measurement of pH in small systems has to be done near the pK of the buffer groups in order that measurement errors using fluorescent probes be minimized.

Comparing Figs. 6.3 and 6.6, we can observe that the charge fluctuation has a maximum where pH fluctuations are at a minimum. This is a result of the fluctuation-dissipation theorem [3], where the pH fluctuations can be be viewed as a response of the medium to the protonic charge fluctuations of the system and vice versa, namely:

$$< (\Delta q)^2 >< (\delta V)^2 >= (kT)^2 \tag{6.42}$$

or

$$< (\Delta q)^2 >< (\delta \mathrm{pH})^2 >= \left(\frac{e_0}{2.3}\right)^2 \tag{6.43}$$

We can also observe from Figs. 6.5 and 6.6 that the pH fluctuations diminish with decreasing surface negativity due to decreasing the number of buffer molecules on the inner vesicular surface.

In Fig. 6.7 can be observed that pH fluctuations diminish with increasing the size of the SUVs, this being an expected result in accordance with [17].

From the above results we can predict that there will be measurable effects on the fluorescence detection due to protonic fluctuations close to the pH sensing region of the probes.

Many probes used as pH indicators show a shift in absorption and emission spectra between protonated and deprotonated forms, allowing the spectroscopic measurement of the acid dissociation constant K_a in the ground state. The protonation and deprotonation reactions can also be examined in the excited states of the probe, under the assumption that the acid–base equilibrium may be established during the lifetime of the first singlet excited state, typically in the range of ns. As a consequence, the acid dissociation constants in the excited state can be determined using fluorometric techniques [4, 24]. As pointed by Rettig and Lapouyade [19], the knowledge of prototropic reactions of chromophores in the ground and excited states results in probes which can monitor the pH of its microscopic surroundings. As a rule, absorption and emission spectra are largely dependent on pH over circa 2 pH units around its pKa and, since probes with a wide range of pKa values are available, detailed monitoring of pH from 0 to 10 is possible. In particular, probes like hydroxycoumarin, pyranine, fluoresceine, seminaphtofluorescein (SNAFLs) and seminaphtorhodafluors (SNARFs) are employed as physiological pH indicators. Szmacinski and Lakowicz [20] indicated that the fluorescence sensors assays are based mainly on intensity measurements, following the intensity changes resulting from the different electronic properties and interactions with the surroundings presented by the protonated and deprotonated forms of the probes. It is suggested by these authors, however, that lifetime-based sensing methods would be developed to be applied mainly to overcome difficulties with intensity measurements as, for example, in the case of turbid samples, imprecise or dirty optical surfaces or variations in optical alignment of different samples. Use could be made from the fact that many probes display changes in fluorescence lifetime on protonated/deprotonated states. For example, the SNAFL-1 probe has a lifetime of 1.19 ns in the acid form and 3.74 ns in the basic form [20]. It would be expected then an heterogeneous decay of fluorescence in time-resolved experiments performed in a sample in which there is a mixture of two populations of the probe having different lifetimes. With the instrumentation presently available, it is possible the measurement of lifetimes with precision in the picosecond range and also the discrimination of the different contributions to a heterogeneous fluorescence decay. Thus, in the context of the present work, and with adequate choice of the probes, it would be possible to detect

pH fluctuations within the small internal volumes of vesicles, using fluorometric techniques. As natural candidates to such probes we have lipophilic derivatives of hydroxycoumarins and fluorescein. Using probes as described by Fernandez and Fromherz [2], and Kraayenhof et al. [12], that monitor precise positions in the neighbourhood of the membrane surface, one could follow pH fluctuations in nanometer space range and picosecond time range.

References

1. Cevc, G., Marsh, D.: Phospholipid Bilayers. Wiley, New York (1987)
2. Fernández, M.S., Fromherz, P.: Lipoid pH-indicators as probes of electrical potential and polarity in micelles. J. Phys. Chem. **81**, 1755 (1977)
3. Fornés, J.A.: Fluctuation-dissipation theorem and the polarizability of rodlike polyelectrolytes: an electric circuit view. Phys. Rev. E **57**, 2110 (1998)
4. Grabowski, Z.R., Grabowska, A.: The Förster cycle reconsidered. Z. Phys. Chem. **101**, 197 (1976)
5. Gutknecht, J.: Proton conductance caused by long-chain fatty acids in phospholipid bilayer membranes. J. Membr. Biol. **106**, 83 (1988)
6. Gutman, M., Nachliel, E.: The dynamic aspects of proton transfer processes. Biochim. Biophys. Acta **1015**, 391 (1990)
7. Hamilton, J.A.: Fatty acid transport: difficult or easy? J. Lipid Res. **39**, 467 (1998)
8. Hamilton, J.A., Cistola, D.P.: Transfer of oleic acid between albumin and phospholipid vesicles. Proc. Natl. Acad. Sci. **83**, 82 (1986)
9. Kamp, F., Hamilton, J.A.: pH gradients across phospholipid membranes caused by fast flip-flop of un-ionized fatty acids. Proc. Natl. Acad. Sci. **89**, 11367 (1992)
10. Kamp, F., Hamilton, J.A.: Movement of fatty acids, fatty acids analogues, and bile acids across phospholipid bilayers. Biochemistry **32**, 11074 (1993)
11. Kamp, F., Zakim, D., Zhang, F., Noy, N., Hamilton, J.A.: Fatty acid flip-flop in phospholipid bilayers is extremely fast. Biochemistry **34**, 11928 (1995)
12. Kraayenhof, R., Sterk, G.J., Sang, H.W.F.: Probing biomembrane interfacial ... at varing distance from the membrane surface. Biochemistry **32**, 10057 (1993)
13. Kirkwood, J.G., Shumaker, J.B.: Forces between protein molecules in solution arising from fluctuations in proton charge and configuration. Proc. Natl. Acad. Sci. **38**, 863 (1952)
14. Mitchell, P., Moyle, J.: Estimation of membrane potential and pH difference across the cristae membrane of rat liver . . . Biochem. J. **104**, 588 (1967)
15. Miyazaki, J., Hideg, K., Marsh, D.: Interfacial ionization and partitioning of membrane-bound local anaesthetics. Biochim. Biophys. Acta **1103**, 62 (1984)
16. Procopio, J., Fornés, J.A.: Fluctuation-dissipation theorem imposes high-voltage fluctuations in biological ionic channels. Phys. Rev. E **51**, 829 (1995)
17. Procopio, J., Fornés, J.A.: Fluctuations of the proton- electromotive force across the inner mitochondrial membrane. Phys. Rev. E **55**, 6285 (1997)
18. Putnam, R.W.: In: Sperelakis, N. (ed.) Cell Physiology Source Book. Academic, New York (1998)
19. Rettig, W., Lapouyade, R.: Fluorescence probes based in TICT states. Chap. 5. In: Lakowicz, J.R. (ed.) *Topics in Fluorescence Spectroscopy*, vol. 4. Plenum Press, New York (1994)
20. Szmacinski, H., Lakowicz, J. R.: Lifetime-based sensing, Chap. 10. In: Lakowicz, J. R. (ed.) *Topics in Fluorescence Spectroscopy*, vol. 4. Plenum Press, New York (1994)

21. Tanford, C.: The interpretation of hydrogen ion titration curves of proteins. Adv. Protein Chem. **17**, 69 (1962)
22. Timasheff, S.N.: In: *Biological Polyelectrolytes*, vol. 3, Chap. 1. Marcel Dekker, New York (1970)
23. Thelen, M., Petrone, G., O'Shea, P.S., Azzi, A.: The use of fluoresce in dipalmitoylphosphatidylethanolamine for measuring pH-changes in the internal compartment of phospholipid vesicles. Biochim. Biochim. Biophys. Acta **766**, 161 (1984)
24. Van der Donckt, E.: Acid-base-properties of excited states. Prog. React. Kinet. **5**, 273 (1970)

Chapter 7
Electrical Fluctuations on the Surfaces of Proteins from Hydrodynamic Data

Abstract We calculate the electrical capacitance on the surface of protein molecules from hydrodynamic data of the proteins. Then, we estimate the electrical fluctuations (charge, voltage) through the fluctuation-dissipation theorem which links the electrical capacitance of the system with these fluctuations. From the intrinsic viscosity of the proteins we estimate the polarizability which leads to the knowledge of the field and dipole fluctuations. From the fitting of the capacitance, polarizability and electrical fluctuations as a function of the molecular weight of the proteins we report numerical equations which allow to estimate these physical magnitudes for a given protein knowing the molecular weight. Charge fluctuations are in the fraction of unit charge range, voltage fluctuations are in the three mV digit range, field fluctuations are in the two digit mV/nm (10^6 V/m) range and the dipole moment fluctuations range from the two to three digit times the dipole moment of water molecule. These surface properties of proteins have not been reported before.

Keywords Proteins electrical fluctuations • Proteins dipole fluctuations • Proteins field fluctuations • Proteins voltage fluctuations

7.1 Electrical Fluctuations on the Surface of Proteins from Hydrodynamic Data

In this chapter we estimate the electrical capacitance, from hydrodynamic data, of several proteins in order to estimate the electrical fluctuations on their surfaces. It has long been inferred from a variety of experimental studies that substantial structural fluctuations occur in proteins, and that these fluctuations are essential to protein function (Edsall [7]; Careri et al. [4]; Weber [23]). Charged groups are

Part reprinted from [José A. Fornés, *J. Colloid Interface Sci.* **323**, 255, (2008)] Copyright (2008), with permission from Elsevier.

J.A. Fornés, *Electrical Fluctuations in Polyelectrolytes*, SpringerBriefs in Molecular Science, DOI 10.1007/978-3-319-33840-8_7

extruded from the protein interior towards the higher dielectric solvent, the protein surface is often highly charged, and the dielectric properties of this interfacial region are quite different from the protein bulk. Simonson and Perahia [19] studied the polar fluctuations of yeast cytochrome c using nanosecond molecular-dynamic simulations in a spherical droplet of water, they found an important component of dipole moment fluctuations consisting of diffusive, mutually independent, motions of the charged side chains at the protein surface.

7.2 Relation Between Friction Coefficient and Capacitance

Hubbard and Douglas [14] performed a simple and accurate method of estimating the translational hydrodynamic friction on Brownian particles of arbitrary shape. The Brownian friction coefficient f takes the form

$$f = 6\pi\eta C \tag{7.1}$$

where C is the equivalent to the electrostatic capacitance of the particle in units where the capacity of a sphere equals its radius and η is the fluid viscosity. They arrived to this result by angular averaging of the Oseen tensor [5, 6, 15, 22]. The connection between hydrodynamic and electrostatic properties was also recognized by Zhou [24–26], from the fact that the Oseen Tensor, i.e. the Green function for the Navier–Stokes equation, when orientationally averaged is proportion to the Green function for the Laplace equation. In this way Zhou obtained the same Eq. 7.1. In order to calculate the charge and voltage fluctuations we make use of the hydrodynamic data for proteins reported in [20]. In Table 7.1 f_0 was calculated using the equation given also in [20], namely

$$f_0 = 6\pi\eta r_0 = 6\pi\eta\left(\frac{3M\overline{v}}{4\pi N_A}\right)^{1/3} \tag{7.2}$$

where r_0 is the radius of an anhydrous spherical particle having the same mass and partial specific volume, $\overline{v}$, as the protein under consideration, N_A is Avogadro's number and M is the molecular weight. Knowing f_0 we can calculate f from Table 7.1 and from Eq. 7.1 we determine C, see Table 7.2. With the knowledge of C, using Eqs. 1.27 we determine the voltage, δV, and charge fluctuations, δq.

7.3 Relation Between Polarizability and Intrinsic Viscosity

For determining the polarizability α, we use the equation given by Zhou in [24], namely,

$$\alpha = \frac{1}{3}\left(4\,[\eta] - V_h\right) \tag{7.3}$$

Table 7.1 Hydrodynamic properties of proteins[a]

Protein (source)	PDB	$f_0\ 10^{-8}$ g/s	f/f_0	$f\ 10^{-8}$ g/s	$\overline{v}$ (cm^3/g)	$[\eta]$ (cm^3/g)	Molecular weight	$\frac{gH_2O}{gprotein}$ Hydration
Pancreatic trypsin Inhibitor (bovine)	4pti	2.346	1.321	3.099	0.718	3.83 [16]	6670	0.86
Cytochrome c (equine)	1hrc	2.848	1.116	3.178	0.715	2.50 [8]	11,990	0.24
Ribonuclease A (bovine)	7rsa	2.954	1.290	3.210	0.703	3.30 [12]	13,600	0.73
Lysozyme (hen)	6lys	2.968	1.240	3.680	0.703	3 [3, 25]	13,800	0.57
Myoglobin (sperm whale)	1mbo	3.218	1.170	3.765	0.745	3.25 [12]	16,600	0.35
Adenylate kinase (porcine)	1ake	3.474	1.167	4.055	0.740	2.96[b]	21,030	0.41
Bence Jones REI (human)	1b6d	3.558	1.156	4.113	0.726	2.55[b]	23,020	0.35
Chymotrypsinogen (bovine)	2cga	3.582	1.262	4.521	0.721	2.8 [17, 21]	23,660	0.71
Trypsin (bovine)	1tpo	3.604	1.187	4.278	0.727	2.93[b]	23,890	0.47
Elastase (porcine)	1est	3.644	1.214	4.424	0.730	3.14[b]	24,600	0.53
Carbonic anhydrase (human)	2cab	3.758	1.053	3.957	0.729	2.76 [1]	27,020	0.12
Subtilisin novo (B. amyloliq.)	1sup	3.790	1.181	4.476	0.731	2.91[b]	27,630	0.47
Superoxide dismutase (bovine)	2sod	4.041	1.132	4.575	0.729	2.64[b]	33,600	0.23
Carboxypeptidase A (bovine)	1cps	4.106	1.063	4.365	0.733	2.50[b]	35,040	0.14
Phosphoglycerate kinase (yeast)	3pgk	4.554	1.377	6.271	0.749	4.73[b]	46,800	1.04
Concanavalin A	1con	4.747	1.299	6.167	0.732	4.11[b]	54,240	0.64
Hemoglobin, oxy (equine)	1hho	5.168	1.263	6.517	0.750	3.60 [3]	67,980	0.74
Malate dehydrogenase (porcine)	1mld	5.287	1.344	7.106	0.742	4.27[b]	73,900	1.00
Alcohol dehydrogenase (porcine)	1axe	5.427	1.208	6.556	0.750	2.23[b]	79,070	0.37
Lactate dehydrogenase (dogfish)	6ldh	6.551	1.273	8.340	0.740	3.80 [27]	141,000	0.77

[a]Measured data from [20] except $[\eta]$

[b]Calculated with Eq. 7.5 using for ν the formalism of [13], knowing the shape dimensions of the molecules reported in [20]

Table 7.2 Electrical properties of proteins

Protein (source)	PDB	C nm[a]	aF[b]	α nm^3	$\delta q/e_0$	δV mV	δE mV/nm	$\delta p/p^c_{H_2O}$
Pancreatic trypsin inhibitor (bovine)	4pti	1.63	0.182	51.03	0.171	150.3	26.86	24.90
Cytochrome c (equine)	1hrc	1.68	0.187	60.17	0.173	148.4	24.8	27.04
Ribonuclease A (bovine)	7rsa	2.01	0.224	89.10	0.189	135.6	20.37	32.90
Lysozyme (hen)	6lys	1.94	0.216	82.35	0.186	137.9	21.17	31.63
Myoglobin (sperm whale)	1mbo	1.98	0.221	109.69	0.188	136.4	18.32	36.51
Adenylate kinase (porcine)	1ake	2.14	0.238	124.7	0.195	131.4	17.2	38.93
Bence Jones REI (human)	1b6d	2.17	0.242	116.9	0.197	130.5	17.8	37.70
Chymotrypsinogen (bovine)	2cga	2.39	0.266	128.8	0.206	124.5	16.96	39.56
Trypsin (bovine)	1tpo	2.25	0.251	139.6	0.200	127.9	16.2	41.18
Elastase (porcine)	1est	2.34	0.260	148.3	0.204	125.8	15.8	42.45
Carbonic anhydrase (human)	2cab	2.08	0.232	152.6	0.193	133.0	15.53	43.06
Subtilisin novo (B. amyloliq.)	1sup	2.36	0.263	160.5	0.205	125.1	15.2	44.16
Superoxide dismutase (bovine)	2sod	2.44	0.269	178.8	0.207	123.7	14.4	46.62
Carboxypeptidase A (bovine)	1cps	2.30	0.256	177.3	0.203	126.7	14.4	46.41
Phosphoglycerate kinase (yeast)	3pgk	3.31	0.368	446.8	0.243	105.7	9.1	73.68
Concanavalin A	1con	3.25	0.362	454.0	0.241	106.6	9.02	74.27
Hemoglobin, oxy (equine)	1hho	3.44	0.383	488.4	0.248	103.7	8.70	77.03
Malate dehydrogenase (porcine)	1mld	3.75	0.417	630.9	0.259	99.3	7.65	87.55
Alcohol dehydrogenase (porcine)	1axe	3.46	0.385	343.8	0.248	103.4	10.37	64.64
Lactate dehydrogenase (dogfish)	6ldh	4.40	0.490	1074.1	0.280	91.6	5.86	114.2

[a] $1F \equiv 8.985 \times 10^{18}$ nm
[b] $aF \equiv attoF = 10^{-18}$ F
[c] $p_{H_2O} = 1.84D = 6.138 \times 10^{-30}$ cm

V_h is the hydrated volume of a molecule and is given by

$$V_h = \left(\frac{M}{N_A}\right)\left(\overline{v} + \frac{1}{\rho_h}H\right) \tag{7.4}$$

ρ_h is the density of hydration water in units of g/cm^3, it has been found to have a somewhat higher density than bulk water, with a value of $\rho_h = 1.104\,\text{g/cm}^3$ (Bull and Breece [2]) and $[\eta]$ is the intrinsic viscosity, which measures the contribution of the molecule to the viscosity of the solution in which it is dissolved [24, 25]. Also represents the space occupied by a gram of solute at infinite dilution. In volume units the intrinsic viscosity is given by Cantor and Schimmel [3],

$$[\eta] = \nu V_h \tag{7.5}$$

In units of $(volume/g)$ is given by,

$$[\eta] = \frac{N_A}{M}\nu V_h \tag{7.6}$$

In the former equations ν is the Simha factor [18].

7.4 Relations of the Polarizability to Electric Field and Dipole Moment Fluctuations

In [11] we also gave a relation between the polarizability and electric field and dipole moment fluctuations, namely

$$\delta p = \sqrt{\alpha kT} \tag{7.7}$$

and

$$\delta E = \sqrt{\frac{kT}{\alpha}} \tag{7.8}$$

The values of δp and δE are also reported in Table 7.2.

In Fig. 7.1a is plotted the capacitance as a function of the molecular weight, M, of the proteins. We can fit the curve by a second order polynomial. We observe very low values of the capacitance of the proteins, C, in the range [0.18–0.5] aF, with a corresponding increase of the capacitance with the size of the molecule. In Fig. 7.1b we observe a linear fitting relation between the polarizability and M, the polarizability, α varies in the range [50–1100] nm^3. Correspondingly to the low values of the capacitance, C, the fluctuations of charge are negligible, in units of the elementary charge the range is [0.17–0.28]$\delta q/e_0$, this could be

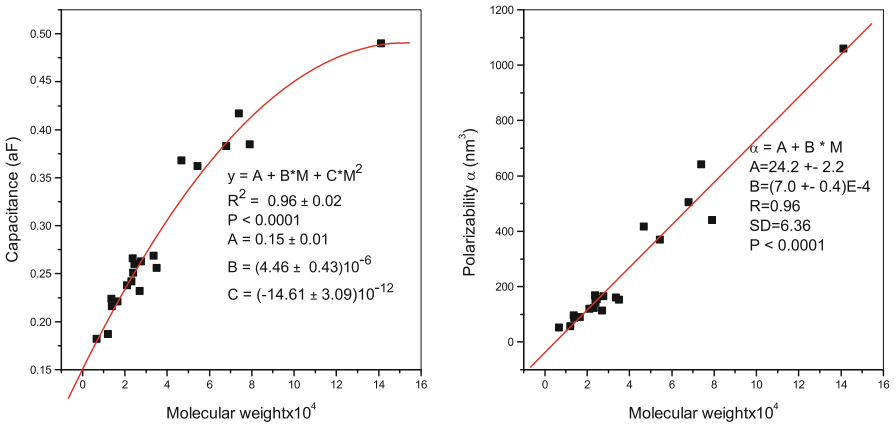

Fig. 7.1 Electrical parameters of proteins

interpreted as the probability of producing a unit charge variation in the protein. In Fig. 7.2a we observe an exponential growth with M for these charge fluctuations. In Fig. 7.2b we observe the voltage fluctuations as a function of the molecular weight, these fluctuations are in the [90–150] mV range, decreasing with the size of the protein molecule. This effect was already predicted for colloidal particles and polyelectrolytes in [9, 10]. We observe a good fitting of data with a first order exponential decay curve. In Fig. 7.2c is plotted the field fluctuations δE versus M showing a first order exponential decay. These high field fluctuations are in the [5–30] mV/nm range. Finally in Fig. 7.2d is plotted the dipole moment fluctuations in units of the water molecule dipole moment versus M, we observe a second order polynomial fitting in the range $[25–115]\delta p/p_{H_2O}$. In conclusion using phenomenological equations (FDT) we predict high electrical fluctuations on the protein surfaces. We developed numerical equations which allow us to estimate these fluctuations for a given protein knowing the molecular weight. It is possible that these fluctuations are important for explaining some biological phenomena.

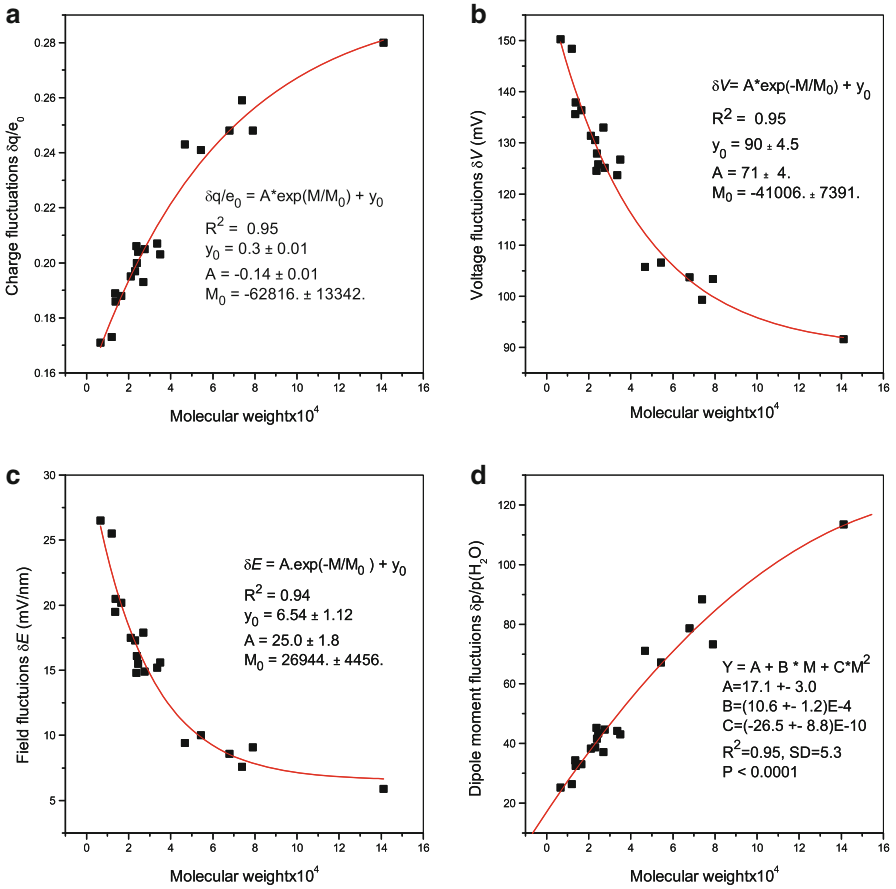

Fig. 7.2 Electrical fluctuations of proteins

References

1. Armstrong, J.McD., Myers, D.V., Verpoorte, J.A., Edsall, J.T.: Purification and properties of human erythrocyte carbonic anhydrases. J. Biol. Chem. **241**(21), 5137–5149 (1966)
2. Bull, H.B., Breese, K.: Protein hydration. II. Specific heat of egg albumin. Arch. Biochem. Biophys. **128**, 497–502 (1968)
3. Cantor, C.R., Schimmel, P.R.: Biophysical Chemistry - Part II. W. H. Freeman, New York (1980)
4. Careri, G., Fasella, P., Gratton, E.: CRC Crit. Rev. Biochem. **3**, 141 (1975). Ann. Rev. Biophys. Bioengng. **132**, 69 (1979)
5. Carrasco, B., de la Torre, J.G.: Hydrodynamic properties of rigid particles: comparison of different modeling and computational procedures. Biophys. J. **75**, 3044–3057 (1999)
6. Deutch, J.M., Felderhof, B.U.: Frictional properties of dilute polymer solutions. II. The effect of preaveraging. J. Chem. Phys. **62**, 2398–2405 (1975)

7. Edsall, J.T.: In: Rich, A., Davidson, N. (ed.) Structural Chemistry and Molecular Biology, p. 88. Freeman, San Francisco (1968)
8. Fisher, W.R., Taniuchi, H., Anfinsen, C.B.: On the role of heme in the formation of the structure of cytochrome c. J. Biol. Chem. **248**, 3188–3195 (1973)
9. Fornés, J.A.: Electrical fluctuations in colloid and ionic solutions. J. Colloid Interface Sci. **186**, 90–101 (1997)
10. Fornés, J.A.: Thermal electrical fluctuations around a charged colloidal cylinder in an electrolyte. Phys. Rev. E **57**, 2104–2109 (1998)
11. Fornés, J.A.: Fluctuation-dissipation theorem and the polarizability of rodlike polyelectrolytes: an electric circuit view. Phys. Rev. E **57**, 2110–2114 (1998)
12. Harding, S.E.: The intrinsic viscosity of biological macromolecules. Progress in measurement, interpretation and application to structures in dilute solutions. Prog. Biophys. Mol. Biol. **68**, 207–262 (1997)
13. Harding, S.E., Dampier, M., Rowe, A.J.: The viscosity increment for a dilute suspension of triaxial ellipsoids in dominant Brownian motion. J. Colloid Interface Sci. **79**(1), 7–13 (1981)
14. Hubbard, J.B., Douglas, J.F.: Hydrodynamic friction of arbitrarily shaped Brownian particles. Phys. Rev. E **47**(5), R2983–R2986 (1993)
15. Kirkwood, J.G., Riseman, J.: The intrinsic viscosities and diffusion constants of flexible macromolecules in solution. J. Chem. Phys. **16**, 565–573 (1948)
16. Rai, N., Nöllmann, M., Spotorno, B., Tassara, G., Byron, O.: SOMO(SOlution MOdeler): Differences between X-Ray- and NMR-derived bead models suggest a role for side chain flexibility in protein hydrodynamics. Structure **13**, 723–734 (2005)
17. Schwert, G.W.: The molecular size and shape of the pancreatic proteases. II. Chymotrypsinogen. J. Biol. Chem. **190**, 799–806 (1951)
18. Simha, R.: The influence of Brownian movement on the viscosity of solutions. J. Phys. Chem. **44**, 25–34 (1940)
19. Simonson, T., Perahia, D.: Polar fluctuations in proteins: molecular-dynamic studies of cytochrome c in aqueous solution. Faraday Discuss. **103**, 71–90 (1996)
20. Squire, P.G., Himmel, M.E.: Hydrodynamic and protein hydration. Q. Rev. Biophys. **1**, 165–177 (1979)
21. Tanford, C.: Protein denaturation. Adv. Protein. Chem. **23**, 121–282 (1968)
22. de la Torre, J.G., Bloomfield, V.A.: Hydrodynamic properties of complex, rigid, biological macromolecules. Theory and applications. Quart. Rev. Biophys. **14**, 81–139 (1981)
23. Weber, G.: Adv. Protein Chem. **29**, 1 (1975)
24. Zhou, H.-X.: Calculation of translational friction and intrinsic viscosity. I. General formulation for arbitrarily shaped particles. Biophys. J. **69**, 2286–2297 (1995)
25. Zhou, H.-X.: Calculation of translational friction and intrinsic viscosity. II. Application to Globular Proteins. Biophys. J. **69**, 2298–2303 (1995)
26. Zhou, H.-X.: A unified picture of protein hydration: prediction of hydrodynamic properties from known structures. Biophys. Chem. **93**, 171–179 (2001)
27. Zipper, P., Durchschlag, H.: Calculation of hydrodynamic parameters of proteins from crystallographic data using multibody approaches. Prog. Colloid Polym. Sci. **107**, 58–71 (1997)

Index

J.A. Fornés, *Electrical Fluctuations in Polyelectrolytes*, SpringerBriefs in Molecular Science, DOI 10.1007/978-3-319-33840-8